ATRIAL FIBRILLATION AND OBESITY:

CHARACTERIZATION OF ELECTRO-STRUCTURAL ATRIAL SUBSTRATE WITH SUSTAINED OBESITY AND REVERSAL UPON WEIGHT REDUCTION

Rajiv Mahajan MBBS, MD, FRACP

Department of Cardiology

Royal Adelaide Hospital

and

Discipline of Medicine

University of Adelaide

A thesis submitted to the University of Adelaide

in fulfillment of the requirements for the degree of

Doctor of Philosophy

February 2014

To my parents Sabita and Bal,

my soulmate Kavita

and

my daughter Idhika

Table of contents

Abstract

Atrial fibrillation (AF) is the most prevalent arrhythmia affecting humans. The identification of risk factors for AF has ushered a risk factor based approach for management. Obesity is a highly prevalent and novel risk factor for AF with a potential for reversibility. The epidemiological link between obesity and AF has been established in population based studies; however the atrial substrate remains to be fully characterized. Furthermore, mechanism and degree of reversibility with weight reduction has not been described. This thesis evaluates the various aspects of endocardial and epicardial atrial remodeling with sustained obesity and the underlying mechanisms in an ovine model. It also examines the endocardial atrial remodeling with obesity in humans and its relationship with epicardial adipose tissue. In addition, the reversal of obesity related atrial substrate with weight reduction has been characterized in a sustained obesity ovine model.

Chapter 2 examines the endocardial electrophysiological remodeling with sustained obesity in an ovine model. Sustained obesity was associated bi-atrial slow and heterogeneous atrial conduction with increased fractionation and greater vulnerability for AF. There is no significant alteration in endocardial atrial refractoriness. Although there was no difference in mean voltage there was increased voltage heterogeneity. Obesity was associated with overexpression of pro-fibrotic TGFβ1 and increased atrial fibrosis. Infiltration of the epicardial atrial musculature by the contiguous fat was seen and this could represent a unique substrate for AF in obesity.

Chapter 3 describes the reversal of the obesity related atrial substrate with weight reduction in an ovine model. Sustained obesity was associated with bi-atrial epicardial slow and heterogeneous conduction, reduced atrial refractoriness (epicardial) and increased propensity for AF. This was associated with hemodynamic stress and diastolic dysfunction. Histologically obesity was associated with atrial fibrosis, inflammation and fatty infiltration. There was up-regulation of atrial TGFβ1 expression and Endothelin receptor B. The TGFβ1 expression correlated with electrophysiological changes and atrial fibrosis, and this relationship persisted even after adjusting for left atrial pressure. There was decreased expression of atrial gap junction protein Connexin43 expression. The changes observed with sustained obesity were reversed with moderate weight reduction.

Chapter 4 describes the electrophysiological reverse remodeling with weight reduction in an ovine model. Weight reduction resulted in improvement in endocardial atrial conduction velocity and decrease in conduction heterogeneity. However, the atrial refractoriness from endocardial sites did not change with either obesity or weight reduction. This is in contrast to epicardial atrial refractoriness which shortened with sustained obesity and improved to control values with weight reduction. This endocardial- epicardial dissociation in atrial refractoriness may represent part of the unique substrate for AF in obesity.

Chapter 5 describes the validation of atrial pericardial fat assessment on cardiac magnetic resonance imaging against the gold standard of autopsy.

Chapter 6 describes the electroanatomic remodeling with obesity in humans and describes the association with atrial pericardial fat.

NOTE: Pagination of the digital copy does not correspond with the pagination of the print copy

Declaration

I certify that this work contains no material which has been accepted for the award of any other degree or diploma in my name, in any university or other tertiary institution and, to the best of my knowledge and belief, contains no material previously published or written by another person, except where due reference has been made in the text. In addition, I certify that no part of this work will, in the future, be used in a submission in my name, for any other degree or diploma in any university or other tertiary institution without the prior approval of the University of Adelaide and where applicable, any partner institution responsible for the joint-award of this degree.

I give consent to this copy of my thesis when deposited in the University Library, being made available for loan and photocopying, subject to the provisions of the Copyright Act 1968.

The author acknowledges that copyright of published works contained within this thesis resides with the copyright holder(s) of those works. I also give permission for the digital version of my thesis to be made available on the web, via the University's digital research repository, the Library Search and also through web search engines, unless permission has been granted by the University to restrict access for a period of time.

Rajiv Mahajan
February 2014

Acknowledgements

I would like to thank Professor Prashanthan Sanders, my primary supervisor, for his mentorship and support during my doctoral training. I am particularly encouraged by his enthusiasm, originality of ideas, and the drive to lead projects successfully to completion. He has demonstrated the fine art in balancing a successful career as a clinician, scientist, teacher and a family person. I am also thankful to my co-supervisors, Prof Joseph Selva, Dr Anthony Brooks and Dr Pawel Kuklik for their guidance. I am grateful for the scholarship support from the University of Adelaide (Australian Post Graduate Award, Leo J Mahar Scholarship).

I cherish my clinical electrophysiology training at The Royal Adelaide Hospital with Prof Prashanthan Sanders, Drs Glenn Young and Kurt Roberts-Thomson. I also enjoyed working alongside co-fellows: Drs Dennis Lau, Muayad Alasady, Han Lim, Anand Ganesan, Rajeev Pathak and Darragh Twomey. I would like to convey special thanks to Drs Dennis Lau and Muayad Alasady for their guidance and support at difficult times during this incredible journey. Support from the following was also crucial: Drs Nicholas Shipp, John Wood, Jim Manavis, Chrishan Samuel, Shiv Thaigaimani, Melissa Middeldorp and Aimie Paukner. All these individuals contributed to a very productive & successful research environment. I am also thankful to the contribution made by Adam Nelson and Christopher Wong and the support from Loren Mathews and Dr Tim Kuchel at LARIF.

In particular, I am blessed by the understanding and unwavering support from my beloved wife, Kavita and our beautiful daughter Idhika who have walked every step with me in my pursuit of academia. I am also blessed to have the support and

blessings of our parents and siblings who have shared my tribulations and joys during this journey. Above all, I thank our great God for being so kind.

Publications and Communications to Learned Societies

Chapter 2

1. **Presentation:** Presented at the Annual Scientific Sessions of the Heart Rhythm Society, May 2013, Denver, USA and published in abstract form (Heart Rhythm 2013:10: S259).
2. **Presentation:** Presented at the Annual Scientific Sessions of the Heart Rhythm Society, May 2012, Boston, USA and published in abstract form (Heart Rhythm 2012; 9: S185).
3. **Presentation:** Presented at the Annual Scientific Sessions of Cardiology Society of Australia, August 2012, Brisbane, Australia and published in abstract form New Zealand (Heart, Lung and Circulation 2012; 21;S125)

Chapter 3

1. **Young Investigator Award Presentation:** Presented at the Annual Scientific Sessions of the Heart Rhythm Society, May 2013, Denver, USA and published in abstract form (Heart Rhythm 2013; 10: S484).
2. **Young Investigator Award, Ralph Reader prize Presentation:** Presented at the Annual Scientific Sessions of Cardiology Society of Australia and New Zealand, August 2013, Goldcoast, Australia and published in abstract form (Heart, Lung and Circulation 2013; 22:S1-2)
3. **Best Oral Abstract Presentation:** Presented at the Annual Scientific Sessions of the Asia Pacific Heart Rhythm Society, October 2013, Hong

Kong, Hong Kong and published in abstract form (Journal of Arrhythmia 2013; 29:i1-130)

Chapter 4

1. **Presentation:** Presented at the Annual Scientific Sessions of Cardiology Society of Australia, August 2012, Brisbane, Australia and published in abstract form New Zealand (Heart, Lung and Circulation 2012; 21;S109-110)
2. **Presentation:** Presented at the Annual Scientific Sessions of the Heart Rhythm Society, May 2012, Boston, USA and published in abstract form (Heart Rhythm 2012; 9: S405).

Chapter 5

1. **Manuscript:** Mahajan R, Kuklik P, Grover S, Brooks AG, Sanders P, Selvanayagam JB. Cardiovascular magnetic resonance of total and atrial pericardial adipose tissue: A validation study and development of a 3 dimensional pericardial adipose tissue model. Journal of Cardiovascular Magnetic Resonance. 2013;15;73
2. **Presentation:** Presented at the Annual Scientific Sessions of Cardiology Society of Australia, August 2012, Brisbane, Australia and published in abstract form New Zealand (Heart, Lung and Circulation 2012; 21;S233)
3. **Presentation:** Presented at the Annual Scientific Sessions of the Heart Rhythm Society, May 2012, Boston, USA and published in abstract form (Heart Rhythm 2012; 9: S413).

Prizes and Awards during Candidature

1. Best Oral Abstract (First prize), Asia Pacific Heart Rhythm Society, 2013.
2. Ralph Reader Young Investigator Award (First prize), Cardiology Society of Australia and New Zealand, 2013.
3. Young Investigator Award (First prize), Heart Rhythm Society, Denver, 2013.
4. SA Heart Research Award (First prize), Adelaide Australia, 2013.
5. Cardiac Society of Australia and New Zealand Travelling Fellowship: 2013
6. First prize, Nimmo Prize, Royal Adelaide Hospital Research Forum, Adelaide Australia, 2012.
7. International Postgraduate Research Scholarship (2011). *University of Adelaide*.
8. Australian Post Graduate Award (2011). *University of Adelaide*.
9. Leo J Mahar Electrophysiology Scholarship (2011). *University of Adelaide*.

Chapter 1

Literature Review

1.1 Atrial Fibrillation: background

Atrial fibrillation(AF) is the most common sustained arrhythmia in humans. Its prevalence is estimated to be 1% in the general population(1-3). The lifetime risk of developing AF at age 40 or older is one in four(4). AF is encountered more frequently with age, with the prevalence increasing to one in 10 in those aged older than 80 years(5). The prevalence of AF continues to rise and is projected to affect more than 10 million Americans by 2050(6). AF is rapidly overtaking other cardiovascular causes for hospitalization(7) and is responsible for a huge economic burden(8). AF results in a gamut of clinical sequel ranging from symptomatic distress , heart failure(9), to thromboembolic events(10) culminating in reduced quality of life(11), frequent hospitalization and increased mortality(11-13). Of these, thromboembolic events remain the most devastating complications of AF(10). Cardioembolic strokes are more severe, with greater disability and mortality(14). Recent data suggests a link between AF and cognitive decline(15-17). Recent data highlights that the risk of dementia is comparable in magnitude to stroke risk(16). As a potential consequence of these several morbidities, AF increases the risk of dying, 1.5- 1.9 fold, after adjusting for other cardiovascular factors(11,18).

AF is often associated with significant structural heart disease. The Framingham heart study identified several independent risk factors for AF. These are increasing

age (odds ratio (OR) 2.1 for men and 2.2 for women), diabetes (OR 1.4 for men and 1.6 for women), hypertension (OR 1.5 for men and 1.4 for women), congestive heart failure (OR 4.5 for men and 5.9 for women), myocardial infarction (OR 1.4 for men and 1.2 for women), and valvular disease (OR 1.8 for men and 3.4 for women)(19). After adjusting for the above risk factors, men were also found to have a 1.5 times greater likelihood of developing AF than women(19). Smaller studies have also identified atrial septal defects(20), pericardial disease(20), myocarditis(20), hypertrophic cardiomyopathies(21), conduction system disorders such as sinus node disease(22), thyrotoxicosis, alcohol use and pulmonary pathology as risk factors for AF. More recently genetic predisposition has been identified in some patients(23). AF can occur in the absence of structural risk factors and is considered "lone AF"(24,25). Although, recent evidence suggests that these patients also may not be without concurrent abnormalities(26-28). With the identification of novel risk factors like obstructive sleep apnoea(29,30) and obesity(29,31-33) in the last decade, this group of lone AF is shrinking further. Furthermore, there is familial aggregation in lone AF(34,35). While an association with the above conditions is recognized, the mechanisms of AF are still not completely understood.

1.2 Electrophysiological basis of AF

Over the last century much has been learned of the electrophysiological basis of atrial fibrillation, which has shaped our current understanding and management this arrhythmia.

1.2.1 Mechanisms of AF

As early as the turn of the 20th century, mechanisms underlying AF were hypothesized along two main themes- rapidly discharging ectopic foci and circus movement. In the first known experiments conducted by Mayer in 1906, he observed isolated rings of jellyfish muscle could sustain circulating activity for long periods of time(36). Mines(37,38) and Garrey(39), further developed the concept of reentry in independently performed experiments in cold blooded animal hearts. Following this, Lewis postulated that AF and atrial flutter could be attributed to a circulating reentrant wavefront that encroached on its own partially refractory tail(40,41). He proposed that the main difference between fibrillation and flutter was the degree and nature of the encroachment of the leading edge into the tail which was smaller in flutter, whereas greater and intermingled front and tail in AF. In the 1960s, Moe postulated the 'multiple wave hypothesis' for AF supported with computer modeling studies(42,43). More than a decade later, Allessie et al(44,45) proposed the concept of leading circle hypothesis and subsequently provided the first experimental proof for Moe's multiple wavelet hypothesis of AF. It differed from Mines' concept of re-entry that it explained re-entry in absence of an anatomical barrier and forced the crest of the leading wave to encroach on its own refractory tail. This concept remained the most acceptable explanation for functional re-entry until it was demonstrated to be inadequate to explain the dynamics of fibrillation(46). High resolution recording studies later demonstrated the drifting and meandering nature of circulating waves which could not be explained by the leading circle concept(47,48). Meanwhile, the concept of rotors generating spiral waves was developed via theoretical studies by Krinsky(49) and

Winfree(50,51) independently. The first experimental demonstration proof of a spiral wave in the heart was provided by Davidenko et al an isolated sheep ventricular muscle slice high-resolution optical mapping(48). The rotor concept differs from the leading circle hypothesis in several aspects, importantly, absence of refractory core which can allow the rotor to meander. More recently rotors have been mapped in humans (52); and ablation successfully targeted based on this information (53,54).

1.2.2 Left atrial dominance in AF

Schuessler et al. showed the transition of activation patterns characterised by multiple re-entrant circuits converted to a single, relatively stable, high-frequency re-entrant circuit that resulted in fibrillatory conduction in isolated canine right atrial preparations that with increasing concentrations of acetylcholine(55). Thereafter, not only dominant frequencies were found in the left atrium(56-58) but also that there was a significant left to right atrial gradient in fibrillatory intervals(58,59). Based on this, Mansour et al postulate that these of high frequency waves sources within the left atrium may act as drivers or a dominant rotor, which maintains AF(59). This was supported work demonstrating termination of AF on targeting areas with the shortest cycle length in the posterior LA in a canine rapid atrial pacing model of atrial fibrillation(60). Li et al have also provided evidence that there may in fact be intrinsic differences between the left and right atrium myocardium(61).

While these observations suggested left atrial dominant rotors, they could also be explained by the existence of multiple anatomical structures within the left atrium that result in greater fractionation of the wavelet and therefore higher frequency

waves(62). However, the demonstration of surgical isolation of the left atrium, resulting in sinus rhythm in the right atrium with persistent AF in the left atrium in half the cases provided support to the left atrium being the dominant location of rotors(63,64).

However recent data from mapping and ablation in humans suggest the presence of rotors in right atrium as well.

1.2.3 Importance of atrial foci in AF

While the concepts of the mechanism of AF were been developed in animal and computer models, seminal observations in humans led Haissaguerre et al (65) to propose that sources in thoracic veins, particularly the pulmonary veins, play an important role in initiation and maintenance of AF.

Clinically it is now apparent that the pulmonary veins not only result in ectopy but also atrial tachycardia and initiate atrial fibrillation(65-67). It was soon realized that patients who develop ectopy from the pulmonary veins frequently have more than one pulmonary venous source of ectopy(68,69). Based on these finding, PV isolation forms the integral part of AF ablation strategy today.

The atrial muscle fibers at the atrio-venous junction are variably arranged (sphincter like) and that the peripheral zones of these myocardial sleeves are variably associated with connective tissue(70-72). This creates regions of anisotropy and therefore substrate for micro re-entry. The electrophysiological consequences were supported by a study of the canine pulmonary veins, in which significant conduction delay correlated with myocardial fiber orientation producing non-uniform anisotropy and fractionated electrograms(73). Clinically this is confirmed with the observation of decremented conduction to the atrium

and the documentation of long fractionated electrograms in close juxtaposition to the sharp spikes within the pulmonary veins(74,75). Further histological evidence of cardiac conduction tissue within the pulmonary veins in embryonal stage suggests potential for automaticity(76). A higher incidence of DADs or EADs has been observed in PV cardiomyocytes in AT remodeling canine model further providing evidence that sustained atrial tachyarrhythmias may promote to PV firing(77,78). The evidence for the pulmonary veins to act as drivers comes from cardioversion studies in chronic AF where pulmonary vein ectopy re-initiate AF(79-81). Non-re-entrant focal activations have also been reported in the PVs of a canine model of pacing-induced sustained AF (82). However, PVs are not essential for AT-induced atrial tachyarrhythmia promotion in this model as resection of all PVs does not prevent atrial tachyarrhythmia inducibility in AT-remodeled LA preparations. High recurrence rate of AF during long term follow up persistent AF also suggest that non-pulmonary vein triggers may be important in this subset(83).

1.2.4 Substrate and triggers in the genesis of AF

With advances in our knowledge of AF, it is clear that AF results from a complex interaction of several mechanisms, which can be broadly classified as the triggers, initiators, and substrate. The triggers are varied yet do not initiate AF in the absence of an appropriate initiator or substrate. The initiation and maintenance of atrial fibrillation may depend on the uninterrupted periodic activity of a few discrete re-entrant sources, which propagates and interacts with anatomical and/or functional obstacles, leading to fragmentation and wavelet formation(84).

Once initiated a host of factors act as perpetuators to sustain AF. AF causes electrical and structural remodeling of the atrium and begets more AF(85).

1.3 Atrial remodeling and AF

Significant advances have been made in understanding the substrate underlying AF in the last two decades. Experimental and clinical studies have identified ionic, cellular and histological remodeling culminating into a substrate for AF. A great deal of understanding of the remodeling processes has emerged from preclinical models which can be broadly classified as atrial tachycardia remodeling models and atrial structural remodeling models. *Wijffel et al.* in the seminal work on chronically instrumented goats demonstrated electrical remodeling and put forward the concept of *'AF begets AF'*(85). Alteration in ionic currents and properties of cellular excitability resulting in *abbreviated ERP* was termed as '*electrical remodeling*'. Subsequently a '*different sort of remodeling*' involving *conduction abnormalities* and structural changes in atrial architecture, particularly *diffuse atrial fibrosis* was described in an experimental heart failure model. (86). These findings were subsequently confirmed to be the unifying feature of structural remodeling in other conditions, both in pre-clinical studies (87-91) and clinical studies (92-99).

1.3.1 Atrial tachycardia remodeling model

Wijffels et al. demonstrated experimentally that maintained AF modifies atrial electrophysiology to enhance AF vulnerability and persistence in chronically instrumented goats, positing that AF begets AF (85). Atrial burst pacing led to atrial ERP shortening, lack of ERP adaptation to rate changes and enhanced

perpetuation of AF. These changes in atrial refractoriness secondary to AF and in turn promoting AF have been termed as 'atrial tachycardia remodeling'. Atrial tachycardia remodeling has since been demonstrated in other large animal models (100,101). Rapid atrial rates cause dispersion of refractoriness, increased AF Inducibility and persistence.

1.3.1.1 Alteration in ion channel in atrial tachycardia remodeling

Atrial tachycardia remodeling alters Ionic currents and gene expression of ion channels. Rapid atrial rates causes intracellular Ca^{2+} overload(102). This in turn activates the Ca^{2+}-dependent calmodulin–calcineurin–nuclear factor causing transcriptional down regulation of I_{CaL} in an attempt to restore intracellular Ca^{2+}(103). The reduction in I_{CaL} is mediated by down regulation of $Ca_v1.2$ mRNA and protein expression (104,105). Reduction in I_{CaL} causes action potential duration (APD) shortening and reduced rate adaptation. In addition to this, atrial tachycardia causes spontaneous I_{KACh} channel opening (106). This further contributes to APD shorting. Abnormal channel phosphorylation by PKC has been described in chronic AF and result in increased I_{KACh} activity and APD abbreviation (107).

In addition to APD abbreviation, long-term rate-related remodeling is associated with conduction velocity slowing (108). This is thought to be mediated by down regulation of the Na^+ channel α-subunit expression, thereby resulting in a decreased Na^+ current (I_{Na}) (108). Rapid atrial activation over a period of time reduces transient outward current (I_{to}) and increases background inward-rectifier K^+ current (I_{K1} and I_{KACh}). This can modulate conduction by opposing early depolarizing currents and I_{Na} inactivation by hyperpolarizing atrial cells

respectively (104,106,109). Furthermore, decreased expression of gap junction proteins and their altered distribution are thought to contribute to conduction slowing (110).

1.3.1.2 Long term atrial tachycardia remodeling causes structural changes

Preclinical studies have shown that structural changes can develop after prolonged AT remodeling (111). This includes loss of myofibrils, accumulation of glycogen, altered mitochondrial shape and size, fragmentation of SR, and dispersion of nuclear chromatin are observed (112). Remodeling of the cellular ultrastructure develops progressively over 16 week of AF, and recovery remains incomplete 16 week post-AF (111,113).

Rapid ventricular response to AT and tachycardia-induced ventricular dysfunction may contribute to atrial stretch and fibrosis. This has been elegantly demonstrated in ovine model. In comparison to sheep with His bundle ablation and ventricular pacing, sheep with intact atrio-ventricular conduction and rapid ventricular response were associated with diminished atrial matrix metalloproteinase (MMP)-2, increased tissue inhibitor of metalloproteinase (TIMP)-2 expression, and more extensive atrial fibrosis and AF(101). Inhibition of the angiotensin pathway has been shown to suppress fibrosis and the development of persistent AF in sheep. Atrial fibrosis and structural changes have also been observed in a canine atrial tachypacing model in the absence of LV dysfunction (114). Canine atrial fibroblasts cultured in the medium from rapidly paced atrial cardiomyocytes adopt an activated myofibroblast phenotype, as indicated by increased α-smooth muscle

actin (SMA) protein expression (115). Furthermore, increased secretion of collagen and fibronectin by fibroblasts may explain increased atrial fibrosis with AT. In summary, maintained AF especially in the setting of tachycardiomyopathy may result in structural changes in addition to the electrical remodeling.

1.3.2 Atrial structural remodeling model

In contrast to ERP shortening with electrical remodeling, *slow and heterogeneous conduction* is the electrophysiological hallmark of structural remodeling and is represented by *atrial fibrosis* at the ultra-structural level and left atrial enlargement grossly. The importance of diffuse atrial fibrosis and conduction abnormalities within the atria for the substrate for AF was initially described in experimental heart failure (86). In this ventricular tachypacing canine model, the AF inducibility was increased, atrial refractoriness unchanged or increased with localized regions of conduction slowing occurring in association with marked interstitial fibrosis (86). Expansion of extracellular connective tissue, myolysis, alteration in myocyte size and hypertrophy are other features of structural remodeling. Atrial structural remodeling has been demonstrated in several pre-clinical studies evaluating substrate in heart failure(87), hypertension(88-90) and coronary artery disease(91,116). Consistent are the observations in several clinical studies that have studied the substrate predisposing to AF due to heart failure(92), sinus node disease(93), aging(94), hypertension(96), valvular heart disease(97,98), congenital heart disease(99), and sleep apnea(95). Interestingly, evaluation of patients with "lone AF(117)" has also demonstrated similar findings, suggesting the presence of under recognized(118) or novel risk factors.

1.4 Structural remodeling in common clinical substrates

Observations from the Framingham Heart study cohort have shown that cardiovascular risk factors like hypertension, diabetes, smoking , congestive heart failure, myocardial infarction, valvular heart disease, male gender and advanced age are associated with increased risk for AF (5,19). Atrial septal defect has also been shown to be associated with AF. Further studies have shown that obesity (29,31,32), obstructive sleep apnoea (29) and end stage renal disease (119) are independently associated with atrial fibrillation. In contrast to electrical remodeling, these disease processes have been associated with '*remodeling of a different sort'*. This type of remodeling as earlier described has been labelled as structural remodeling with conduction abnormalities and interstitial fibrosis being the prominent and constant features. Structural remodeling has been observed in animal models (86-89,91,116,120-122) and clinical studies (92,95,96,123) with a number of these clinical conditions associated with AF. They provide insight into the mechanism of structural changes that predispose to AF. The following section will discuss the structural remodeling with important risk factors for AF.

1.4.1 Age

AF is uncommon in individuals younger than 40 years. However, the lifetime risk of developing AF after the age of 40 is one in four (4). The estimated prevalence of AF increases from 2.3% in those older than 40 years to 5.9% beyond 65 years of age(124). After the age of 50years, the prevalence of AF doubles every passing decade, from incidence increasing from 0.5% at age 50 to 59 years to almost 9% at age 80 to 89 years (125). In fact, approximately 70% of individuals with AF are

aged 65 to 85 years. With increasing age, there is structural remodeling and increase in interstitial fibrosis (126,127). Aging is associated with increased regions of low voltage areas, electrograms fractionation and importantly conduction slowing and anisotropy (94,128-132). In one study, the increased electrograms fractionation correlated with age and occurred in regions of low voltage and conduction slowing (133).

1.4.2 Hypertension

Hypertension is one of the most common known risk factors for AF. Population based studies have demonstrated a robust association between hypertension and AF (5,19). Observations from the Framingham Heart Study show an increase risk of 1.5- and 1.4 –fold in men and women respectively. Similarly, analysis from the Women health Study cohort of initially healthy 34,221 women, BP was strongly associated with incident AF (134). In this study, systolic BP was a better predictor than diastolic BP. Systolic blood pressure levels within the non-hypertensive range were independently associated with incident AF even after adjusting for BP changes over time. The study hypothesized that this association with in the non-hypertensive range may have been secondary to unmeasured confounders in participants with low systolic BP, such as coronary artery disease. Increased brachial pulse pressure has also been shown to be an important determinant of the incidence of AF. Analysis from 5331 Framingham Heart Study participants showed that the incidence rates of AF were 5.6% for pulse pressure of 40 mm Hg or less (25th percentile) and 23.3% for pulse pressure greater than 61 mm Hg (75th percentile). After adjusting for other risk factors, pulse pressure was associated with an increased risk of AF (HR of 1.26 per 20-mm Hg increment). This has been

confirmed in another study evaluating the relationship between aortic stiffness indices and AF (118).

Observations from preclinical studies have shown that hypertension was associated with widespread conduction slowing, increased conduction heterogeneity, no change/ increase in atrial refractoriness, inflammation, atrial fibrosis and increase duration of induced AF (88-90). Similar conduction abnormalities have been confirmed in humans (96). The time course of development of these changes has been studied in an ovine model. In the 'one kidney one clip' hypertensive ovine model, hypertension was associated with early and progressive changes in atrial remodeling suggesting that short term elevated blood pressure may cause significant atrial remodeling suggesting timely intervention may be required to prevent such changes after onset of hypertension (88,89).

1.4.3 Congestive heart failure

Chronic heart failure was the strongest predictor for incident AF, with a nearly 5-fold risk in men and 6-fold in women in the Framingham Heart study (19). Not only is heart failure a strong predictor, the prevalence of AF increases with severity of heart failure. In clinical trials enrolling chronic heart failure patients, the prevalence of AF increased stepwise from 4% in functional class I (135), 10%-27% in class II-III (136,137), to 50% in class IV patients (138).

Chronic heart failure is associated with elevated left atrial pressure atria; dilatation and stretch. Atrial structural remodeling has been first described in an experimental heart failure canine model (86). In this ventricular tachypacing canine model, the AF inducibility was increased, atrial refractoriness unchanged

or increased with localized regions of conduction slowing occurring in association with marked interstitial fibrosis (86). Cessation of ventricular tachypacing allowed ventricular function and atrial dilatation to reverse completely with resolution of congestive heart failure. However, fibrosis persisted after 4 weeks of tachypacing cessation and so did the ability to induce prolonged AF (139). Similar changes have been observed in an anthracycline-induced non-ischemic heart failure ovine model (87). The electrophysiological substrate in human heart failure has been further characterised by Sanders and coworkers (92). They demonstrated increased atrial refractoriness, conduction slowing, sinus node dysfunction, increased fractionation, low voltage area and electrical scars in ischemic and non-ischemic cardiomyopathy.

Increased angiotensin II expression in heart failure promotes atrial interstitial fibrosis and structural remodeling that create areas of slowed conduction and heterogeneity in repolarization, serving as substrates for AF generation (140). Activation of the sympathetic nervous system causes abnormalities of atrial action potentials and automaticity that can trigger arrhythmias as well (141). Alterations in the matrix metalloproteinase signaling pathway have been shown to be associated with myocardial infarction related heart failure in rats (142). Heart failure causes profound changes in calcium handling in the atrial cardiomyocyte that promotes triggered activity and AF (143). Experimental CHF in canine tachypacing model selectively has been shown to decrease atrial I_{to}, I_{Ca}, and I_{Ks}, increase NCX current. This, in particular NCX increased current, may promote afterdepolarizations and triggered activity (144).

1.4.4 Mitral valve disease

Mitral valve stenosis and incompetence are both recognised risk factors for AF (19,145). There is 5% annual risk of AF with increased morbidity and mortality in patients with mitral valve incompetence over a 10 year follow up period (146). Other studies have reported greater progression to AF with mitral stenosis than with incompetence (147,148).

A preclinical study evaluating the AF substrate in a canine mitral regurgitation model has reported increased interstitial fibrosis and fibrosis (149). This was accompanied by glycogen deposition ultra-structurally. However the atrial conduction pattern and velocities were not significantly altered. The atrial refractory periods were increase. The authors explained the absence of conduction changes to potential subtlety of changes undetected by their epicardial mapping techniques. In keeping with this, the degree of interstitial fibrosis was modest as compared to heart failure model (86,144).

Electrical substrate for AF has been investigated in patients with mitral stenosis (97,98,150). John and co-workers have demonstrated no change/ elevated effective refractory periods, site specific conduction slowing, low voltage areas, electrical scarring in both left and right atria of patients with mitral stenosis (98). Of considerable interest, they also demonstrated that conduction velocity improved immediately after removing chronic stretch by mitral valvotomy in mitral stenosis. The improvement was maintained at when re-evaluated at 6 months (97).

1.4.5 Atrial septal defect

Atrial septal defect (ASD) is associated with atrial arrhythmias that may persist even after closure of these defects (151,152). ASD is associated with reduction in peak myocardial strain and strain rate which reached statistical significance for the right atria indicating there was decrease in reservoir function of the atria and increased atrial stiffness (153).

Left to right shunt associated with ASD results in right atrial stretch and result in electrical remodeling with modest increases in right atrial refractoriness, conduction delay at the crista terminalis, and sinus node dysfunction (154). Although the shunt in ASD is pre- tricuspid with predominant right heart overload, there is left atrial remodeling characterized by loss of myocardium, and electrical scar that results in widespread conduction abnormalities but with no change or an increase in ERP. These abnormalities were associated with a greater propensity for sustained AF (99).

ASD closure is associated with incomplete right atrial reverse remodeling with pre-closure RA size predicting degree of reverse remodeling (155). Similarly, electrophysiological abnormalities may not completely reverse after ASD closure (154).

1.4.6 Coronary artery disease

Myocardial infarction increases the risk of AF by 1.4 fold (19). In another study, both myocardial infarction and angina are associated with an increase AF risk of 3.6 and 2.8 respectively (156). AF is often encountered at the time of myocardial infarction and is associated with adverse prognosis (156-158). The occurrence of AF during the index myocardial infarction increases the risk of subsequent AF

(159,160). In fact, a number of post-mortem studies have demonstrated atrial infarction in patients who has AF complicating myocardial infarction (161,162). However, the pathogenesis of AF in myocardial ischemia is thought to be multi-factorial with ventricular dysfunction (163), pericarditis (164), increase atrial stretch (163,165,166), hypoxia (167,168) and neuro-hormonal changes (169) contributing to it . Recent data implicates an important role of atrial ischemia (170).There is evidence from a preclinical ovine study that atrial infarction results in greater atrial electrophysiological changes and propensity for AF and is the predominant substrate for AF (91). This study demonstrated reduced atrial refractoriness, slow and heterogeneous atrial conduction with atrial infarction that resulted in greater propensity for AF. Similar findings have been reported by other investigators in a canine model (116,171). An experimental study in a canine model has further shown increased spontaneous atrial ectopy associated with calcium handing and substrate for re-entry at the infarct border zone further elucidating the mechanism of atrial arrhythmias in chronic coronary artery disease (116).

1.4.7 Obstructive sleep apnoea

Obstructive sleep apnea (OSA) has been shown to be an independent risk factor for AF (30). OSA increases the risk of AF by 2.4 folds as compared to the control population. OSA commonly occurs in association with obesity; the latter being an important risk factor for OSA (172,173). Furthermore, there is a graded increase in the risk of OSA with increasing obesity. Patients with untreated OSA have also been found to have a higher incidence of recurrent AF after cardioversion than

patients with treated OSA or patients without OSA (217). Several studies have shown a strong association between OSA and AF (29,30,174,175).
Possible mechanisms by which OSA predisposes to AF include intermittent nocturnal hypoxemia and hypercapnia (176); enhanced sympathetic tone with surges in blood pressure during apneic episodes leading to left atrial stretch through pressure and volume overload (177,178); and increased oxidative stress and inflammatory signaling pathway activation contributing to left atrial remodeling and fibrosis (176,179). Blood pressure surges and left ventricular afterload due to sympathetically mediated vasoconstriction during an apneic episode may lead to left atrial enlargement. There is evidence from an experimental study in an obese rat model that forced inspiration induced acute atrial stretch and diastolic dysfunction may have an important role in predisposing to AF (122). Dimitri and co-workers have further described low voltage area, site specific and widespread conduction abnormalities and abnormal sinus node recovery in patients with OSA (95).

Several studies indicate that OSA may also be an independent factor for AF recurrence after catheter ablation (175,180). The likely mechanism could be the presence of AF triggers outside the PVs, recurrent acute and chronic atrial stretch related to apneic episodes or possibly more extensive arrhythmic substrate (181,182). The use of continuous positive airway pressure (CPAP) significantly reduces AF recurrence after ablation (181,183,184). In one such study, the CPAP therapy resulted in 71.9% AF free survival after AF ablation as compared to 36.7% AF free survival in control patients undergoing AF ablation (183).

1.4.8 Obesity

This risk factor is covered under a separate section 1.7.

1.5 Histological abnormalities with atrial structural remodeling

The altered cytokine milieu contributes to the alteration in atrial tissue structure resulting in a substrate for AF. These structural changes have not only been described with different risk factors but also with lone AF. Frustaci and coworkers described the presence of myocardial necrosis, myocarditis and fibrosis in septal biopsies of patients with lone AF (26). Atrial fibrosis, inflammation, myolysis, myocyte hypertrophy and altered gap junction protein expression and distribution have been described with risk factors for AF.

1.5.1 Atrial fibrosis

Atrial fibrosis is considered an important factor in the development of substrate for AF (185,186). Atrial fibrosis has been observed in both preclinical (88,89) and clinical studies (187-189) with structural heart disease and with lone AF (26) as well.

The cardiomyocytes are organized in bundles which are separated by perimysial fibrous tissue. Within each bundle, the muscle fibres are further separated from each other by endomysial fibrous tissue. Structural remodeling is associated with increased extracellular tissue volume in experimental models (89) as well in humans (187). Furthermore difference in endo-epicardial endomysial fibrosis has been shown to be associated with AF complexity and potentially progression to permanent AF in an experimental goat model (190). In addition to this increase in interstitial fibrosis, experimental canine model of congestive heart failure (86) has

demonstrated large areas of fibrosis, similar to “replacement fibrosis” secondary to tissue damage and cell death.

Atrial fibrosis alone may be sufficient to increase AF vulnerability (191). Although atrial fibrosis has been shown to be correlated with AF in post-operative patient, significant fibrosis may be seen in absence of AF (126). However the quantitative relationship between atrial fibrosis is still not clear. In addition it is not clear whether there is a ‘threshold effect’ exists for fibrosis beyond which it predisposes the AF. Despite the lacunae in the knowledge, experimental and clinical studies have shown that therapies directed at prevention of atrial fibrosis may delay development of substrate for AF (140,192,193).

1.5.2 Myocyte hypertrophy

Myocyte hypertrophy has been observed with structural remodeling in experimental rapid atrial pacing models (111), congestive heart failure (86) and right atrial dilatation (194). Spash and coworkers have demonstrated that cell hypertrophy, in contrary to the cable theory, would lead to conduction delays and anisotropy during transverse propagation (185,186). This finding explains the conduction disturbances seen with myocyte hypertrophy in absence of fibrosis in the experimental chronic AV block model (194).

1.5.3 Atrial architecture

Structural remodeling can accentuate the anisotropy in regions of strong preferential orientation like bundle of Bachmann, crista terminates and posterior left atrium. Increased fractionation has been described in these regions in congestive heart failure and sleep apnoea. With intrinsic anisotropy in these regions, structural remodeling predisposed to abnormal conduction.

1.5.4 Connexin expression and AF

Revel and Karnovsky described gap junctions for the first time in 1967 when they observed membrane associated particle aggregates that allowed tracer lanthanum hydroxide to pass through small gaps in them (195). These particle aggregates were located at the long ends of the cardiomyocytes, identified as intercalated discs (ID)(196). The primary component of these gap junctions were subsequently identified as a 43-kD protein and named connexin43 (Cx43) (197). The Cx43 were identified to be located primarily at the ID, staining as a straight line at the cardiomyocyte ends. However, on transverse sections of the ID, connexins stain as a ring demonstrating that the ID is not covered with gap junction proteins. The Cx43 is anchored to the ID by the zonula occludens-1 (ZO-1) (198). The gap junction proteins and their distribution are highly conserved across different species (199,200) and they are understood to act as electrical conduits between cells. Five different types of connexins are seen in the heart with Cx43, connexin-40 (Cx40) and connexin-45 (Cx45) being most abundant in the atria. Cx40 is distributed heterogeneously in the atria with greater expression in the right atrium. Cx43 is more homogeneously distributed. Unlike in the ventricle, the presence of several connexin isoforms in the atria may results in different types of gap junctions (heteromers / homomers of different isoforms) in the atrial make it difficult to interpret alteration of connexin expression and distribution of individual isoforms (201).

The degree of reduction in gap junction expression that can alter conduction is a matter of debate. Observations from a transgenic mouse model suggests a high degree of safety factor, with no alteration in atrial conduction velocity in Cx40

heterozygous mice and 30% reduction in Cx40 knockout mice (202). However, a reduction of a lesser degree of connexin expression creating conduction abnormalities at rapid rates during AF is potentially possible. Prolonged AF in a rapid atrial pacing goat model resulted in 60% reduction in Cx43 expression and this, unlike the expanded extracellular matrix, completely reversed after 4 months of sinus rhythm (113). Bikou and coworkers have reported that restoration of Cx43 protein to control levels by gene therapy prevented progression to persistent AF in a pacing induced AF porcine model (203). It is also hypothesized that alteration in distribution may alter transverse conduction predisposing to AF. Lateralization of Cx43 has been demonstrated in response to ischemia in the ventricle. Endothelin dependent reduction in connexin43 expression with reduction in conduction velocity has been described in a mouse model suggesting the possibility of endothelin system playing a role in creating a substrate for AF by altering Cx43 expression(204).

1.6 Atrial fibrosis and signal transduction alterations in atrial structural remodeling

Fibrosis occurs as a result of persistent tissue repair process due to dys-regulated profibrotic signaling pathways. During tissue repair, activated fibroblasts migrate to the injured tissue and synthesize and remodel newly laid extracellular matrix. The special type of fibroblast involved in the tissue repair is the α-smooth muscle expressing myofibroblast. Abnormal persistence of this myofibroblast is the *'sine quo non'* of fibrosis(205). Cardiac fibroblasts and myofibroblasts lack the ion channels necessary to initiate an action potential and are considered unexcitable.

Interstitial fibrosis is therefore postulated to increase AF vulnerability by causing separating muscle fibre resulting in slow and circuitous conduction promoting AF(206).

The signaling pathways that participate in atrial fibrosis are incompletely understood and their relative contribution governed by the inciting injury. Often a common feature to most disease processes is chronic stretch which activates these signaling pathways. Angiotensin II, Transforming growth factor β (TGFβ) and Endothelin pathways are the more established with emerging role of platelet-derived growth factor (PDGF) and matricellular protein connective tissue growth factor (CTGF). The TGFβ is central to the fibro-proliferative signaling pathways with endothelin pathway works downstream to both Angiotensin II and TGFβ in a highly interactive signaling network. Figure 1 shows the fibro-infiltrative signaling network.

1.6.1 Transforming growth factor β

There is robust data supporting the role of TGFβ1 in atrial fibrosis. Overexpression of constitutional TGFβ1 in transgenic mice led to selective atrial fibrosis, conduction heterogeneity and AF(191). TGFβ acts downstream to Angiotensin II and acts in a paracrine-autocrine fashion(207). Angiotensin induces the synthesis of TGFβ1 which in turn stimulates fibroblast to produce Angiotensin II.

TGFβ has three isoforms, the most important being TGFβ1. TGFβ1 acts primarily via the SMAD signaling pathway(208). It also activates a variety of noncanonical signaling pathways including: ras/MEK/ERK; p38(209); and c-Jun N-terminal kinase (JNK)(210). To activate the SMAD signalling pathway, it binds to TGFβ receptor type I (activin linked kinase [ALK]5) and type II receptor (TFGβR2) to

form a complex. ALK5 phosphorylates Smad2 and -3, which bind to Smad4, translocate into the nucleus, and activate transcription of target genes(208). Smad7, however, inhibits TGFβ signaling. Cross talk adds another level of complexity with mitogen activated protein kinases (ERK, JNK, p38) also phosphorylating SMAD proteins(211). TGFβ, in addition, induces fibroblasts to differentiate into α-SMA expressing myofibroblasts(212) with CTFG acting as a co-factor(213). When applied to fibroblasts, TGFβ directly induces ECM gene expression and promotes ECM deposition by simultaneously suppressing matrix metalloproteinase gene expression and inducing tissue inhibitors of matrix metalloproteinase gene expression (214). Experiments in SMAD3$^{-/-}$ fibroblasts(215) and intervention study in organculture model(216) have shown that SMAD3(215) and Activin(216) are essential for TGFβ1 mediated collagen deposition.

ALK5 inhibitor and TGFβ1 antibody have shown promise in animal models to supress TGFβ1 mediated fibrosis (217).

1.6.2 Angiotensin II

Angiotensin II (Ang II) has been studies in varies cardiac pathologies including hypertensive heart disease, myocardial infarction and congestive heart failure. Chronic atrial stretch increase atrial synthesis of Ang II. Ang II mediates fibrosis through the AT I receptor. The signaling pathways associated with AT I receptor are linked to G proteins and mediate fibrosis through mitogen activated protein kinases, viz., ERK1/2 (218) , JAK/ STAT 1,3(219) and Ang II/Rac1/STAT3 signaling pathways(220).

The signaling pathways of Ang II and TGFβ1 are interwined and act as part of an integrated signaling network to mediate fibrosis(221). Ang II upregulates TGFβ1

expression through the angiotensin type 1 (AT1) receptor in cardiac fibroblasts and cadiomyocytes(221). Ang II induces collagen in cardiac fibroblasts through TGFβ and ERK (222). In addition, Ang II has been shown to require TGFβ to be able to induce cardiac hypertrophy and fibrosis in vivo(223).

Angiotensin receptor inhibitors have been shown to be effective in suppressing cardiac fibrosis in animal models (224) and in humans (225).

1.6.3 Endothelin-1

There are 3 isoforms of Endothelin (ET), the most important being ET1 in humans. It is secreted predominantly from endothelial cells but is also expressed by epithelial cells, bone marrow mast cells, macrophages, polymorphonuclear leukocytes, cardiomyocytes, and fibroblasts. Endothelin is a vasoconstrictor with mitogenic properties, acting through 2 subtypes of receptors (ET receptor subtype A [ETA] and ET receptor subtype B [ETB]). Endothelin system acts downstream to TGFβ1 and activates the procollagen I promoter and collagen synthesis in fibroblasts (226). It also stimulates aldosterone release via ET-B receptor (227). ET1 induces ECM production and in association with TGFβ1 promotes differentiation of fibroblasts to myofibroblasts (214,228). However, constitutive ET signaling, operating through an ALK5 (TGFβ superfamily) - independent mechanism, is also responsible for the persistent myofibroblast phenotype of fibrotic lung fibroblasts (229). Moreover, Ang II also induces ET-1 via ERK and reactive oxygen species (230). These results suggest that ET operates downstream of both TGFβ and Ang II pathways in the fibrosis signaling network.

Previous studies in hypertensive and heart failure rat models have shown that the effect of cardiac fibrosis is mediated through the ET-B receptor (231,232). Since there are no truly selective ET-B receptor blockers available, the effect has been

observed by subtraction i.e. intervention with non-selective blockers prevented fibrosis while ET-A receptor blockers did not prevent fibrosis (231). Considering the dowmstream position of ET1 in the signaling network, ET receptor antagonism represents a potential candidate as an inhibitor of atrial fibrosis.

1.6.4 Connective tissue growth factor

CCN2 is a matricellular protein which promotes angiogenesis (213). CCN2 acts through various integrins and HSPGs or receptor trkA to promote cell adhesion (213). CCN2 is induced by TGFβ1, Ang II and ET1 and is potentially a downstream mediator of these proteins (214,233). CCN2 acts as a cofactor with TGFβ1 to induce fibrogenesis (234,235). CCN2, on its own accord, is weakly fibrogenic. However, CCN2 enhances the ability of TGFβ1 to induce (236,237). CCN2 is not essential for all of TGFβ's actions, but in constitutively expressing CCN2 mouse embryonic fibroblasts, it is vital for TGFβ to maximally induce type I collagen and α-SMA mRNA and protein (235,237). Though direct evidence functionally linking CCN2 to cardiac disease is sparse, CCN2 has been shown both in vitro and in vivo to cause hypertrophy of rat cardiomyocytes (236).

1.6.5 Platelet derived growth factor

PDGF consist of a family of growth factors comprising PDGF-AA, PDGF-AB, PDGF-BB, PDGF-CC, and PDGF-DD (238). There are 2 different PDGF receptors, α and β. PDGF stimulates proliferation and differentiation of fibroblasts and pericyte migration to the injury site. PDGF receptor inhibitor imatinib mesylate has been shown to delay wound closure by predominantly by inhibiting fibroblast proliferation and migration and pericyte migration in a collagen type I transgenic reporter mouse (239). The gene expression of PDGF and its receptors is stronger

in the atrial than ventricular rat fibroblasts and PDGF receptor inhibition exerts greater suppression atrial myofibroblast suppression (240). PDGF has been shown to up regulate TGFβ mRNA in rat cardiac allografts, thereby demonstrating the close interaction of profibrotic signaling molecules (241).

1.6.6 Oxidative stress and Inflammation

There is preclinical and clinical evidence to suggest that inflammation plays an important pathological role leading to fibrosis in several cardiovascular conditions (242-244). Liu et al conducted a systematic review and meta-analysis to examine the association between baseline CRP and recurrence of AF after successful electrical cardioversion (245). Seven prospective studies with 420 patients were analyzed. Overall, baseline CRP levels were greater in patients who experience a recurrence of AF. Similarly, Aviles et al showed in a prospective cohort study that, with regards to baseline CRP, patients in the highest quartile had an odds ratio of 1.8 compared to those in the lowest quartile, for having atrial fibrillation (246). The risk of atrial fibrillation persisted even after adjusting for relevant variables. Despite this evidence whether inflammation is the cause or effect of atrial fibrillation is not clear. The high rate activity of AF may lead to myocyte calcium overload and in some cases to the initiation of apoptotic loss of atrial myocytes (247). CRP has been shown to act as an opsonin and may participate in the clearance of apoptotic myocytes (248). Myocyte loss is typically accompanied by replacement fibrosis. This low-level inflammatory response may thus be part of the structural remodeling process associated with persistence of AF (249). Alternatively, the inflammatory state may predispose to the frequent triggering of the foci in the pulmonary veins. It is well established that baseline CRP is related to metabolic syndrome and vascular risk.

In addition to elevation of CRP, AF is considered to promote AF with evidence arising from experimental (242) and human studies (242,243) showing an association between chronic AF and elevated atrial oxidative stress and peroxynitrite formation. Rapid atrial pacing has been shown to be associated with increased activity of matrix metalloproteinases (MMP 2, 9) and its tissue inhibitor (TIMP1, 3) in a porcine model (250).

Cardiovascular disease mediated tissue injury result in secretion of proinflammatory cytokines and hormones, such as tumour necrosis factor (TNF α), interleukin 6 (IL6), interleukin 8 (IL8). These cytokines promote activation of leucocytes with subsequent release of cytokines and reactive oxygen species (ROS) (251). Inflammatory stimuli such as myeloperoxidase (MPO), nicotine adenine dinucleotide phosphate (NADP) oxidase, and ROS are established triggers of fibroblast proliferation, migration and differentiation into myofibroblasts, which are important players in development of fibrosis. Leucocyte derived haeme enzyme myeloperoxidase (MPO), via generating hypochlorous acid, has been shown to be a critical regulatory switch modulating matrix metalloproteinases (MMP), a key enzyme in extracellular matrix (ECM) turnover leading to atrial fibrosis (250,252). MPO mediated MMP activity regulation is an important contributor to increased extracellular matrix (ECM) and atrial fibrosis. MPO increases NADPH oxidase related ROS production which in turns enhances expression of Rac 1. The Rac1 protein, a member of Rho GTPase superfamily and a target for statins, mediates upregulating of CTGF, fibronectin and transcriptional factors involved in collagen deposition.

The histological proof for the role of inflammation in AF was first provided by *Frustaci et al* (26). They demonstrate the presence of inflammatory infiltrates in

atrial septum biopsy of patients with atrial fibrillation (26). Patients with history of AF have also been shown to have inflammatory $CD45^{+}$ cell infiltration in the atrial myocardium as compared to those without history of AF (253).

1.6.7 Matrix metalloproteinase proteins (MMP) and tissue inhibitor of MMP (TIMP)

MMPs are a family of zinc-dependent endopeptidases that are essentially involved in extracellular matrix (ECM) protein degradation by cleavage of internal peptide bonds. They are secreted by a variety of endothelial cells, monocyte derived- and tissue macrophages. MMP-1, -8, -13 and -18 are collagenases that cleave interstitial collagen I, II and III at a specific site and also cleave other ECM and non-ECM molecules. The fragments of collagen are then degraded by gelatinases (MMP- 2 and -9). They are responsible for type IV collagen degradation. Stomelysins (MMP-3) degrade fibronectins, laminin, gelatins I, III, IV and proteoglycans. MMPs activity is regulated by tissue inhibitors of MMP (TIMPS). An abnormal increase in MMP activity results in degradation of the matrix proteins(254,255) while TIMPs directly inhibit the proteolytic activity of MMPs by binding to them (256).
Several clinical and preclinical studies in AF have focussed on altered MMP and TIMP expression heart failure and myocardial infarction (257-259). MMP-9 protein level was up-regulated and TIMP-1 protein level down-regulated in a canine model with AF as compared to controls (260). The MMP-9 activity was increased in a rapid atrial pacing canine model (261). Similarly, up-regulation of MMP-9, TIMP-1 and -3 was reported in a rapid atrial pacing porcine model (250). Similar changes in MMP-9 and TIMP-1 activity has been confirmed in clinical studies. Atrial ECM remodeling in conjunction with up-regulation of MMP-2 and

down-regulation of TIMP-2 have been associated with development of sustained AF in patients with cardiomyopathy and heart failure (262).

1.7 Obesity

The risk factors for AF have a common feature of 'atrial stretch' which causes structural remodeling and predisposes to AF. The presence of structural and electrical remodeling in patients with apparently 'lone AF' could suggest the presence of unknown risk factors. Obesity has been identified as a risk factor for AF only in the last decade. Considering the obesity epidemic, this risk factor is of considerable public health importance.

Obesity has been a rampant epidemic with more than one third of the population being overweight or obese. The prevalence of obesity in some parts of the western world has increased by 50% over the last few decades with 75% of adults over 40 years being classified as overweight or obese (263). Obesity is associated with several co-morbidities like diabetes, hypertension, obstructive sleep apnea and sleep related disorders, ventricular hypertrophy, left atrial enlargement and congestive heart failure. Several studies have reported an association between obesity and stroke. For every 1 unit increase in BMI there was a 4% increase in ischemic and 6% increase in haemorrhagic stroke (264).

1.7.1 Obesity and Atrial Fibrillation- the epidemiologic link

The increasing prevalence of AF despite the improved prognosis of hypertension, coronary artery disease and heart failure, has been attributed to the aging population. However, there is evidence that obesity is contributing to it. Analyses of the Framingham Heart study and Women Health Study suggest that obesity is

associated with long term increased risk of AF independent of other traditional risk factors (31,32). This has been confirmed in other population based studies (29,265,266). The study from Mayo clinic in particular demonstrated that the risk of developing incident AF was additive for obesity and obstructive sleep apnea (29). This is important considering the close association of obesity and sleep apnoea. In a meta-analysis performed by Wanahita and co-workers, they reviewed 16 studies enrolling 123,243 patients to assess the impact of obesity on AF (33). In the subgroup of 5 population-based cohort studies enrolling 78,602 patients, obese patients had a 49% increased risk of developing AF that rose with increasing BMI. On the other hand, post-cardiac surgery studies enrolling 44,647 patients failed to show an increased risk of AF in obesity, possibly suggesting an alternative mechanism. Importantly, there was a graded 'dose-response relationship' in the general population cohort with the relative risk of developing AF incrementally rising from 1.3% to 2.1% to 3.2% in the normal weight, overweight and obese population respectively (33).

1.7.2 Obesity mediators of Atrial Fibrillation

Obesity is closely association with obstructive sleep apnea, components of metabolic syndrome namely hypertension and diabetes mellitus, and coronary artery disease and congestive heart failure. This clouds the elucidation of the mechanistic link between obesity and AF. Nonetheless, left atrial enlargement, direct lipotoxicity and inflammation and excessive activation of signaling pathways have been hypothesized to mediate the effect of obesity in creating a substrate for AF.

1.7.2.1 Left atrial enlargement and diastolic dysfunction

Data from the Framingham Heart study suggest that left atrial enlargement and diastolic dysfunction may be the mediators of atrial fibrillation (31). A substudy of Framingham Heart study, demonstrated that with every 5mm rise in left atrial diameter, there was a corresponding increase in risk of AF by 39% (267). In a study of 5,881 Framingham Heart Study participants, Kenchaiah et al. demonstrated a graded increase in the risk of HF was observed across all categories of BMI (268). During a 14-year follow-up, the risk of heart failure increased 5% in men and 7% in women for every 1 kg/m2 increment in BMI (268).

1.7.2.2 Inflammatory milieu

Histological studies have demonstrated the presence of inflammation in biopsies of patients with isolated AF (26). It is well-established that several cardiovascular diseases, such as coronary artery disease and hypertension, involve an inflammatory mechanism. A recent study has demonstrated inflammatory infiltrates in atrial tissue with short term weight gain in an ovine model (121). Obesity has been shown to be associated with over expression of the endothelin (269) and TGFβ superfamily (270,271) signalling pathways. An experimental study has demonstrated increased expression of endothelin receptors with short term weight gain (121).

1.7.2.3 Direct Lipotoxicity

Knockout Zucker rat model (leptin receptor deficient) and acyl-CoA sythetase deficit models have demonstrated the accumulation of triglycerides in the myocardial cells with lipo-apoptosis and replacement fibrosis (272,273).

1.7.2.4 Obstructive sleep apnea

OSA is often commonly associated with obesity (172,173) and the data from Mayo clinic suggest additive effect of both OSA and obesity on the risk of developing new AF (29,30). Intermittent hypoxia and hypercapnea (176), forced inspiration induced acute atrial stretch (122), autonomic surges (177,178) are the likely mechanism by which OSA predisposes to AF.

1.7.3 Electrical remodeling in obesity

A preclinical study has demonstrated conduction slowing, fibrosis without alteration of the atrial refractory periods with progressive weight gain (121). A human study has shown similar findings with slower conduction from the LA entering into the pulmonary veins in obese patients undergoing AF ablation (123).

1.7.4 Pericardial fat and Atrial Fibrillation

Evidence is mounting that pericardial lipid, which surrounds the heart, may also play a significant role in the development of both cardiac and vascular disease. While population based studies have reported the association between obesity and AF using BMI, there are reports to suggest that pericardial fat measures are more precise in predicting AF than the traditional measures of obesity (274,275). Data from the Framingham Heart Study Offspring and Third Generation Cohorts involving over two thousand participants, Thanassaulis et al measured pericardial fat with computed tomography (CT) and showed that each SD increase in pericardial fat volume increased AF risk 1.28 fold independent of other measures of adiposity (276). Total pericardial fat, but not the intra-thoracic or visceral fat was associated with AF. In keeping with this, Batal et al, studied 169 consecutive patients with CT angiograms for either coronary artery disease or AF and

demonstrated that posterior LA fat thickness predicted AF burden, independent of LA area and body mass index (277). In this study, a 10mm increase in posterior LA fat thickness was increased the risk of AF by 6.06 fold. The association between cardiac ectopic fat depots and AF was further confirmed by Al Chekakie et al, who demonstrate that pericardial fat volume (CT) was associated with AF with an OR of 1.13 (for every 10ml increase in pericardial fat volume) after adjusting for BMI and other risk factors (278). Wong and co-workers studied pericardial fat with cardiac magnetic resonance (CMR) in 130 patients and reported the association between pericardial fat volumes with prevalence and severity of AF(274). In this study, both periatrial fat (odds ratio 5.33, 95% CI: 1.25-22.66; p=0.02) and periventricular fat (odds ratio 11.97, 95% CI: 1.69 to 84.88; p=0.01) were predictive of AF after adjusting for other risk factors and BMI. Recently, Shin et al also reported that CT measured epicardial fat volume and peri-atrial fat thickness were associated with prevalence and chronicity of AF(279). The term 'pericardial and epicardial fat' has been used interchangeably in AF literature, with some studies defining pericardial fat as fat inside the pericardial sac(276,278) while others defining pericardial fat as a sum of epicardial (fat inside pericardial sac) and paracardial adipose tissue (outside pericardial sac) (274) and others reporting epicardial fat (fat inside pericardial sac) (279). Nonetheless, these studies have shown that cardiac ectopic fat depots predict the presence and severity of AF independent of the traditional measures of obesity. More recently, Nagashima and co-workers have shown a spatial relationship with epicardial fat with high dominant frequency sites but poor correlation with complex fractionated signals(280).These studies has evoked interest into the mechanism by which local cardiac fat deposits create a substrate for AF.

As adipose tissue is highly vascular, it has been hypothesized that mediators of lipid metabolism and inflammation may be supplied by the pericardial adipose tissue surrounding the heart, thereby directly affecting cardiac function in a site-specific manner. Venteclef et al have provided insights in the mechanistic link between epicardial fat and AF substrate. They performed experiments in an rat organo-culture model and demonstrate atrial fibrosis in rat tissue incubated with a secretrome isolated from human epicardial fat (216). They then performed an intervention showing that the fibrosis is mediated by activin A, a member of the TGFβ superfamily. In summary, there is indirect evidence to suggest that pericardial fat is metabolically active and may act in a paracrine fashion to create a substrate for AF.

1.7.5 Weight reduction and risk of atrial fibrillation

Analyses from the Women health study have shown that the risk for incident AF changes with alteration in weight (32). The women in whom obesity developed during follow-up in the study showed a significant 41% increase in AF risk compared with women who maintained a BMI <30 kg/m2. This increased risk even exceeded the risk of women who were obese at baseline and remained obese. In contrast, the AF risk of women who were obese at baseline but lost weight and reached a BMI <30 kg/m2 during follow-up did not differ from the risk of women who were non-obese at baseline and remained non-obese during follow-up. Although the strength of the latter analysis is somewhat limited by the relatively small number of subjects (n - 599) who lost weight during follow-up, these findings suggest a potential reversibility of the obesity associated AF risk increase. Moreover, the authors estimated the proportion of the observed AF cases that

were attributable to short-term BMI increases and found that this proportion was significant (18%).

Although the reversibility of risk for AF was suggested by this study, the underlying mechanism is unclear. Reversal of electrophysiological substrate has been scarcely studied. In addition, degree of reversibility with removal of inciting factor or intervention in previous studies has been variable and not fully characterized. Improvement in conduction abnormalities with reduced fractionation has been previously demonstrated following mitral commissurotomy in mitral stenosis and this was associated with decreased propensity to AF(97). However, another study reported persistence of conduction abnormalities in right atrium after closure of atrial septal defect (154). Reversibility of substrate has been addressed in an experimental heart failure canine model, which demonstrated extensive electrical abnormalities and atrial fibrosis with 5 weeks of ventricular tachypacing (139). In this study, despite the reversal in atrial size and AF inducibility over the next five weeks of recovery, the atrial fibrosis persisted. However, the study was limited by the short period of recovery phase. The degree of recovery may depend on the underlying inciting factor, extent of changes and degree of removal of the inciting factor.

This thesis examines the mechanism of development of substrate for AF in an ovine model of sustained obesity, a state more analogous to human obesity. The changes occurring at the electrophysiological, histological and molecular level are evaluated. Following this, the effect of weight reduction on the AF substrate in sustained obesity is examined. The latter half of the thesis evaluates the AF substrate in humans with focus on the role of pericardial fat in electroanatomic remodeling. The cardiac MRI measures of pericardial fat were also validated.

Figure 1 Signaling pathways in fibrosis

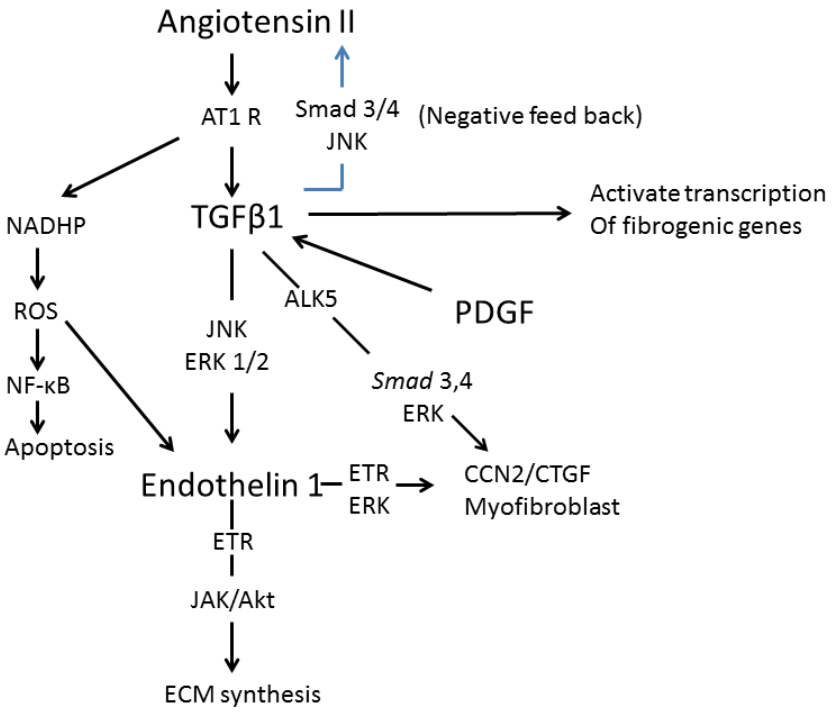

Chapter 2

Electrophysiological, electroanatomical and structural remodeling of the atria as a consequence of sustained obesity

2.1 Introduction

Obesity is a rampant epidemic with more than one third of the population being overweight or obese(263). Similarly, atrial fibrillation is an important heath problem especially in the aging population. It is estimated that nearly 1% of the population suffers from atrial fibrillation and the prevalence is projected to increase 2.5 fold by 2050.(2,3,7) Atrial fibrillation is an independent risk factor for stroke and causes significant cardiovascular morbidity in the form of congestive heart failure and impaired quality of life.(10,281,282). Thus obesity and atrial fibrillation are two important present day public health issues.

The increasing prevalence of atrial fibrillation has been previously attributed to the aging population. However, emerging evidence over the last decade has observed that aging alone does not account for the exponential rise in the prevalence of AF.(6) It is in this setting that new risk factors such as obesity have been proposed as important contributors to the epidemic of atrial fibrillation. Analysis of the Framingham Heart study, Women Health Study and other population based studies suggest that obesity is associated with long term increased risk of AF independent of other traditional risk

factors.(29,32,266,283,284) In a recent meta-analysis by Wanahita et al, there was a graded 'dose-response relationship' in the general population cohort with the incidence of developing atrial fibrillation incrementally rising from 1.3% to 2.1% to 3.2% in the normal weight, overweight and obese population respectively.(33) The mechanism by which obesity predisposes to AF is confounded by the coexistence of obstructive sleep apnea, hypertension, diabetes and coronary artery disease, all well-established pre-cursors for the development of atrial fibrillation; thereby clouding interpretation in population based studies. We have previously shown using limited epicardial mapping conduction slowing and atrial fibrosis with short term weight gain in an open chest ovine model(121). In the present study we investigate the global endocardial electrophysiological structural changes with sustained obesity, a state more comparable with humans.

2.2 Methods

All animal handling was conducted in accordance to the guidelines for use and care of animals for research by the National Health and Medical Research Council of Australia on research animal use. The study was approved by the Animal Research Ethics Committee of the University of Adelaide and SA Pathology, Adelaide, Australia.

2.2.1 Obese Ovine Model

A total of 10 sheep had obesity induced through a previously described protocol based on ad-libitum regimen of hay and high energy pellets, was utilized to induce progressive weight gain.(285) At baseline, healthy sheep were commenced on a high caloric diet of energy-dense soybean oil (2.2%) and molasses fortified grain

and maintenance hay with weekly weight measurement. Excess voluntary intake was predominantly of grass alfalfa silage and hay. For the obese sheep, pellets were gradually introduced at 8% excess basal energy requirements, and rationed to ≥70% of total dry matter intake. Blood samples were periodically collected to ensure electrolyte and acid-base homeostasis. The sheep gradually gained weight to peak obesity in 36 weeks and were subsequently maintained in this state for 36 weeks.

2.2.2 Control Group

Ten age-matched sheep were maintained as controls at their baseline weight. To do this, high quality hay was provided ad-libitum, while energy dense pellets were rationed at 0.75% of live weight to maintain weight. Nutritional content of food and housing conditions were identical between both groups, but only the amount of food intake was varied.

2.2.3 Study Preparation

Animals were pre-acclimatized for at least one week prior to any surgery. Shorn weight was recorded immediately prior to surgery.

2.2.4 Body Composition

The Dual-energy x-ray absorptiometry (DEXA) scan was performed to determine total body fat in the animals. The DEXA scan was performed under general anesthesia.

2.2.5 Transthoracic echocardiography

An echocardiogram was performed under general anesthesia prior to the electrophysiology study. The left atrial dimensions were measured in apical 4-

chamber view. The left ventricular dimensions were measured in M-Mode in parasternal long axis view at the level of mitral leaflet tips. The left ventricular dimensions were utilized for determination of global left ventricular function by Teicholz formula.

2.2.6 Hemodynamic assessment

Invasive blood pressure monitoring was performed during the electrophysiology study. Left atrial, right atrial and pulmonary artery pressures were recorded.

2.2.7 Electrophysiological study

Electrophysiological study was performed in the post absorptive state under general anesthesia. A 10-pole catheter with 2-5-2 mm inter-electrode spacing (Daig Electrophysiology, Minnetonka, MN) was positioned in the coronary sinus with the proximal bipole positioned at the ostium of coronary sinus in the best left anterior oblique view. A conventional transeptal puncture was performed using an SLO sheath and a BRK1 needle (St Jude Medical) using fluoroscopic and pressure monitoring to access to the left atrium.

Surface electrocardiogram (ECG) and bipolar endocardial electrograms were continuously monitored and stored on a computer based digital amplifier/recorder system for off-line analysis (LabSystem Pro, Bard Electrophysiology, Lowell, MA, USA). Intracardiac electrograms were filtered from 30 to 500 Hz, and measured with computer assisted calipers at a sweep speed of 200 mm/s.

2.2.8 Electroanatomical mapping

Electroanatomic maps of the right and left atrium was created during sinus rhythm and pacing from proximal CS (CL 300ms) using the CARTO XP mapping system and a 3.5-mm tip catheter (Navistar, Biosense Webster, Diamond Bar, CA, USA). The electroanatomic mapping system has been previously described in detail(286); the accuracy of the sensor position has been previously validated and is 0.8 mm and 5°. In brief, the system records the surface ECG and bipolar electrograms filtered at 30 to 400 Hz from the mapping and reference catheters. Endocardial contact during point acquisition was facilitated by electrogram stability, fluoroscopy, and the catheter icon on the CARTO system. Points were acquired in the auto-freeze mode if the stability criteria in space (≤6mm) and local activation time (LAT; ≤5ms) were met. Mapping was performed with an equal distribution of points using a fill-threshold of 15 mm. Editing of points was performed offline. Local activation time was manually annotated to the peak of the largest amplitude deflection on bipolar electrograms. In the presence of double potentials, the LAT was annotated at the largest potential. If the bipolar electrogram displayed equivalent maximum positive and negative deflections, the maximum negative deflection on the simultaneously acquired unipolar electrogram was used to annotate the LAT. Points were excluded if they were not conforming to the surface ECG P-wave morphology or if they were < 75% of the maximum voltage of the preceding electrogram. Regional atrial bipolar voltage and conduction velocity were analyzed offline and are detailed below.

2.2.9 Effective Refractory Period

Effective refractory period (ERP) testing was performed after the electroanatomic mapping. Atrial ERPs were evaluated at twice the diastolic threshold at cycle lengths (CLs) of 450 and 300ms using an 8-beat drive train followed by an extra-stimuli (S_2), starting with an S2 coupling interval of 120ms increasing in 10ms increments. The ERP was defined as the longest coupling interval failing to propagate to the atrium. ERP was measures from the following 7 sites: (1) right atrial appendage, (2) right atrial lateral wall- upper, (3) right atrial free wall-lower, (4) proximal CS, (5) distal CS, (6) left atrial appendage and (7) left atrial posterior wall. ERP was measured 3 times at each cycle length at each site and averaged. If ERP varied by more than 10ms, an additional 2 measurements were made and the total number averaged. ERP heterogeneity was determined by the coefficient of ERP variation at each cycle length (CoV = SD/mean × 100%).

2.2.10 Atrial conduction velocity

Isochronal activation maps (5-ms intervals) of the atria were created and regional conduction velocity determined in the direction of the wave-front propagation (least isochronal crowding). The CARTO system determines conduction velocity by expressing the distance between 2 points as a function of the difference in local activation time. For analysis, each atrium was segmented as previously described.(92,99) The mean conduction velocity for each segment was determined by averaging the conduction velocity between 3-5 pairs of points, as previously described.(92,99)

The proportion of points demonstrating delayed conduction was determined using the following definitions: 1) fractionated signals: complex activity of 50ms

duration with 3 or more deflections crossing baseline; and 2) double potentials: potentials separated by an isoelectric interval and the total electrogram duration ≥50ms. (92,99)

2.2.11 Atrial voltage

For the purpose of evaluating regional bipolar voltage, the atria were segmented as above. For each region the mean voltage was obtained by determining the mean of the bipolar voltage of the points within the given region. The global voltage of the chamber was obtained by calculating the mean of the means of the different segments. An index of heterogeneity of the bipolar voltage amplitude was determined by calculating the coefficient of variation of the different regions in each chamber. Low voltage areas were defined as three contiguous points with a bipolar voltage <0.5 mV. Electrically silent areas (scar) was defined as three contiguous points with absence of recordable activity or a bipolar voltage amplitude <0.05 mV (the noise level of the system).

2.2.12 AF vulnerability and duration

AF vulnerability was assessed during ERP testing. Atrial fibrillation was defined as irregular atrial activity lasting at least 2 seconds. AF lasting more than 10 minutes was considered sustained; when this occurred no further data was acquired.

2.2.13 Histological assessment

The animals were euthanized following the electrophysiology study. Isolated atrial tissues from the left atrial posterior wall (LAPW) and left atrial appendage (LAA) of the control, obese and weight loss sheep were perfusion-fixed with 4% paraformaldehyde and immersed in 10% buffered formalin. Sections were processed and embedded in paraffin. From each site at 1cm intervals, 5μ serial

sections were then taken from each block and stained with hematoxylin and eosin and Masson's trichrome. In addition, samples were frozen at -70^{o}C.

Fatty infiltration of atrial muscle by epicardial fat: The fat infiltration of the atrial muscle from the epicardial fat was evaluated in low power (X1.25) magnification with hematoxylin and eosin (HE) staining. Fatty infiltration of the atrium by the overlying epicardial adipose tissue was graded 1-3 based on severity.

1. None or focal infiltration of adjacent outer third of the atrial muscle layer by the overlying epicardial adipose tissue.
2. Coalescent infiltration of outer third and/or focal infiltration up to the middle third of the atrial muscle layer.
3. Coalescent infiltration extending from the epicardial adipose tissue to the middle or inner third of the atrial muscle layer.

Fibrosis assessment: Morphometric analysis of Masson's trichrome-stained sections was performed utilizing 'analySIS LS Professional' software (Olympus Soft Imaging Solutions, Münster, Germany) to obtain a quantitative estimate of collagen within the tissue. Stained sections from LAPW and LAA from of 6-8 animals per group were digitally captured (from 5 random fields per section using NanoZoomer Digital Pathology System software (Hamamatsu Phonetics, Japan); at a magnification of x5) with an area of Masson's trichrome selected for its colour range and the proportional area of tissue with this range of colour quantified, as previously described(89).

Atrial TGFβ1 assessment: Western blotting was used to assess changes in TGFβ1 tissue concentration in left atrial myocardium. TGFβ1 concentration in atrial tissue was assessed with western blot. Cells were sonicated in homogenization buffer

(20mM Tris-HCl, pH 7.4, 25oC; containing 2mM EDTA, 0.5mM EGTA, 1mM dithiothreitol, 50μg/ml leupeptin, 50μg/ml pepstatin A, 50μg/ml aprotinin and 0.1mM phenylmethylsulphonyl fluoride). An equal volume of sample buffer (62.5mM Tris-HCl, pH 7.4, containing 4% SDS, 10% glycerol, 10% β-mercaptoethanol and 0.002% bromophenol blue) was then added and samples were boiled for 3 minutes; protein concentrations in each sample were equalized according to the method of Bradford(287).

Electrophoresis was performed using a Mini-PROTEAN® TGX™ precast gel system (Bio-Rad Laboratories Pty Ltd, Gladesville, New South Wales, Australia). Denaturing polyacrylamide gels (10% w/v) were employed for protein separation, which was undertaken as described previously(288). After separation, proteins were transferred to polyvinylidine fluoride (PVDF) membranes for immunoprobing (Bio-Rad Laboratories Pty Ltd). Membranes were incubated with antiserum for TGF-β1 overnight (1:1000), and labeling carried out using a two-step detection procedure: first, biotinylated secondary antibody (Vector Laboratories; 1:500; 30 minutes) was reacted with membranes and then streptavidin-peroxidase conjugate was applied (Pierce, Rockford, Il, USA). Positive antibody labeling was detected as described previously(288) and quantification of detected proteins was achieved using the program, Adobe PhotoShop CS2. Detection of β-actin (Sigma; mouse anti-β-actin; 1:10000) was assessed in all samples as a positive gel-loading control.

2.3 Statistical Analysis

Normally distributed continuous data were expressed as mean ± standard deviation and tested with unpaired t-tests between groups. Skewed distributions

were expressed as median and inter-quartile and means tested using Mann-Whitney U. To compare voltage, conduction velocity, and atrial refractory period across regions, chambers, rhythm and group (obese and control), mixed effects models were fitted to the data. Fixed effects included combinations of group (obese, control), map type (sinus rhythm or pace), region and chamber (RA, LA) with a maximum of two fixed effects entered into the statistical model at one time. Main effects and their interaction were tested. Random effects of sheep ID were fitted to all models to account for the dependence in observations from the same animal. In the case of skewed distribution (i.e. for fibrosis assessment via Masson Trichrome staining), the data were log transformed prior to further analysis. Two sided p-values of less than 0.05 were considered statistically significant. All analyses were performed using SPSS/PASW version18 (SPSS Inc. Chicago, IL).

2.4 Results

2.4.1 Group characteristics

The study sheep achieved peak obesity over a period of 36 weeks and remained in this state of sustained obesity for another 36 weeks. The control sheep were maintained lean during this period. The obese sheep weighted twice the control animals and had significantly greater total body fat. Table 1 presents the characteristics of the two groups.

2.4.2 Structural and hemodynamic remodeling

Table 1 describes the hemodynamic characteristics of the two groups. The left atrium (LA) was enlarged ($p=0.01$) with increase in left atrial pressure ($p<0.001$) without a change in left ventricular ejection fraction ($p=0.8$) in the obese sheep as

compared to the controls. In addition, there was significant increase in right atrial and pulmonary artery pressures ($p<0.001$) with obesity. The systemic blood pressure was also elevated in the obese as compared to the controls (p 0.02).

2.4.3 Electroanatomic remodeling

The electroanatomic maps of the atria were created in sinus rhythm and during proximal coronary sinus (PCS) pacing (CL=300ms). The electrophysiology data has been summarized in Table 2. Both the left and right atria (RA) volumes were increased in the obese sheep as compared to the controls ($p<0.001$).

2.4.4 Atrial refractoriness

The atrial ERP, at both 450 and 300 ms cycle length, from the seven sites did not differ significantly between the two groups (CL 300ms p=0.8, CL 450ms p=0.9) (Table 2, Figure 1). The ERP heterogeneity, at both 450 and 300ms cycle length, from the seven sites, also did not significantly differ between the obese and control groups (CL 300ms p=0.8; CL 450ms p=0.1) (Table 2).

2.4.5 Conduction velocity

The mean conduction velocity was greater in the left atrium compared to the right atrium in both obese and control groups both during sinus rhythm ($p<0.001$) and PCS pacing ($p<0.001$). However, the mean conduction velocity was significantly slower in the obese group (LA 1.18±0.04m/s and RA 1.03±0.04m/s) in both atrial chambers as compared to the controls (LA 1.58±0.04m/s and RA 1.43±0.04) ($p <0.001$) in sinus rhythm (Figure 2). Similarly during PCS pacing, the mean conduction velocity was significantly slower in the obese group (LA 0.99±0.05m/s and RA 0.92±0.05m/s) in both atrial chambers as compared to the controls (LA 1.41±0.04m/s and RA 1.33±0.04) ($p <0.001$). Importantly, the conduction was

more heterogeneous in the obese as compared to the controls (CoV: 22.0 ±6.1% vs 9.1± 4.9%) in sinus rhythm (p<0.001) (Figure 1). Likewise, the conduction was more heterogeneous during PCS pacing (p< 0.001) in obese as compared to controls (CoV: 21.4±6.1% vs 8.3±3.0%).

In addition, conduction velocity (p<0.001) was reduced and conduction heterogeneity (p<0.001) increased in the obese animals even after adjusting for LA pressure.

2.4.6 Complex fractionation

The left atrium demonstrated greater fractionation/ double potentials (FP/DP) as compared to the right atrium in both obese and control groups during sinus rhythm (p<0.001) and PCS pacing (p<0.001). During sinus rhythm, 53.2±13.5% and 36.0±2.8% of the signals in the LA and RA respectively were FD/DP in the obese group. In contrast, only 10.8±4.4% and 8.2±2.8% of all signals in the LA and RA respectively were FD/DP in the control group (p <0.001). Similarly during PCS pacing, 34.2±3.1% and 32.8±11.9% of signals were FP/DP in left and right atria respectively in the obese sheep as compared to 9.8±3.0% and 6.1±3.9% in LA and RA respectively in control group (p<0.001).

2.4.7 Voltage

The mean voltage did not differ between obese (LA 4.5±1.7 mV; RA 4.1±1.6 mV) and controls (LA 4.4±1.4 mV; RA 3.6±0.9) in sinus rhythm (p=0.3) (Figure 3). There was no areas of low voltage or scar in either chamber in both control or obese. However, regional voltage heterogeneity was elevated in the obese group (CoV: 32.1±8.8%) as compared to the controls (CoV: 24.6±7.5%) in sinus rhythm (p<0.001) (Figure 2).

2.4.8 Vulnerability for atrial fibrillation

Figure 4 shows the AF vulnerability in the two groups. The median number of AF episode were 4.5 (2.0-7.0) were greater in the obese group as compared to controls 1 (0.0-2.0) (p=0.02)). The total AF episode duration per animal was increased in the obese group (75.2±90.4 seconds) as compared to the controls (12.0±16.4 seconds) (p=0.05). Likewise, the average AF episode length was longer in the obese (11.4±9.1 seconds) as compared to controls (3.2±1.7 seconds) (p=0.01).

2.4.9 Atrial musculature infiltration by epicardial adipose tissue

Distribution of epicardial adipose tissue: The epicardial adipose tissue, in relation to the atria, was distributed adjacent to left atrial posterior wall and atrioventricular groove. There was minimal epicardial adipose tissue adherent to the appendage. In contrast the paracardial adipose tissue was more diffuse in distribution with prominent deposit between the appendage and great arteries.

Fatty infiltration by epicardial fat: Moderate (Grade II) to severe infiltration (Grade III) of the left atrial posterior wall by the overlying epicardial fat was seen significantly more in the obese sheep (mean grade: obese-2.5±0.7, controls-1.0±0.0; p value <0.001). There was minimal fatty infiltration in the left atrial appendage in both groups (p=0.18) (mean grade: 1.2±0.4 and 1±0 for obese and control groups respectively). The Grade III Fatty infiltration was not seen in the left atrial appendage in either group, where epicardial fat was minimal. Figure 5 depicts representative HE stained sections (X1.25) demonstrating fatty infiltration of the atrial musculature by the epicardial adipose tissue in the obese and control groups.

2.4.10 Fibrosis

Morphometric analysis of the Masson trichrome stained sections of the left atrial demonstrated 8.14±2.39%, and 5.31±0.95% staining in the obese and control groups respectively. There was increase in interstitial fibrosis in the obese as compared to the control animals (p=0.003). Figure 6, upper panel shows representative Masson trichrome stained sections from the two groups.

2.4.11 Atrial TGFβ1 protein

Atrial TGFβ1 protein was assessed by Western blot (Figure 6, lower panel). The atrial TGFβ1 protein expression increased 5 fold in the obese as compared to control group (p=0.002, table 2).

2.5 Discussion

2.5.1 Major Findings

This study presents new information on the global endocardial electrophysiological and electroanatomical remodeling of the atria due to sustained obesity. In the present study, animals gained weight over 36 weeks to achieve stable obesity and maintained at this sustained obesity for another 36 weeks to replicate a state more analogous with chronic obesity in humans. The obese group accumulated fivefold greater total body fat (34.5kg) as compared to controls (8.7 kg). The obese sheep model is unique as it does not suffer from obstructive sleep apnea, due to the typical habitus and sleeping posture. Hence this model allows us to study the relationship between obesity and AF in absence of confounding effects of sleep apnea. It demonstrates:

Structural and hemodynamic changes

- Bi-atrial enlargement with diastolic dysfunction reflected by elevated left atrial pressure in presence of normal ventricular function,
- Elevated right heart pressures and
- Elevation of systemic blood pressure.
- Increased expression of pro-fibrotic TGFβ1 and increased interstitial fibrosis.
- Decreased connexin-43 expression

Electrophysiological remodeling

- Slowed and heterogeneous conduction,
- Increased complex fractionated electrograms and double potentials,
- Increased voltage heterogeneity without significant change in mean voltage or appearance of scar/low voltage and,
- No change in mean endocardial ERP and ERP heterogeneity,

As a result of these hemodynamic and electrophysiological changes, obese animals were more vulnerable to AF. Importantly, this study provides causative evidence that links obesity directly with the development of AF substrate.

2.5.2 Atrial substrate in AF

Wijffel et al. in the pivotal work on chronically instrumented goats demonstrated electrical remodeling and put forward the concept of *'AF begets AF'*(85). They showed that rapid atrial rates caused alteration in ionic currents and cellular excitability resulting in *abbreviated ERP.* This was termed as '*electrical remodeling*'. Subsequently a '*different sort of remodeling*' involving *conduction abnormalities* and structural changes, particularly *diffuse atrial fibrosis* was described in an experimental heart failure model. (86). These findings were subsequently

confirmed to be the unifying feature of structural remodeling in other conditions, both in pre-clinical studies (87-91) and clinical studies (92-99).

2.5.3 AF substrate in Obesity

Although an epidemiological link has been established between obesity and atrial fibrillation over the last decade, the underlying electrophysiological changes and mechanism still remain to be clearly defined.(29,32,266,283,284,289) Obstructive sleep apnea (OSA) is closely associated with obesity in humans and predisposes to AF by causing hypertension, diastolic dysfunction and heart failure, and catecholaminergic surges during sleep.(30,290) Iwasaki and coworkers have demonstrated obesity facilitated AF inducibility in presence of acute obstructive sleep apnea. However, in absence of obstruction, the basic electrophysiological parameters were unaltered and AF inducibility not enhanced in obese rate despite structural remodeling. The ovine model allows evaluation of obesity in absence of OSA and in this study demonstrated diffuse conduction abnormalities and interstitial fibrosis with chronic obesity alone.

2.5.3.1 Electroanatomic remodeling with Obesity

The chronically obese animals demonstrated global endocardial bi-atrial conduction slowing. However the degree of slowing varied in different regions resulting in increased conduction heterogeneity. This is consistent with finding with limited epicardial mapping with short term weight gain in an ovine model(121). Munger and coworkers have also reported slowed longitudinal conduction velocities from the left atrium to the pulmonary veins in obese patients with AF(123). However, this human study did not observe any significant change in conduction velocity along the coronary sinus. The obese animals did not

demonstrate electrical scars or alteration in mean voltage. Despite this increased voltage heterogeneity was observed in obese animals. We hypothesize that fatty infiltration and interstitial fibrosis could explain the heterogeneity. As with other studies evaluating clinical substrate for AF, endocardial atrial refractoriness was not altered with sustained obesity. This finding differs from those reported by Munger et al who reported shortened atrial refractoriness in obese patients undergoing ablation for AF. They however acknowledged that AF induced during ERP testing could potentially impact atrial refractoriness. In addition, marked increase in complex fractionated signals was observed with sustained obesity in our study.

2.5.3.2 Atrial fibrosis and atrial TGFβ1 with sustained obesity

Sustained obesity was associated with diffuse atrial interstitial fibrosis. This is consistent with changes observed with heart failure(86) and chronic hypertension(89). Spach and coworkers have demonstrated elegantly that fibrosis can produce conduction abnormalities promoting re-entry and AF(185,186). The fibrosis observed in the study was only interstitial in nature without areas of replacement fibrosis usually seen with infarction(116) and with congestive heart failure(86). This may suggest a more subtle insult occurring with sustained obesity, albeit sufficient to cause interstitial fibrosis.

TGFβ1 has been shown to be a crucial cytokine in the signal transduction pathways responsible for fibrosis. It occupies a central position, downstream to angiotensin and upstream to endothelin pathways and acts in a paracrine- autocrine fashion(207,291). Verhuele and coworkers have shown that overexpression of constitutional TGFβ1 in transgenic mice led to selective atrial fibrosis, conduction heterogeneity and AF(191). TGFβ1 expression was increased fivefold with

sustained obesity in our study and could explain the increase in interstitial fibrosis. We have previously reported increased endothelin receptor expression with short term weight gain. Overexpression of the TGFβ superfamily(270,271) and endothelin(269) signaling pathways has been similarly reported in humans.

2.5.4 Pericardial fat and AF

There is emerging evidence that localized epicardial fat depots may have a significant role in development of AF. Several groups including ours have shown an association of pericardial fat with AF independent of other measures of obesity(274,276-278). Epicardial fat, a kind of visceral fat, behaves like an endocrine organ secreting a myriad of adipo-cytokines including TGFβ superfamily. The further absence of fascial barriers and common vascular supply with the underlying myocardium may facilitate paracrine action. This has been elegantly demonstrated in an organo-culture model by Venteclef and coworkers(216). They incubated rat atrial tissue in a secretome derived from human epicardial fat and demonstrated that atrial fibrosis mediated by members of TGFβ superfamily. We demonstrated several fold increased expression of TGFβ1 in atrial tissue but source of this cytokine was not evaluated. In addition, a new finding was observed with epicardial fat infiltrating the underlying myocardium. We hypothesize that fat infiltration separates myocytes and could result in conduction abnormalities in a fashion similar to microfibrosis(186). Considering the infiltration was observed only adjacent to epicardial fat depots, the distribution of epicardial fat could be contributing to conduction heterogeneity.

2.5.5 Study limitations

This study addressed substrate development with sustained obesity. Although the observed electrical and structural abnormalities predispose to AF, the development of clinical AF is a complex process, with other factors such as triggers and perpetuators which the not addressed in the current study. We also did not address the impact of fluctuating weight which is often observed in clinical obesity. Furthermore, the pro-fibrotic signal transducing pathways responsible for AF in obesity have not been fully elucidated in this study.

2.5.6 Conclusion

Sustained chronic obesity results in chronic stretch, diffuse interstitial fibrosis and conduction abnormalities and increased vulnerability to AF. TGFβ signaling pathway may have an important role in mediating interstitial fibrosis in sustained obesity. Infiltration of underlying atrial musculature by the epicardial fat may be a unique feature of AF substrate in obesity. This study provided direct evidence for the role of obesity in the development of AF.

Table 1: Structural and hemodynamic characteristics of the control and obese groups.

	Controls	Obese	P value
Weight (Kg)	60±7	110±9	<0.001
Total Body fat (Kg)	9±6	35±6	<0.001
TBF/TST	15.2±7.8	36.9±4.3	<0.001
LA major axis (mm)	36.2±1.3	38.3±1.9	0.01
LA minor axis (mm)	27.7±1.1	30.1±1.4	<0.001
LVEF (%)	67±5	70±6	0.81
LA Pressure (mmHg)	3.7±1.4	8.1±1.6	<0.001
RA Pressure (mmHg)	1.8±1.1	4.6±1.2	<0.001
PA Pressure (mmHg)	9.8±2.6	15.0±0.9	<0.001
Systemic Mean BP (mmHg)	71±12	86±13	0.02

TBF/TST- Total body fat/ total soft tissue (DEXA); LA-Left atrium; LVEF- Left ventricular ejection fraction; RA- Right Atrium; PA- Pulmonary Artery; BP- Blood Pressure.

Table 2: Electrophysiology and structural characteristics of the control and obese groups.

	Controls	Obese	P value
LA CARTO volume (ml)	74±13	86±15	<0.001
RA CARTO volume (ml)	75±15	89±16	<0.001
FP/DP LA sinus rhythm (%)	10.8±4.4	53.2±13.5	<0.001
FP/DP RA sinus rhythm (%)	8.2±2.8	36.0±2.8	<0.001
CV LA (sinus rhythm) (m/s)	1.58±0.04	1.18±0.04	<0.001
CV RA (sinus rhythm)(m/s)	1.43±0.04	1.03±0.04	<0.001
Conduction heterogeneity (SR) (%)	9.1± 4.9	22.0 ±6.1	<0.001
Voltage LA (SR) (mV)	4.4±1.4	4.5±1.7	0.3
Voltage RA (SR) (mV)	3.6±0.9	4.1±1.6	0.3
Voltage heterogeneity (Sinus rhythm) (%)	24.6±7.5	32.1±8.8	<0.001
ERP mean (ms) CL 300ms	180	182	0.8
ERP heterogeneity at CL 300ms (%)	10.0±4.2	10.5±3.3	0.70
ERP mean (ms) CL 450ms	190	190	0.99
ERP heterogeneity at CL 450ms (%)	10.3±3.3	13.6±5.4	0.32
AF episodes- total (median)	1(0-2)	4.5(2-7)	0.02
AF cumulative duration (median)(seconds)	4.1(3-15)	46(10-112)	0.05
AF episode duration (median)(seconds)	2.7(2-5)	7.9(5-17.7)	0.005
Fatty infiltration posterior LA (Grade)	1±0	2.5±0.7	<0.001
Fibrosis (% staining-morphometry)	5.31±0.95	8.14±2.39	0.003
Atrial TGFβ1 protein OD	0.41±0.35	2.07±1.04	0.002

LA- Left atrium; RA- Right atrium; FP/DP- Fractionated potential/ Double potential; PCS- proximal coronary sinus; SR- sinus rhythm; ERP- Effective refractory period

Figure 1: Distribution of ERP in obese and control groups at two cycle lengths.

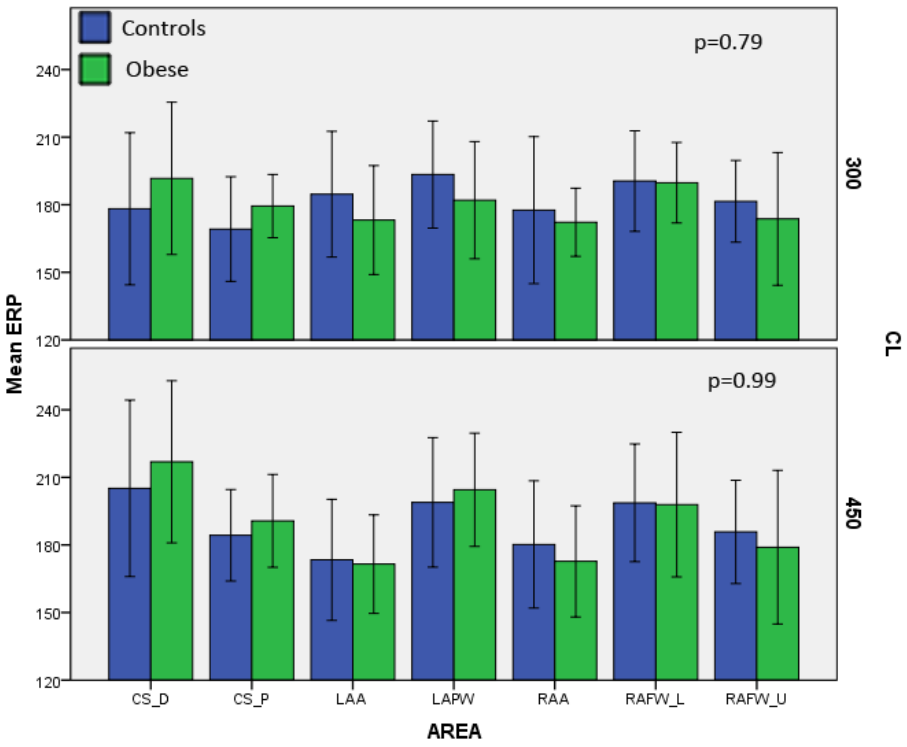

The top and the bottom panels depict ERP at 300 and 450ms cycle length respectively. CS_P- proximal coronary sinus; CS_D- distal coronary sinus; LAA- left atrial appendage; LAPW- left atrial posterior wall; RAA- right atrial appendage; RAFW_U- upper right atrial free wall; RAFW_L- lower right atrial free wall.

Figure 2: Conduction velocity slowing and increased conduction heterogeneity with obesity

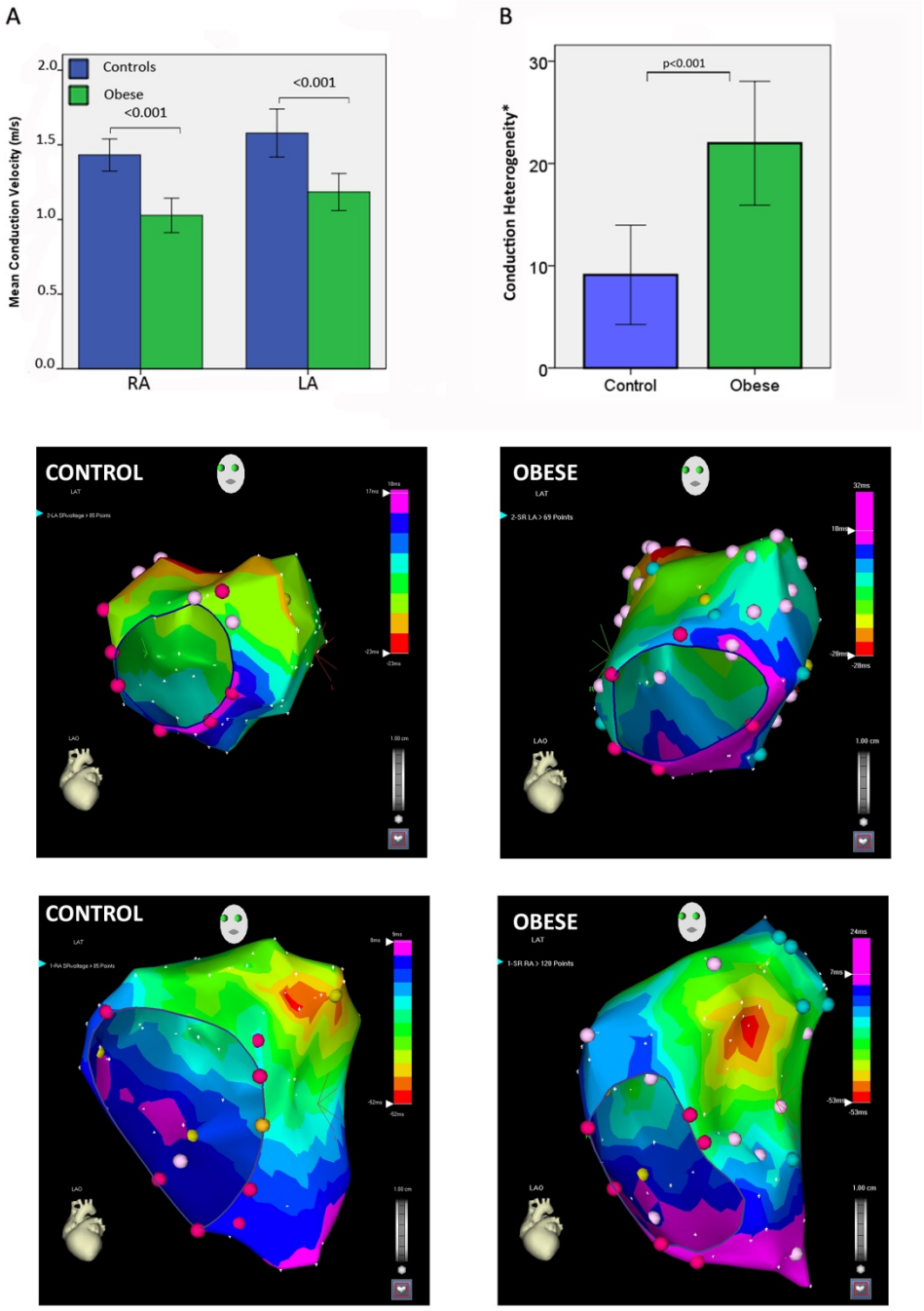

The top panel shows the mean conduction velocity (A) and conduction heterogeneity (B) in obese and control groups in sinus rhythm. * Conduction heterogeneity= Coefficient of CV variation (SD/mean × 100%). The middle and bottom panel shows representative left and right atrial isochronal maps (5ms) demonstrating conduction in obese and control groups in sinus rhythm. The isochrones in the obese sheep are more crowded and greater time to activate the atria.

Figure 3: Changes in mean endocardial voltage and voltage heterogeneity with obesity

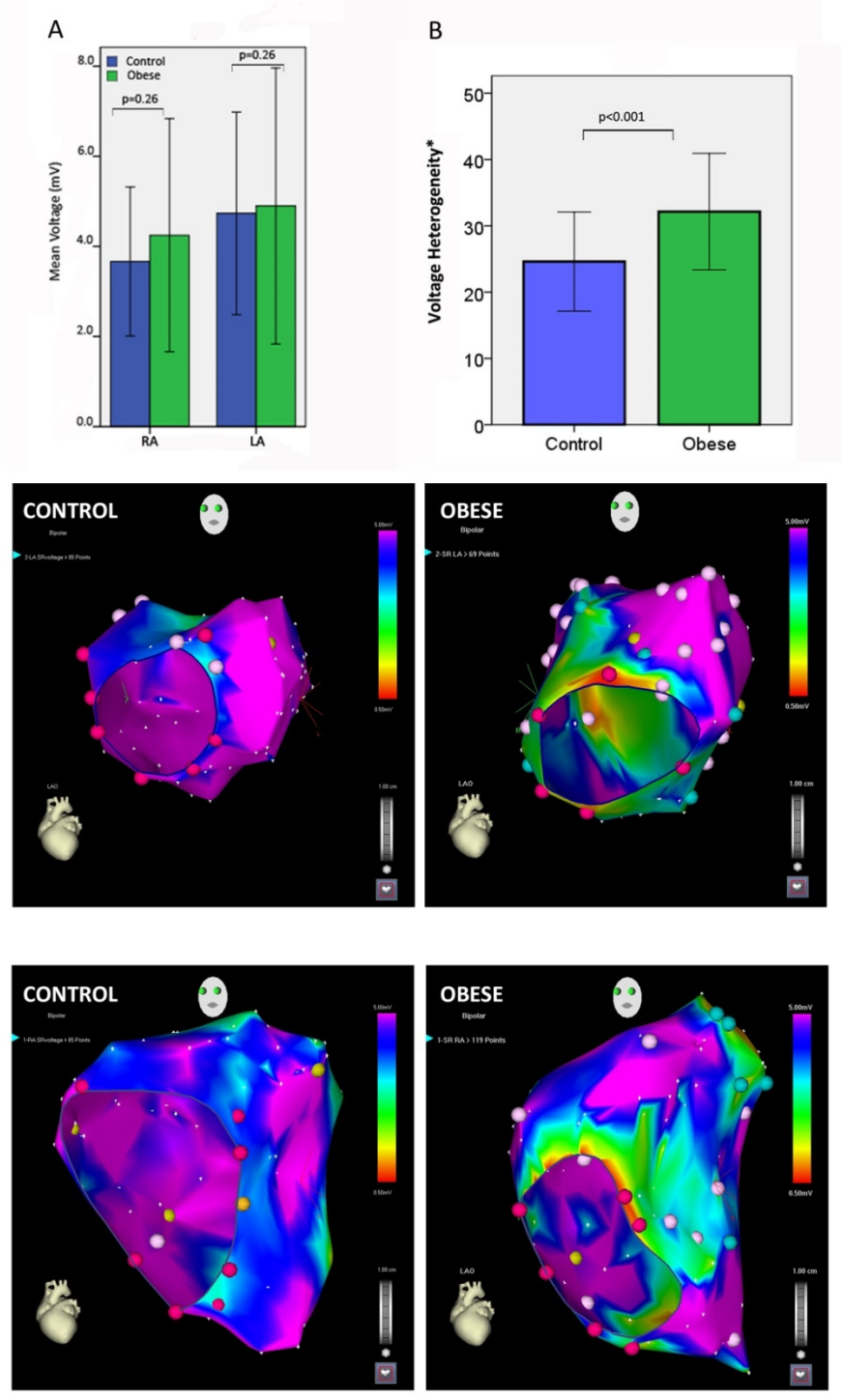

Representative left atrial voltage maps of the control and obese group upper limit 5.0mV. Note the heterogeneity in the voltage across different regions in the obese sheep. There was no area of electrical scar. There was increased number of fractionated/double potentials in the obese animal.

Figure 4: Atrial fibrillation vulnerability in the obese and control groups.

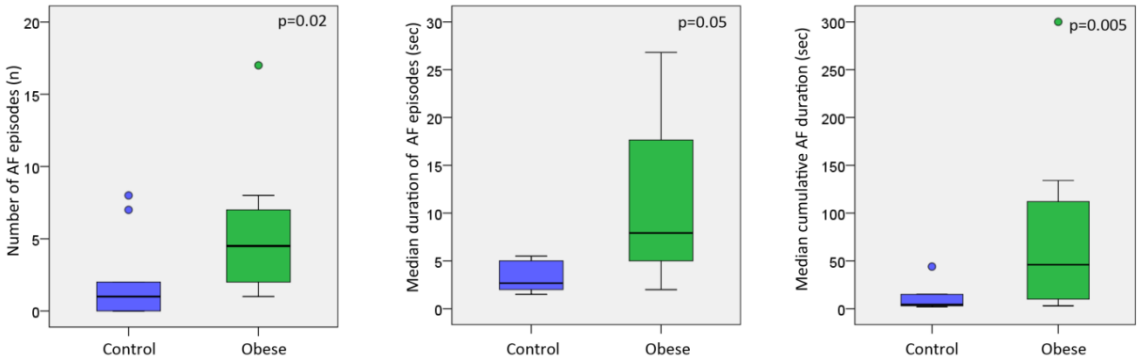

Figure 5 Distribution of epicardial fat and infiltration of atrial myocardium by contiguous epicardial fat

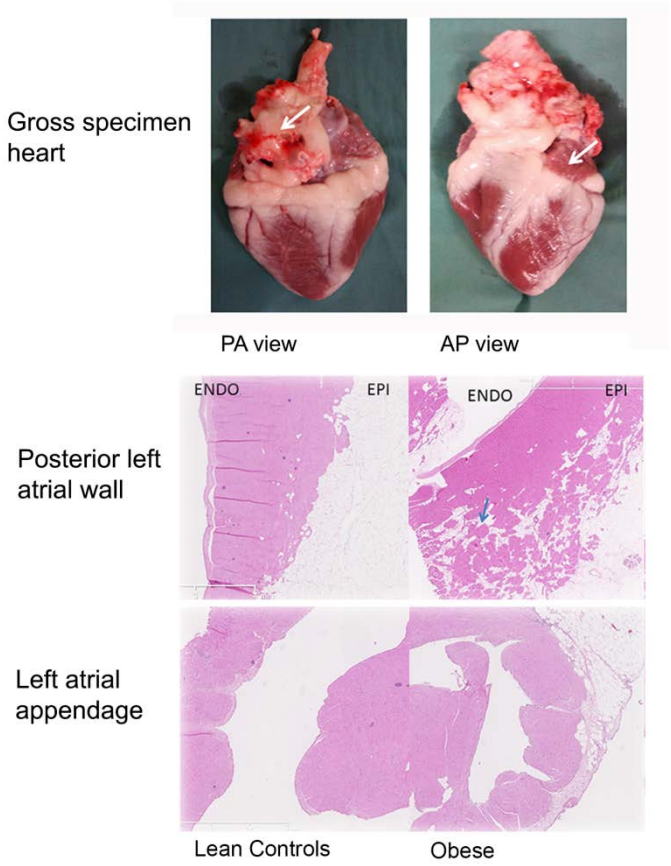

Top panel shows gross specimen of sheep heart after removal of parietal pericardium with the paracardial fat. PA View- arrow points to epicardial fat adjacent to left atrial posterior wall. AP view- arrow points to left atrial appendage which has very little epicardial fat. Middle and bottom panels show representative H&E stained sections (X1.25) of LA posterior wall and appendage respectively from control and obese groups. Arrow shows infiltration of atrial musculature with fat cells.

Figure 6: Atrial fibrosis and atrial TGFβ1 expression with obesity

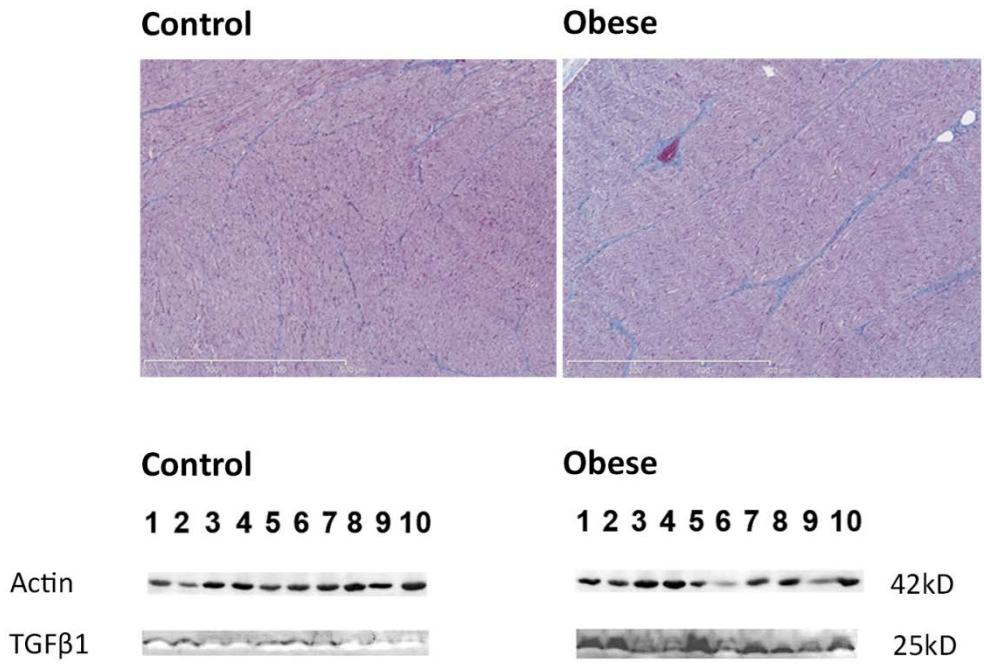

The top panel shows the representative Masson trichome stained sections (X5) of the LA posterior wall in the control and obese groups. Masson trichome stains collagen blue and the fibrosis was assessed morphometically. The bottom panel show the Western blots showing expression of TGFβ1 in the left atrial tissue.

Chapter 3

Atrial fibrillation and obesity: Reversibility of atrial substrate with weight reduction

3.1 Introduction

The rise in prevalence of atrial fibrillation (AF) has been accompanied by its increasing contribution to cardiovascular mortality and morbidity(2,7). This has coincided with the obesity epidemic and the emergence of obesity as a new risk factor for AF(29,31,32,266). The identification of risk factors for AF and improved understanding of the pathophysiology has ushered a paradigm shift in the approach to management of AF from anti-arrhythmic and ablation strategies to upstream therapy and risk factor management. Although the upstream therapies have been successful in primary prevention, the benefits have been equivocal in secondary prevention(292).

The mechanistic link between obesity and AF is confounded by the coexistence of obstructive sleep apnea, hypertension, diabetes and coronary artery disease, thereby clouding interpretation in population based studies. However, left atrial enlargement and recently pericardial fat have been implicated in the role of obesity in AF(31,274). Recent experimental work in an ovine model has shown conduction slowing, atrial fibrosis and alteration in pro-fibrotic markers expression with short term weight gain(121). In addition, there is evidence for a complex interplay in the development of AF due to obesity with the presence of sleep apnea(95,122).

Here we utilized a previously validated obese ovine model; a model not known to suffer from sleep apnea. In this model we evaluated the effect of weight reduction on reversibility of the epicardial electrophysiological, structural and molecular substrate for AF.

3.2 Methods

All procedures were conducted in accordance with guidelines outlined in the "Position of the American Heart Association on Research Animal Use", adopted on November 11, 1984. This study was approved by the Animal Research Ethics Committees of the University of Adelaide and SA Pathology, Adelaide, Australia.

3.2.1 Study Groups

Figure 1 provides the study outline. Thirty sheep had induced obesity by ad-libitum calorie dense diet over a 36 week period and maintained obese for another 36 weeks. Eight lean sheep of similar age were maintained lean to serve as control. The obese animals were randomized to three groups of 10 animals each: obese, 15 and 30% weight reduction groups. The control group of 8 lean sheep was maintained lean over this period.

3.2.2 Obese Ovine Model

Weight gain: A previously described ovine model of progressive weight gain, based on ad-libitum regimen of hay and high energy pellets, was utilized to induce progressive weight gain(285). At baseline, healthy sheep were commenced on a high caloric diet of energy-dense soybean oil (2.2%) and molasses fortified grain and maintenance hay with weekly weight measurement. Excess voluntary intake was predominantly of grass alfalfa silage and hay. For the obese sheep, pellets

were gradually introduced at 8% excess basal energy requirements, and rationed to ≥70% of total dry matter intake. The sheep gradually gained weight to a plateau in weight at 36 weeks and were subsequently maintained at this weight for a further 36 weeks.

Weight reduction: The obese sheep, assigned to weight loss, underwent gradual weight reduction over 32 weeks. The weight loss sheep were housed in groups of fours. The energy-dense soybean oil and molasses fortified feed was gradually withdrawn and replaced with high quality cereal hay which was reduced to two-third of the normal intake. The weight was monitored weekly. If weight loss was inadequate in a particular sheep, it was housed separately. Blood samples were collected four weekly to ensure electrolyte and acid-base homeostasis.

Control sheep: The control sheep were maintained at their baseline weight with high quality cereal hay provided ad-libitum and energy dense pellets rationed at 0.75% of live weight daily. The housing conditions were identical between all groups, but only the amount was varied. Shorn weight was recorded immediately prior to surgery.

3.2.3 Study Protocol

All animals were pre-acclimatized for at least one week prior to the study and underwent: imaging (DEXA, Echocardiography, and cardiac magnetic resonance), hemodynamic assessment, and bi-atrial epicardial electrophysiological studies, histology, immunohistochemistry and molecular analysis.

3.2.4 Body Composition

The Dual-energy x-ray absorptiometry (DEXA) scan was performed under general anesthesia to determine total body fat (TBF) in the animals.

3.2.5 Transthoracic echocardiography

An echocardiogram was performed under general anesthesia prior to the electrophysiology study. The left atrial dimensions were measured in apical 4-chamber view. The left ventricular dimensions were measured in M-Mode in parasternal long axis view at the level of mitral leaflet tips. The left ventricular dimensions were utilized to determine global left ventricular function utilizing Teicholz formula.

3.2.6 Cardiac Magnetic Resonance

Cardiac magnetic resonance (CMR) wcould not be performed in the obese group as they did not fit into the bore of the scanner. Chamber volumes were measured using CMR (Siemens Sonata 1.5 Telsa, MR Imaging Systems, Siemens Medical Solutions, Erlangen Germany) with 6mm slice-thickness and no interslice gaps through both the atrial and the ventricles. The animals were anaesthetized and placed supine within the CMR chamber. The animals were mechanically ventilated to allow breath holding sequences to be performed. Analyses were performed offline by blinded operators using proprietary software, QMass MR (Medis medical imaging systems, Leiden, Netherlands). Chamber size, ventricular mass and pericardial fat volumes were measured using previously described methods.

3.2.7 Electrophysiological study

Electrophysiological study was performed in the post absorptive state under general anesthesia. A midline sternotomy was utilized to facilitate access to pericardium and epicardial application of custom designed 54-electrode plaque with 5mm spacing, spanning the appendage and free wall. This was positioned on the left atria and right atria sequentially. Surface electrocardiogram (ECG) and

bipolar electrograms were continuously monitored and stored on a computer based digital amplifier/recorder system for off-line analysis (LabSystem Pro, Bard Electrophysiology, Lowell, MA, USA). Intracardiac electrograms were filtered from 30 to 500 Hz, and measured with computer assisted calipers at a sweep speed of 200 mm/s. The following parameters were determined:

3.2.7.1 Atrial conduction

Conduction was assessed during stable S1 pacing at 400, and 300 and 200 ms from the RAA, RA free wall, LAA, and LA free wall. Activation maps of the atria were created using semi-automated custom software and verified manually. Isochronal lines were superimposed to further illustrate conduction patterns. Conduction velocity was calculated from the local vectors within each triangle of electrodes as described previously(293).

3.2.7.2 Heterogeneity of conduction (CHI)

Conduction heterogeneity was assessed using an established phase mapping method during S1 pacing. Absolute conduction phase delay was calculated by subtracting the 5th from the 95th percentile of the phase difference distribution (P5-95). Conduction heterogeneity index was derived from dividing P5-95 by the median (P50) as previously described(89).

3.2.7.3 Atrial effective refractory period

Atrial effective refractory period (ERP) was measured at twice diastolic threshold at 400, 300 and 200 ms from 8 sites- 4 corners of plaque positioned on the right and left atrium each. Eight basic (S1) stimuli were followed by a premature (S2) stimulus in 10-ms increments starting at a coupling interval of 80 ms. Atrial ERP

was defined as the longest non-propagated S1-S2. ERP was measured thrice at each cycle length and averaged. If ERP varied by greater than 10 ms, an additional 2 measurements were made and then averaged.

3.2.7.4 AF vulnerability

AF vulnerability was assessed during ERP testing. AF was defined as rapid irregular atrial rhythm. The cumulative duration was calculating by summation of all episodes of AF≥10 seconds.

3.2 8 Hemodynamic assessment

Invasive blood pressure monitoring was performed during the electrophysiology study. Left atrial and pulmonary artery pressures were recorded directly at the end of the electrophysiology study.

3.2.9 Histological assessment

The animals were euthanized following the electrophysiology study. Isolated atrial tissues from the left atrial posterior wall (LAPW) and left atrial appendage (LAA) were perfusion-fixed with 4% paraformaldehyde containing 0.02% heparin and immersed in 10% neutral buffered formalin. They were then paraffin-embedded and, from each site at 1cm intervals, 5μ serial sections were cut and stained with hematoxylin and eosin, Masson's trichrome, and immunohistochemically for connexin43.

3.2.9.1 Inflammation

Morphometric analysis of hematoxylin and eosin stained sections for perivascular inflammation was performed utilizing Image J 1.3 software (National Institutes of Health, Bethesda, MD, USA). Stained sections from LAPW and LAA each from 8-10

animals per group were digitally captured (from 5 random fields per section using NanoZoomer Digital Pathology System software (Hamamatsu Phonetics, Japan). The inflammatory cells were identified to surround the vessel wall and infiltrate the fat and interstitial regions of the tissue. The endogenous cells in the vessel wall were not included for analysis. The results were expressed as the mean inflammatory cells/field in each animal.

3.2.9.2 Fibrosis assessment

Morphometric analysis of Masson's trichrome-stained sections was performed utilizing 'analySIS LS Professional' software (Olympus Soft Imaging Solutions, Münster, Germany) to obtain a quantitative estimate of collagen within the tissue. Stained sections from LAPW and LAA from of 8-10 animals per group were digitally captured (from 5 random fields per section; magnification x5) with an area of Masson's trichrome selected for its color range and the proportional area of tissue with this range of color quantified, as previously described(89).

3.2.9.3 Connexin43 expression

Sections from paraffin embedded atrial tissues were cut and dewaxed using xylene and rehydrated through alcohols and antigen retrieval was performed using citrate buffer (pH 6). Slides were allowed to cool and washed twice in PBS (pH 7.4), then endogenous peroxidise activity was quenched. Non-specific proteins were blocked using normal horse serum for 20 min. Connexin43 (Sigma, USA, Cat No. C6219) was applied at 1:8000 at room temperature overnight. The following day, the sections were given two washes in PBS and then a biotinylated anti-rabbit secondary (Vector Laboratories, USA, Cat # BA-1000) was applied for 60 min at room temperature. Following two PBS washes, the slides were incubated for 1

hour at room temperature with a streptavidin-conjugated peroxidise tertiary (ThermoScientific, USA, Cat # 21127). Sections were then visualized using diaminobenzidinetetrahydrochloride (DAB), washed, counterstained with hematoxylin, dehydrated, cleared and mounted on glass slides. Sections were then visualized using diaminobenzidine tetrahydrochloride (DAB), washed, counterstained with hematoxylin, dehydrated, cleared and mounted on glass slides. Morphometric analysis of DAB-stained sections was performed utilizing Image J 1.3 software (National Institutes of Health, Bethesda, MD, USA) to obtain a quantitative estimate of connexin43 expression within each tissue. Stained sections from LAPW and LAA from 8-10 animals per group were digitally captured (from 10 random fields per section, as above; at a magnification of x20) with an area of Connexin43 selected for its color range and the proportional area of tissue with this range of color quantified, as previously described(89).

3.2.10 Western blot

Left atrial appendage tissue was span frozen in liquid nitrogen and stored at -80° C. Electrophoresis and Western immunoblotting were used to assess changes in the tissue concentration of TGFβ1, Endothelin-1, Endothelin receptor A and B in the left atrium. Tissue samples (approximately 100mg) were sonicated in modified 500ul RIPA buffer (50mM Tris HCl, pH8.0 at 25°C containing 150mM NaCl, 1% IGEPAL, 0.5% sodium deoxycholate, 0.1% sodium dodecyl sulphate, 1mM dithiothreitol, 50µg/ml leupeptin, 50µg/ml pepstatin A, 50µg/ml aprotinin and 0.1mM phenylmethylsulphonyl fluoride). Supernatants were prepared from successive centrifugation of samples at 13000g, 15 minutes, room temperature and then 13000g, 45 minutes, room temperature before an equal volume of sample buffer (62.5mM Tris-HCl, pH 7.4, containing 4% SDS, 10% glycerol, 10% β-

mercaptoethanol and 0.002% bromophenol blue) was added and samples boiled for 5 minutes. Protein concentrations in each sample were equalized according to the method of Bradford(287). Electrophoresis was performed using a Mini-PROTEAN® TGX™ precast gel system (Bio-Rad Laboratories Pty Ltd, Gladesville, New South Wales, Australia). Denaturing polyacrylamide gels (10% w/v) were employed for protein separation, which was undertaken as described previously(288). After separation, proteins were transferred to polyvinylidine fluoride (PVDF) membranes for immunoprobing (Bio-Rad Laboratories Pty Ltd). Membranes were incubated with antiserum for TGFβ1 (mouse anti-TGF-β1; Abcam, Cambridge, UK; 1:1000), endothelin-1 (Acris Antibodies, Herford, Germany; 1:10000), endothelin receptor A (Alomone Labs, Jerusalem, Israel; 1:2000) or endothelin receptor B (Alomone Labs, Jerusalem, Israel; 1:2000), overnight, and labeling carried out using a two-step detection procedure:: first, biotinylated secondary antibody (Vector Laboratories; 1:500; 30 minutes) was reacted with membranes and then streptavidin-peroxidase conjugate was applied (Pierce, Rockford, Il, USA). Positive antibody labeling was detected as described previously and quantification of detected proteins was achieved using the program, Adobe PhotoShop CS2(288). Detection of β-actin (Mouse anti-β-actin; Sigma Chemical Company, North Ryde, Australia; 1:10000) was assessed in all samples as a positive gel-loading control.

3.3 Statistical Analysis

Normally distributed continuous data are expressed as mean ± standard deviation, whilst median and inter-quartile range [in square brackets] were utilized for

middle descriptors for significantly skewed distributions (KS <0.05). Statistical significance was set as p<=0.05 and a trend at p<=0.10.

A mixed effects model was used for all analyses that contained multiple regional measures within each animal (eg. 8 x ERPs, CV, CHI per animal; 2 sites [LAA and LAPW] for Cx43 and Masson's, inflammation). To investigate potential atrial specific changes, atria (left or right) and group (obese, 15% weight loss, 30% weight loss and lean control) were modeled as fixed effects with an interaction term (atria*group). If no interaction was present, the model was re-run with the main effects only, with post-hoc tests using Sidak significance adjustment for multiple comparisons where required. The normality of the residuals of the mixed effects model were visually inspected to ensure that the parametric model was suitable for the dataset).

For data without multiple measures or levels of data within an animal (eg. fat mass, LA size, LVEF) a conventional one way ANOVA methodology was used with Sidak adjusted post-hoc testing as warranted. In the case of skewed distributions (e.g. TGF-β1 protein), the data were log transformed prior to performing an ANOVA. Fatty infiltration was coded into a dichotomous variable (at least moderate fatty infiltration or mild/none) and compared using an overall chi-squared statistic with post-hoc tests if the overall model was significant. The cumulative time of AF episodes (≥10 secs) were calculated for each animal and were compared between groups using the Kruskal Wallis non-parametric test, with post-hoc testing to explore pairwise differences using the Mann-Whitney U statistic.

All analyses were performed using SPSS/PASW version18 (SPSS Inc. Chicago, IL).

All procedures were conducted in accordance with guidelines outlined in the "Position of the American Heart Association on Research Animal Use", adopted on November 11, 1984. This study was approved by the Animal Research Ethics Committees of the University of Adelaide and SA Pathology, Adelaide, Australia.

3.4 Results

The obese, 15-, 30% weight loss and control sheep weighed 111±12, 112±11, 109±9 (p=NS) and 59±7 kg respectively at the time of randomization and weighed 111±12, 94±10, 77±8 and 58±6 kg (p<0.001) respectively at time of electrophysiology study (Table 1)

3.4.1 Hemodynamic and imaging characteristics

Table 1 and 2 show the hemodynamic and imaging characteristics of the different groups. The mean left atrial (LA) and the pulmonary artery pressures was greater in the obese group (vs controls <0.001) and reduced upon 30% weight reduction (LA mean; p=0.01 and PA mean; 0.002). The systemic blood pressure did not differ across the groups (p =NS). The left atrium (LA) was enlarged with obesity and reverse remodeled to control size with weight reduction. The LV mass did not change significantly upon weight reduction but was significantly greater than the control group. The left ventricular ejection fraction did not differ significantly between the different groups (p = NS).

3.4.2 Electrophysiological remodeling

A custom made multi-electrode plaque was placed over the epicardial surface of the left and the right atrium. The plaque was paced from the different corners at

three cycle length to perform the electrophysiology study. Figure 2 shows the representative activation maps and corresponding phase histograms of the left atrium signifying conduction velocity and heterogeneity respectively in the different groups. Figure 3 and table 1 show the electrophysiological characteristics of the groups.

3.4.2.1Conduction velocity

The mean conduction velocity was significantly slower in the obese group as compared to controls ($p<0.001$). It improved progressively with weight loss to achieve control values at 30% weight reduction. There was no difference in conduction velocities between the right and left atrium ($p=0.224$).

3.4.2.2 Conduction heterogeneity Index (CHI):

The conduction heterogeneity (assessed as CHI) in the obese group was greater compared to controls ($p<0.001$). The conduction heterogeneity progressively improved with weight loss (vs obese; $p<0.001$) but did not achieve controls levels ($p=0.09$).

3.4.2.3 Atrial refractoriness

The atrial ERPs (400, 300ms cycle lengths) were shorter in the obese group as compared to controls ($p=0.03$, 0.01 respectively). At both these cycle lengths, atrial ERPs improved with 30% weight loss (vs obese; $p<0.001$ each) to control levels (30% weight loss vs control $p=0.37$). The atrial ERP were significantly shorter in left atrium compared to right atrium in obese and weight loss groups ($p=0.01$) as compared to lean controls ($p=0.11$).

3.4.2.4 Vulnerability for atrial fibrillation

The cumulative AF induced in the control, obese, 15%- and 30% weight reduction groups was 135[34-214], 323[198-1331], 118[20-1671] and 93[0-573] respectively. As compared to the controls, the obese group had greater AF vulnerability during ERP testing (p=0.03). The cumulative duration of induced AF reduced significantly with 30% weight reduction (p=0.05) to control levels (30% weight loss vs control; p=0.9).

3.4.3 Structural and molecular remodeling

3.4.3.1 Inflammation

Morphometric analysis was performed to assess perivascular inflammation in the LA *(Figure 5.I)*. The perivascular space was expanded with increased inflammation in the obese animals as compared to controls (p<0.001). With weight reduction, the inflammation reduced stepwise at each step (obese vs 30% weight loss; p<0.001) but not to control levels (15% weight loss vs controls; p<0.001). The median number of inflammatory cells/field were 0.8 [0.4-2.0], 8.9 [7.6-12.8], 5.1 [3.0-8.0] and 3[1.8-3.8] in the lean controls, obese, 15-, and 30% weight loss groups respectively.

3.4.3.2 Fibrosis

Morphometric analysis of the Masson's trichrome stained sections of the LA demonstrated that there was significantly increased interstitial fibrosis in the obese group as compared to the controls (p=0.01). Fibrosis regressed with 30% weight reduction (p=0.01) to control values (p=0.98). The percentage of staining

for fibrosis were 5.1±0.7, 7.5±2.4, 7.8±2.5 and 5.5±1.5% in the lean controls, obese, 15-, 30% weight loss groups respectively (*Figure 5-II)*. .

3.4.3.3 Atrial TGFβ1 protein expression

Atrial TGFβ1 protein levels were assessed by Western blot *(Figure 6).* Atrial TGFβ1 expression was elevated in the obese group (vs controls $p<0.001$). Furthermore, TGFβ1 showed a trend towards regression upon 30% weight loss ($p=0.07$) to a level that it did not significantly differ from controls ($p=0.10$). There was significant correlation between atrial TGFβ1 and left atrial volume ($r=0.45$, $p=0.004$) and trended to correlate with atrial fibrosis ($r=0.35$, $p=0.07$). After adjustment for mean LA pressure and LA volume, the association with atrial conduction velocity ($r=0.51$; $p=0.01$) and conduction heterogeneity ($r=0.66$; $p=0.004$) was maintained. The atrial pericardial adipose tissue volume significantly correlated atrial TGFβ1 expression ($r=0.61$; $p=0.02$) and this relationship remained after adjustment for total body fat ($p=0.09$).

3.4.3.4 Atrial Endothelin-1 and ER-A and B receptor expression

Endothelin-1 and ER-A and B receptor expression was evaluated with western blot *(Figure 6)*. The endothelin-1 and ER-A receptor expression was similar across the 4 groups (p=NS). However, the ER-B receptor expression was increased with obesity (vs controls; $p=0.04$) and reduced stepwise with weight reduction (obesity vs 30% weight reduction; $p=0.01$) to control levels (control vs 30%weight reduction; $p=1.0$)

3.4.3.5 Connexin43 expression

Connexin43 expression was analyzed in the LA appendage and posterior wall by immune-histochemistry (IHC). Connexin43 was distributed along the intercalated disc and cell membrane of the atrial myocytes. Morphometric analysis of DAB stained connexin43 demonstrated that there was significant reduction in connexin43 expression in the obese group (vs controls; p=0.03). Connexin43 expression improved significantly upon weight loss (p=0.01) to reach control values (p=0.96). The percentage of connexin43 staining was 2.7±0.6, 1.8±0.4, 2.0±0.4, 2.5±0.5% in the lean controls, obese, 15- and 30% weight loss groups respectively. There was no alteration in connexin43 distribution with weight change (*Figure 5.III)*.

3.5 Discussion

3.5.1 Major Findings

This study provides new information on the hemodynamic, structural, electrophysiological, histological and molecular remodeling of the atria with sustained obesity and marked reverse remodeling following modest weight reduction.

Sustained obesity was associated with elevated LA and right heart pressures, perivascular atrial inflammation, over-expression of pro-fibrotic factor TGFβ1 and ER-B receptor, atrial fibrosis, diminution in connexin-43 expression and increased propensity for AF.

Weight reduction resulted in a significant decrease in total body fat from 40±9kg to 20±8kg after 30% weight reduction (albeit still greater than controls) and was associated with:

(i) Decrease in LA size, LA and PA pressures signifying improvement of obesity related diastolic dysfunction and reversal of stretch;

(ii) Reversal of the obesity related atrial fibrosis. This correlated with changes in the expression of pro-fibrotic factor TGFβ1 and ER-B receptor.

(iii) Reversal of the obesity related reduction in atrial connexin43.

(iv) Reversal of the obesity related detrimental changes in atrial conduction and refractoriness.

(v) These improvements in the hemodynamic, structural and molecular milieu associated with reversal of atrial fibrosis culminated in a reduced vulnerability for AF.

3.5.2 AF substrate in Obesity

Population based studies have established a strong epidemiological link between obesity and atrial fibrillation.(29,32,266,283,284,289) However, there is paucity of information on the substrate for AF in obesity. Obstructive sleep apnea (OSA) is closely associated with obesity in humans and predisposes to AF through several mechanisms that include hypertension, diastolic dysfunction, heart failure, and catecholaminergic surges during sleep.(30,290) Iwasaki and coworkers have shown that AF inducibility was facilitated by obesity in acute obstructive apnea.(122) However inducibility for AF was not increased in obese rats in the

absence of obstruction. The ovine model allows evaluation of obesity in absence of obstructive sleep apnea.

3.5.3 Electrophysiological remodeling in sustained obesity

Our study shows diffuse atrial fibrosis and conduction abnormalities with sustained obesity. Similar findings have been observed with structural remodeling in other substrates. In addition, abbreviated atrial refractoriness was seen with sustained obesity. The shortening of refractoriness is consistent the observations of *Munger* and coworkers, who reported shortened ERPs in patients with elevated body mass index.(123) In contrast, shortening of atrial refractoriness has not been observed with short term weight gain.(121) The shortening of the refractoriness could potentially represent changes in the expression of I_{to} and L type I_{Ca} ion channels.(104) These changes could be related to the either obesity per se or secondary to electrical remodeling due to spontaneous AF. However, this cannot be confirmed as the sheep did not undergo ambulatory ECG monitoring.

3.5.4 Determinants of atrial fibrosis in obesity

Atrial fibrosis is postulated to result in conduction abnormalities and increase the propensity for AF. Our study describes several key changes that play a crucial role in deposition of collagen and extracellular matrix proteins. In our study, sustained obesity was associated with perivascular inflammatory infiltrate in the atria. Given the ability of the leucocytes to leave the circulation, these inflammatory cells may contribute to interstitial fibrosis in the atria. Leucocyte derived haeme enzyme myeloperoxidase has been shown to be a critical regulatory switch modulating

matrix metalloproteinases (MMP), a key enzyme in extracellular matrix (ECM) turnover leading to atrial fibrosis.(250,252)

TGFβ superfamily and endothelin-1 system overexpression was seen in our obesity model as has been described in human obesity.(294,295) TGFβ signaling pathway is crucial regulating systems in cardiac fibrogenesis acting primarily through SMAD protein pathway(296). Endothelin system acts downstream to TGFβ1 and activates the procollagen I promoter and collagen synthesis in fibroblasts(226). It also stimulates aldosterone release via ET-B receptor(227). Previous studies in hypertensive and heart failure rat models have demonstrated that the effect of cardiac fibrosis is mediated through the ET-B receptor(231,232). Our study confirmed atrial TGFβ1 protein and ET-B receptor (key endothelin receptor mediating fibrosis) over-expression with obesity. The atrial TGFβ1 protein also correlated strongly with atrial fibrosis, conduction velocity and CHI, even after adjusting for hemodynamic parameters.

Sustained obesity was associated with diminution of connexin-43 expression. The alteration in distribution and degree of expression of gap junction proteins has been shown to predispose to AF by causing slow and/or inhomogeneous conduction(201).

3.5.5 Reversal of obesity related AF substrate with weight reduction

The Women Health study has shown potential reversibility of risk for developing new AF in women reducing weight over a period of 5 years.(32) A recently published randomized study has demonstrated reduction in AF burden and

severity with weight reduction and cardiometabolic risk factor management in obese patients with diagnosed AF.(297)

Our study describes the reversal in electrophysiological substrate with improvement in conduction abnormalities and normalization of atrial refractoriness. The reduction in inflammation, normalization of ER-B receptor expression and reduction in TGFβ1 expression potentially resulted in reabsorption of collagen and reversal of fibrosis leading to reversal of electrophysiological abnormalities. Normalization of connexin-43 expression with weight reduction could have contributed to decreased propensity for AF.(203) Reversal of electrophysiological substrate has previously been scarcely studied. Reversibility of substrate was first addressed in an experimental heart failure canine model, which demonstrated extensive electrical abnormalities and atrial fibrosis with 5 weeks of ventricular tachypacing (139). In this study, despite the reversal in atrial size and AF inducibility over the next five weeks of recovery, the atrial fibrosis persisted. However, the study was limited by the short period of recovery phase. Reversal has also been studied following mitral commissurotomy in mitral stenosis which led to improvement in conduction abnormalities, reduced fractionation and decreased propensity to AF(97). However, another study reported persistence of conduction abnormalities in right atrium after closure of atrial septal defect(154). The difference in the reversibility may be a factor of duration of exposure to underlying condition, degree of changes and effectiveness of the intervention.
The reversal of substrate and reduced propensity for AF seen in this study with weight reduction is in contrast with the conflicting results with ACE inhibitors and statins which target molecular milieu responsible for fibrosis. However, removal of

the ‘stretch stimulus’ and down regulation of the pro-fibrotic factors with weight reduction may produce a larger and more effective intervention than targeting individual molecular pathway, explaining the results in the study.

3.6 Limitations

This study was performed in a sheep model, and as with all animal studies, confirmation is a pre-requisite through clinical investigation. Although, the sheep were maintained obese for nearly twenty percent of their usual life span to mirror long standing human obesity; the degree of substrate development still may not correlate with humans.

3.7 Clinical Implications

This study provides evidence to support the direct role of obesity in forming the substrate for AF. Furthermore, it demonstrates that weight reduction should be an important component of management of AF in obese individuals.

CONCLUSION

Obesity results in the substrate for AF through a pro-fibrotic milieu leading to structural and electrophysiological remodeling. Importantly, this study demonstrates that modest weight reduction leads to reversal of fibrosis culminating in improvement of electrophysiological parameters and less AF. In addition, the study provides evidence that atrial substrate may reverse significantly with reduction in AF if appropriate intervention is undertaken.

Table 1: Body mass, structural, hemodynamic and electrophysiological and molecular characteristics of obese, weight loss and control groups.

	Control group	Obese group	15% Weight loss	30% Weight loss group	Obese vs Control	Obese vs 15% Weight loss	Obese vs 30% Weight loss	30% Weight Loss vs Control
Weight (kg)	58±6	111±12	94±9	77±8	<0.001	0.001	<0.001	0.001
Total Body fat (kg)	7±4	40±9	31±4	20±8	<0.001	0.01	<0.001	0.002
A pressure (mmHg)	3.8±1.5	9.3±2.0	6.5±3.1	5.3±2.9	<0.001	0.1	0.007	0.7
PA pressure (mmHg)	9.5±2.3	15.1±2.5	13.5±2.5	10.9±2.0	<0.001	0.6	0.002	0.7
Systemic BP (mmHg)	69±11	59±8	64±13	73±14	0.4	0.9	0.1	0.9
LA dimension (major axis, mm)	35.4±3.4	38.6±1.6	38.4±2.5	36.0±2.3	0.05	1.0	0.13	0.9
Conduction velocity(mean, m/s) 400ms CL pacing	1.06±0.23	0.81±0.12	0.83±0.13	1.01±0.20	0.003	1.0	0.01	1.0
Conduction velocity(mean, m/s) 300ms CL pacing	1.08±0.19	0.78±0.11	0.81±0.10	1.03±0.20	0.001	1.0	0.001	1.0
Conduction velocity(mean, m/s) 200ms CL pacing	1.04±0.19	0.78±0.16	0.80±0.11	0.93±0.22	0.02	1.0	0.2	0.6
Conduction heterogeneity (CHI)	1.07±0.19	1.70±0.59	1.50±0.53	1.23±0.28	<0.001	0.05	<0.001	0.09
ERP (CL=400)	190±36	147±33	161±33	210±36	0.003	0.7	<0.001	0.4
ERP (Cl=300)	177±20	145±29	153±33	191±29	0.001	0.9	<0.001	0.6
ERP (CL=200)	145±15	128±20	126±21	138±22	0.06	1.0	0.6	0.7
Cumulative AF (seconds)	135[34-214]	323[198-1331]	118[20-1671]	93[0-573]	0.03	0.1	0.05	0.9
Inflammation (Inflammatory cell/hpf)	0.8 [0.4-2.0]	8.9 [7.6-12.8]	5.1 [3.0-8.0]	3[1.8-3.8]	<0.001	<0.01	<0.001	<0.001
Fibrosis (%Staining; morphometry)	5.1±0.7	7.5±2.4	7.8 ±2.5	5.5±1.5	0.01	1.0	0.01	1.00
Atrial TGFβ1 protein expression	0.30[0.18-0.55]	1.64[1.44-2.25]	1.62[1.33-1.96]	0.83[0.42-1.41]	<0.001	1.0	0.07	0.01
Endothelin 1	0.71±0.13	0.69±023	0.72±0.41	0.84±0.36	NS*	NS*	NS*	NS*
Endothelin Receptor A	0.50±0.19	0.79±0.52	0.54±0.54	0.82±0.51	NS**	NS**	NS**	NS**

Endothelin Receptor B	0.87±0.30	1.32±0.36	0.89±0.38	0.77±0.28	0.04	0.04	0.01	1.0
Connexin43 (%Stain; morphometry)	2.7±0.6	1.8±0.4	2.0±0.4	2.5±0.5	0.03	1.0	0.01	1.0

* Group main effect p=0.4. Post doc test not performed.

** Group main effect p=0.4. Post doc test not performed.

Figure1: Study Outline.

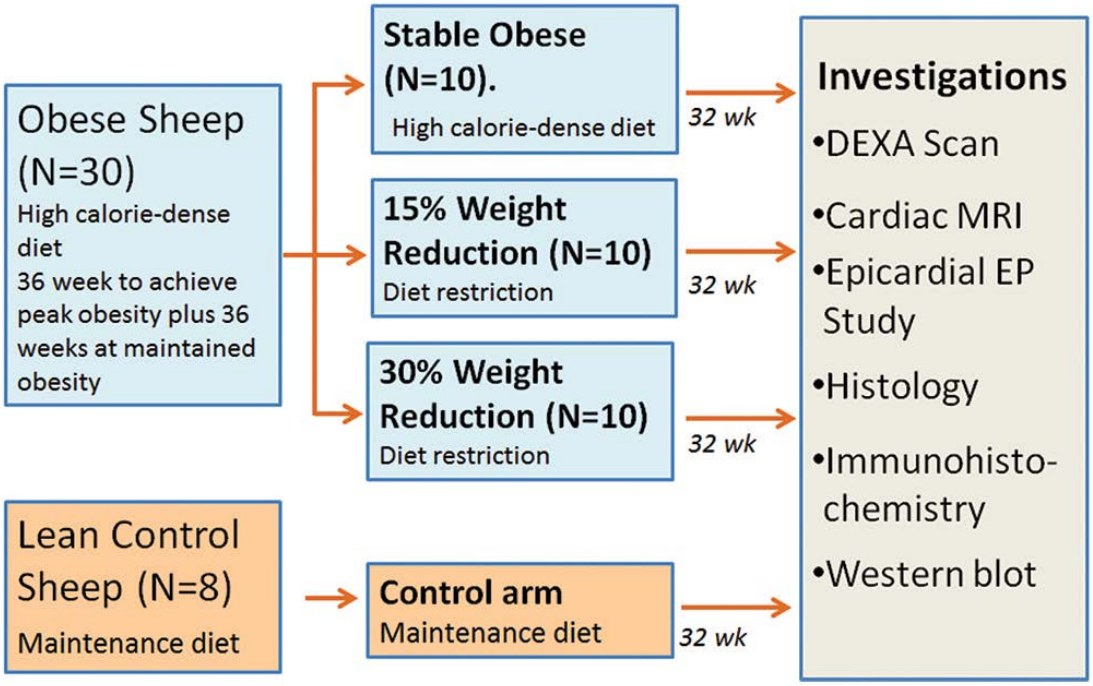

The weight of the obese sheep reached the maximum at 36 weeks. These obese sheep were subsequently maintained at this weight for another 36 weeks prior to randomization to three groups i.e. obese, 15% and 30% weight loss. Weight reduction was achieved by restricting dietary intake over 32 weeks. Eight sheep were maintained lean to serve as controls.

Figure 2: Representative activation maps (panel I) and corresponding phase histograms (panel II) of left atrium (300ms cycle length) in control, obese, 15- and 30% weight reduction groups.

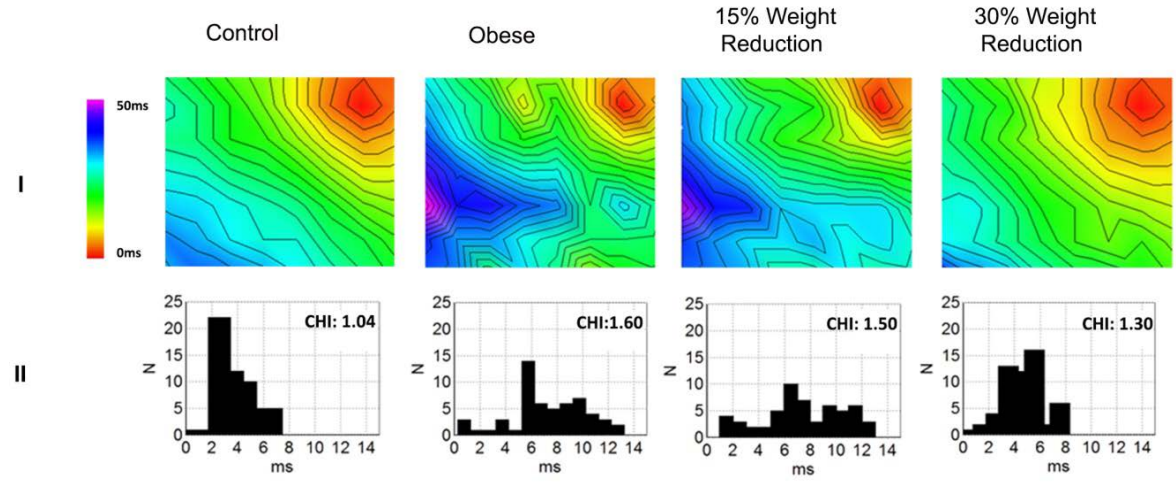

The plaque was paced from the corner. The maps are drawn to the same scale and 2ms Isochrones are superimposed to facilitate visualization of isochronal crowding that represent conduction slowing and block. The phase histograms represent conduction heterogeneity, a measure of conduction variability, with greater dispersion representing greater heterogeneity. Increase isochronal crowding and longer activation times are noted in obese group and improvement with 30% weight loss. Elevated conduction heterogeneity index (CHI), as reflected in greater dispersion on phase histograms was seen in the obese group with improvement with 30% weight reduction.

Figure 3: I) ERP distribution II) Conduction velocity and III) Conduction heterogeneity in control, obese, 15- and 30% weight loss groups.

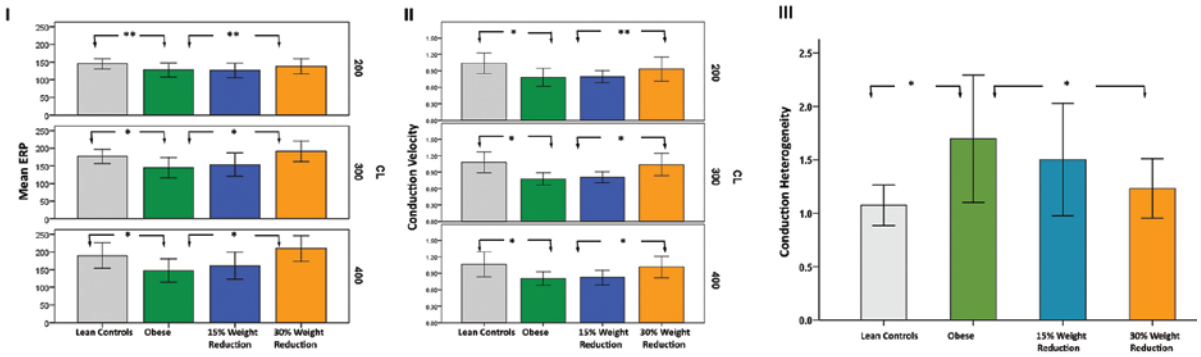

*: Significant, **: Non-significant.

Figure 4: Inflammation, fibrosis and connexin expression with weight loss

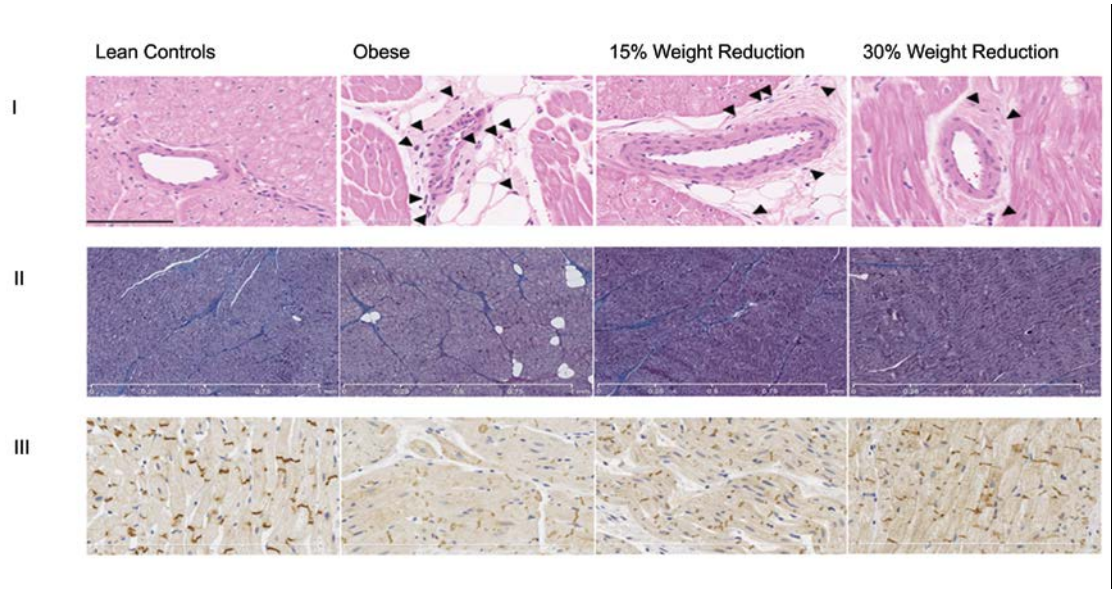

I) H&E stained high sections showing inflammatory infiltrate in the perivascular space in the LA posterior wall. The perivascular space was expanded in obesity and infiltrated with inflammatory cells. Some of the inflammatory cells are marked by arrowheads. The inflammation reduced stepwise with weight reduction. Scale bar 100μm. II) Masson trichome stained sections (X5) of the LA posterior wall. Fibrosis was quantified morphometrically. There was increased deposition of fibrous tissue in obesity which reversed with weight reduction III) DAB stain Connexin43 sections (X20) of the LA posterior wall. The Connexin43 expression was analyzed morphometrically. The connexin43 was distributed along the intercalated discs. Connexin43 expression was diminished with obesity without alteration in distribution. Weight reduction restored the normal expression.

Figure 5: Atrial TGFβ1 and Endothelin, ER-A and B expression with weight reduction

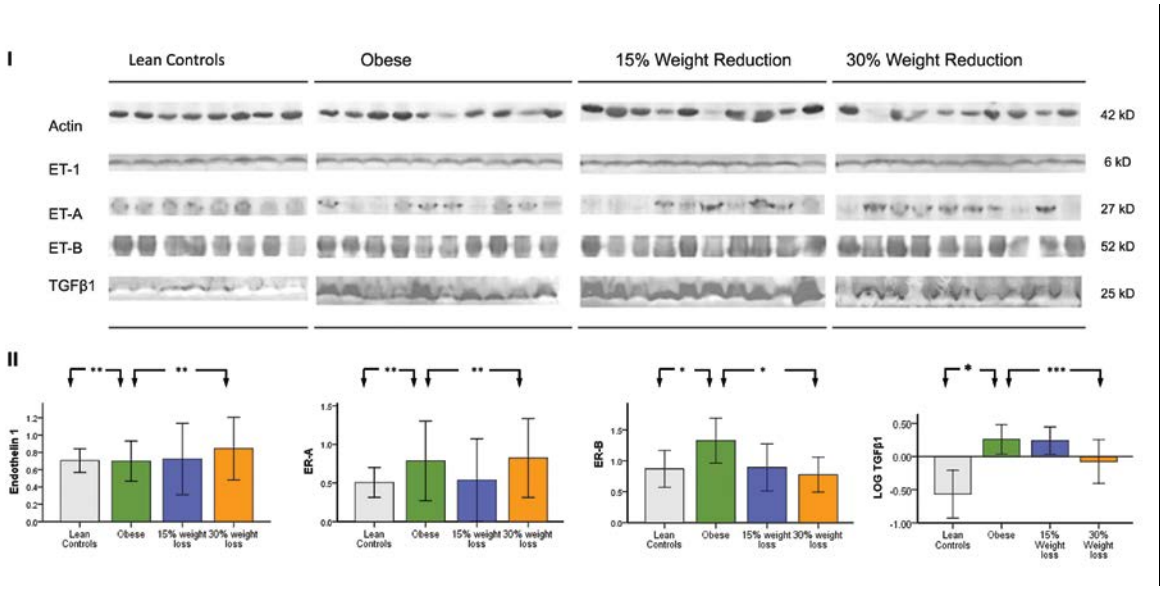

I) Western Blot analysis of atrial Endothelin-1, Endothelin receptor A and B, TGFβ1protein expression in control, obese, 15- and 30% weight loss groups. Data was densitometrically scanned from blots of each case and then used to determine relative difference in TGFβ1 protein expression. II) Bar graphs showing changes in atrial Endothelin-1, Endothelin receptor A and B, TGFβ1 protein expression with obesity and weight reduction. See text for details. Overall group p values were significant for Endothelin receptor B and TGFβ1 protein and non-significant for Endothelin-1 and Endothelin receptor A. *: Significant, **: Non-significant, ***: Trend.

Chapter 4

Obesity and Weight Reduction: Impact on the endocardial substrate for Atrial Fibrillation

4.1 Introduction

Obesity and atrial fibrillation (AF) are issues of public health importance (2,3,263). The prevalence of obesity has increased by 50% in the last few decades with 75% of adults over 40 years of age being classified as overweight or obese(263). It is this age group which is mainly affected with non valvular AF. Obesity has been implicated as a new factor predisposing to the development of AF(29,32,33,266,284). A meta-analysis of population based studies has demonstrated a graded 'dose response relationship' with the relative risk of developing atrial fibrillation (AF) incrementally rising from 1.3% to 2.1% to 3.2% in the normal weight, overweight and obese population respectively(33). Furthermore, data from Women Health Study, suggests that the risk of developing new AF may diminish with weight reduction(32).

Although experimental studies have suggested that development of substrate may be prevented, reversal has been incompletely demonstrated(292). In this endocardial mapping study in a chronic obese ovine model, we evaluate the effect of weight reduction on reversibility of the endocardial biatrial substrate for AF.

4.2 Methods

All animal handling was conducted in accordance to the guidelines for use and care of animals for research by the National Health and Medical Research Council of Australia on research animal use. The study was approved by the Animal Research Ethics Committee of the University of Adelaide and SA Pathology, Adelaide, Australia.

4.2.1 Study Groups

Figure 1 provides the study outline. Ten sheep had induced obesity by ad-libitum calorie dense diet over a 36 week period and maintained their weight for another 24 weeks. These sheep were then subject to 32 weeks weight reduction. Ten lean sheep of similar age served as control. 10 animals in obese state and of these 8 animals after weight reduction and 10 controls underwent: imaging (DEXA and Echocardiography), hemodynamic assessment, and bi-atrial endocardial electroanatomic mapping and electrophysiological evaluation. The animals will be pre-acclimatized for at least one week prior to study.

4.2.2 Obese Ovine Model

Weight gain: A previously described ovine model of progressive weight gain, based on ad-libitum regimen of hay and high energy pellets, was utilized to induce progressive weight gain(285). At baseline, healthy sheep were commenced on a high caloric diet of energy-dense soybean oil (2.2%) and molasses fortified grain and maintenance hay with weekly weight measurement. Excess voluntary intake was predominantly of grass alfalfa silage and hay. For the obese sheep, pellets were gradually introduced at 8% excess basal energy requirements, and rationed to ≥70% of total dry matter intake. The sheep gradually gained weight to terminal

obesity in 36 weeks and were subsequently maintained at this weight for 24 weeks.

Weight reduction: The obese sheep then underwent gradual weight reduction over 32 weeks. The energy-dense soybean oil and molasses fortified feed was gradually withdrawn and replaced with high quality cereal hay which was reduced to two-third of the normal intake. The weight was monitored weekly. Blood samples were periodically collected to ensure electrolyte and acid-base homeostasis.

The control sheep were maintained at their baseline weight with high quality cereal hay provided ad-libitum and energy dense pellets rationed at 0.75% of live weight. Nutritional content of food and housing conditions were identical between both groups, but only the amount was varied. Shorn weight was recorded immediately prior to surgery.

4.2.3 DEXA scan

The DEXA scan was performed to determine total body fat in the animals. The DEXA scan was performed under general anesthesia.

4.2.4 Transthoracic echocardiography

An echocardiogram was performed under general anesthesia prior to the electrophysiology study. The left atrial diameter and length were measured in apical 4-chamber view. The left ventricular dimensions were measured in M-Mode in parasternal long axis view at the level of mitral leaflet tips. The left ventricular dimensions were utilized to determine global left ventricular function.

4.2.5 Electrophysiological study

Electrophysiological study was performed in the post absorptive state under general anesthesia. A 10-pole catheter with 2-5-2 mm inter-electrode spacing

(Daig Electrophysiology, Minnetonka, MN) was positioned in the coronary sinus with the proximal bipole positioned at the ostium of coronary sinus in the best left anterior oblique view. A transeptal puncture was performed using conventional techniques under fluoroscopy to map the left atrium.

Surface electrocardiogram (ECG) and bipolar endocardial electrograms were continuously monitored and stored on a computer based digital amplifier/recorder system for off-line analysis (LabSystem Pro, Bard Electrophysiology, Lowell, MA, USA). Intracardiac electrograms were filtered from 30 to 500 Hz, and measured with computer assisted calipers at a sweep speed of 200 mm/s.

4.2.5.1 Electroanatomical mapping

Electroanatomic maps of the right and left atrium was created of during sinus rhythm using the CARTO XP mapping system and a 3.5-mm tip catheter (Navistar, Biosense-Webster). The electroanatomic mapping system has been previously described in detail(298); the accuracy of the sensor position has been previously validated and is 0.8 mm and 5°. In brief, the system records the surface ECG and bipolar electrograms filtered at 30 to 400 Hz from the mapping and reference catheters. Endocardial contact during point acquisition was facilitated by electrogram stability, fluoroscopy, and the catheter icon on the CARTO system. Points were acquired in the auto-freeze mode if the stability criteria in space (≤6mm) and local activation time (LAT; ≤5ms) were met. Mapping was performed with an equal distribution of points using a fill-threshold of 15 mm. Editing of points was performed offline. Local activation time was manually annotated to the peak of the largest amplitude deflection on bipolar electrograms. In the presence of double potentials, the LAT was annotated at the largest potential. If the bipolar

electrogram displayed equivalent maximum positive and negative deflections, the maximum dv/dt on the simultaneously acquired unipolar electrogram was used to annotate the LAT. Points were excluded if they were not conforming to the surface ECG P-wave morphology or if they were < 75% of the maximum voltage of the preceding electrogram. Regional atrial bipolar voltage and conduction velocity were analyzed offline and are detailed below.

4.2.5.2 Atrial conduction velocity

Isochronal activation maps (5-ms intervals) of the atria were created and regional conduction velocity determined in the direction of the wave-front propagation (least isochronal crowding). The CARTO system determines conduction velocity by expressing the distance between 2 points as a function of the difference in local activation time. For analysis, each atrium was segmented as previously described(92,98,117,299). The RA was segmented as the high- and low-lateral RA, high- and low posterior RA, high- and low-septal RA, and anterior RA. The LA was segmented as posterior LA, anterior LA, septal LA, inferior LA, lateral LA, and LA roof. Mean conduction velocity for each region was determined by averaging the conduction velocity between 3-5 pairs of points, as previously described(92,98,99,117,299).

The proportion of points demonstrating delayed conduction was determined using the following definitions: 1) fractionated signals: complex activity of 50ms duration with 3 or more deflections from baseline; and 2) double potentials: potentials separated by an isoelectric interval and the total electrogram duration ≥50ms(99).

4.2.5.3 Atrial voltage

For the purpose of evaluating regional bipolar voltage, the atria were segmented as above. For each region the mean voltage was obtained by determining the mean of the bipolar voltage of the points within the given region. The global voltage of the chamber was obtained by calculating the mean of the means of the different segments. An index of heterogeneity of the bipolar voltage amplitude was determined by calculating the coefficient of variation of the different regions in each chamber. Low voltage areas were defined as contiguous points with a bipolar voltage <0.5 mV. Electrically silent areas (scar) was defined as contiguous points with absence of recordable activity or a bipolar voltage amplitude <0.05 mV (the noise level of the system) as previously described(92,117,299).

4.2.5.4 Effective Refractory Period

Effective refractory period (ERP) testing was performed after the electroanatomic mapping. Atrial ERPs were evaluated at twice the diastolic threshold at cycle lengths (CLs) of 450 and 300ms using an 8-beat drive train followed by an extra-stimuli (S2), starting with an S2 coupling interval of 120ms increasing in 10ms increments. The ERP was defined as the longest coupling interval failing to propagate to the atrium. ERP was measures from the following 7 sites: (1) right atrial appendage, (2) right atrial lateral wall- upper, (3) right atrial free wall-lower, (4) proximal CS, (5) distal CS, (6) left atrial appendage and (7) left atrial posterior wall. ERP was measured 3 times at each cycle length and averaged. If ERP varied by more than 10ms, an additional 2 measurements were made and the total number averaged. ERP heterogeneity was determined by the coefficient of ERP variation at each cycle length (CoV = SD/mean × 100%).

4.2.5.5 AF inducibility and duration

AF inducibility was assessed during ERP testing. Atrial fibrillation was defined as irregular atrial activity lasting at least 2 seconds(89). AF occurring in absence of ERP testing or pacing was defined as spontaneous. AF lasting more than 5 minutes was considered sustained; when this occurred no further data was acquired.

4.2.6 Hemodynamic assessment

Invasive blood pressure monitoring was performed during the electrophysiology study. Left atrial, right atrial and pulmonary artery pressures were recorded.

4.3 Statistical Analysis

Normally distributed continuous data are expressed as mean ± standard deviation, whilst median and inter-quartile range [in square brackets] were utilized for middle descriptors for significantly skewed distributions (KS <0.05). Statistical significance was set as $p<0.05$.

A mixed effects model was used for all analyses to account for the nested data within each animal (eg. 7 ERPs, regional conduction velocity and voltage) and also, the repeated measures in eight animals (obese and obese weight loss) as compared to a separate control group. In data containing left and right atrial components, a mixed effects model was created between the groups (obese and obese/weight loss) to examine the main effects of group, atrium (right and left atrium) and their interaction. If no group by atrium interaction was present, the model was re-run with the main effects only. To compare these results against the control group, we developed a three group model with only atrium and group main effects, with Sidak adjusted post-hoc analyses, in the case of a significant group main effect.

For data without multiple measures or levels of data within an animal (e.g. LA size, LVEF) a conventional one way ANOVA methodology was used with Sidak adjusted post-hoc testing as warranted. When log transformation did not result in a satisfactorily normal distribution (ie. number of AF episodes), the data were analyzed using a 3 group Kruskal-Wallis test and group pair-wise post-hoc testing with Mann-Whitney U. All analyses were performed using SPSS/PASW version18 (SPSS Inc. Chicago, IL).

4.4 Results

4.4.1 Group characteristics

Ten obese sheep gained weight over a period of 36 weeks and remained at stable obesity for 24 weeks. These obese sheep underwent gradual weight reduction over 32 weeks. Of these 10, 8 underwent successful weight reduction and underwent repeat evaluation. The control sheep maintain their weight over this period.

4.4.2 Body mass Characteristics

Table 1 describes the body mass characteristics of the two groups. The obese group significantly reduced their weight from 110±9kg to 79±7kg but not to control levels (60±7kg). Concurrently, the obese group significantly reduced their total body fat from 34.5±6.0kg to 17.0±6.1kg but not to control levels (8.7±5.6kg)

4.4.3 Structural and hemodynamic remodeling

The left atrium (LA) dimensions significantly reduced and revere remodeled to control size after weight loss (Table 1). Similarly left ventricular hypertrophy was observed in obese sheep which reversed with weight reduction. However the left

ventricular ejection fraction did not differ significantly between the three groups (p value 0.97).

The mean left atrial and the pulmonary artery pressures significantly reduced with weight loss in obese sheep to a stage that they were no longer significantly different from control group. The systemic blood pressure was did not significantly change with obesity and upon weight loss (p value 1.0).

4.4.4 Electroanatomic remodeling

Both the left and right atria (RA) were enlarged in the obese group ($p<0.001$) and they revere remodeled with significant reduction in volume of both the chambers with weight loss ($p<0.001$) to a level that it was no longer different from controls ($p=0.23$). The electroanatomic maps of both the atria were created in sinus rhythm. The electrophysiology data has been summarized in Table 1.

4.4.4.1 Conduction velocity

The mean conduction velocity improved significantly in both the atrial chambers with weight reduction to a level that it was no longer significantly different from controls (Table 1, Figure 2). Despite the improvement in mean conduction velocity, the reduction in conduction heterogeneity was non-significant with weight loss (22.0 ±6.1% vs 19.7±5.1%, p=0.49).

4.4.4.2 Complex fractionation

The percentages of fractionated potentials/ double potentials (FP/DP) in both the atria reduced significantly with weight loss. The FD/ DP reduced from 53.4±13.6% to 41.4±11.6% in the LA and 36.0±12.2% to 31.2±10.6% in the RA with weight loss ($p<0.001$). Despite the reduction, the signal fractionation was significantly higher than the controls (LA 10.8±4.4%, RA 8.2±2.9%, $p<0.001$).

4.4.4.3 Voltage

The mean voltage in the obese group (LA 4.5±1.7 mV, RA 4.1±1.6 mV), after weight loss (LA 4.9±1.6, RA 3.9±1.2mV) and controls (LA 4.4±1.4 mV, RA 3.6±0.9mV) did not differ significantly in sinus rhythm (Figure 3, Table 1). There was no area of low voltage or scar in either chamber in obese-pre and post weight reduction and control groups. However, regional voltage heterogeneity was elevated in the obese group (32.1±8.8%) as compared to the controls (24.6±7.5%; p=0.01). This increased voltage heterogeneity reduced non-significantly with weight loss (29.1±4.5%, p=0.49), to a level that it was no longer significantly more than control group (p=0.21).

4.4.4.4 Atrial refractoriness

The atrial ERP, at both 450 and 300ms cycle length, from the seven sites did not differ significantly in the obese-pre and post weight reduction and control groups (Table 1, Figure 4A). The ERP heterogeneity, at both 450 and 300ms cycle length, from the seven sites, also did not significantly differ between the obese-pre and post weight reduction and control groups (Table 1).

4.4.4.5 Vulnerability for atrial fibrillation

AF inducibility was evaluated during ERP testing. The median AF episodes did not differ significantly in the obese group pre (4.5 (2.5-6.5)) or post weight loss (4 (2.8-5.5) (p=0.65). Similarly, the mean AF episode duration remained elevated despite weight loss (Table 1).

4.5 Discussion

4.5.1 Major Findings

This study demonstrates new information regarding the reversal of endocardial remodeling that occurs as a consequence of obesity. It observes partial reversal of obesity related AF substrate with modest weight reduction. Weight reduction resulted in reduction of the total body fat 34.5kg to 17kg although still greater than the lean controls (8.7 kg). The following features were observed with weight reduction:

- Reversal of bi-atrial enlargement with weight reduction;
- Normalization of obesity related elevated left atrial and pulmonary artery pressures;
- Improvement in regional conduction velocity to control levels with weight reduction. However, the regional conduction heterogeneity did not significantly reverse with weight loss achieved;
- Reduction in complex fractionated electrograms with weight loss;
- Obesity and weight reduction had no impact on endocardial atrial refractoriness.

4.5.2 Substrate for AF in Obesity

Epidemiology studies have demonstrated a link between obesity and atrial fibrillation(29,32,33,266,283,284,289). Experimental studies in obese ovine model has demonstrated diffuse atrial fibrosis and over-expression of pro-fibrotic factors resulting in epicardial and endocardial conduction abnormalities and increased vulnerability for AF(121,300). The remodeling with obesity is distinct from

electrical remodeling(85) and is consistent with structural remodeling observed with experimental heart failure(86) and hypertension(89) as well as in clinical studies(92,95,96). This has been confirmed by Munger and coworkers in patients undergoing ablation for AF. They reported impaired conduction from the left atrium into the pulmonary veins(123). Atrial refractoriness has been demonstrated to be shortened in clinical as well as epicardial mapping pre-clinical studies.

4.5.3 Mechanism of AF in obesity

Obesity results in chronic stretch and dysregulation of the pro-fibrotic signaling pathways leading to atrial fibrosis (300). This is a common factor with other precursors of AF like hypertension and heart failure (86,91,231,232). In addition, epicardial fat is thought to play a unique role in substrate development in obesity(274,276,279,301-303). Like other visceral fat depots, it is metabolically active and secretes pro-fibrotic adipo-cytokines that promote atrial fibrosis(216). The close association with heart muscle and absence of separating fascia facilitate the paracrine action(304). We have previously demonstrated infiltration of the atrial musculature by the contiguous epicardial fat in obese sheep. This may represents a unique substrate in obesity(305) and could potentially promote re-entry and AF in a fashion that is proposed for fibrosis.

Experimental studies have demonstrated increased expression of the TGFβ and endothelin signaling pathways in sustained obesity(300). Although the signaling pathways for fibrosis are still not well understood, there is evidence to suggest TGFβ1 is central to these pathways(296,306). It interacts with other signaling molecules, including the downstream endothelin pathway, to regulate matrix

protein synthesis. Dysregulation of these pathways leads to deposition of excessive collagen and matrix proteins resulting in fibrosis.

Decreased expression of gap-junction protein connexin-43 has also been demonstrated with obesity. Unlike infarction, there was no distortion of the distribution of connexin-43. However, the overall expression has been reported to be reduced in obesity. Dysregulation of endothelin signaling pathway may play a role in connexin-43 expression(204). In addition, enhanced endothelin system activity has been described in obesity(295) suggesting that endothelin system may have a role in creating a substrate for AF by altering connexin43 expression. However, gaps in knowledge persist in the role of connexin in atrial fibrillation with issues like multiple connexin expression (in atria), heteromeric/ heterotypic gap junction, functionality of the remodeled gap junctions clouding the exact role in AF substrate genesis(201).

4.5.4 Reversal of the substrate for AF due to obesity

Structural remodeling and associated conduction abnormalities have been recognized to be integral to substrate development for AF. The degree of reversibility with removal of inciting factor or intervention is variable and not fully characterized. *John et al* demonstrated improvement in conduction abnormalities with reduced fractionation after mitral commissurotomy in mitral stenosis which was associated with decreased propensity to AF(307). *Lau et al* have described prevention of conduction abnormalities and reduction in interstitial fibrosis with omega-3 polyunsaturated fatty acids in a heart failure model(308). However, *Morton et al*, demonstrated persistence of conduction abnormalities in right atrium after closure of atrial septal defect(154). The difference in the reversibility may be

a factor of duration of exposure to underling condition, degree of changes and effectiveness of the intervention.

We have earlier shown that weight reduction results in improved epicardial conduction, normalization of epicardial atrial refractoriness, reduction in pro-fibrotic atrial TGFβ1 and Endothelin Receptor-B , fibrosis and normalization of connexin-43 expression(300). The endocardial electroanatomic remodeling occurred along a similar line, albeit the reduction in AF vulnerability during endocardial ERP testing was not observed. This could represent a residual endocardial substrate persisting despite weight reduction.

4.6 Limitations

We describe an extremely obese model with fivefold increase in total body fat. The extreme obesity may be possibly responsible for incomplete reversal of electrophysiological changes noted with weight reduction. In addition, even after weight reduction, the body fat was significantly more than the controls. It is not known whether the changes would further regress with further weight loss or even sustained weight loss for a longer duration. Also, the level of obesity beyond which the changes do not completely reverse with weight loss is not known.

Finally, the development of clinical AF is a complex process, with other factors such as triggers and perpetuators which are not addressed in the current study.

4.7 Clinical Implications

This study provides evidence to support the direct role of obesity in forming the substrate for AF. It raises caution that not all of the elements of the AF substrate

may be resolved with weight reduction and highlights the need for prevention of the obesity epidemic.

4.8 Conclusion

Obesity results in structural, hemodynamic, endocardial electrophysiological remodeling. Although structural and hemodynamic changes completely reverse, the endocardial electrophysiological changes only reverse partially with weight reduction.

Table 1: **Body mass, structural, hemodynamic and electrophysiological characteristics of Obese- pre and post weight loss and Control groups**

Parameter	**Control**	**Obese**	**Weight Reduction**	**p value**	**p value**	**p value**
				Control vs Obese	**Obese vs Weight loss**	**Weight loss vs Control**
Weight (kg)	60±7	110±9	79±7	<0.001	<0.001	<0.001
Total Body fat (Kg)	8.7±5.6	34.5±6.0	17.0±6.1	<0.001	<0.001	0.02
LA transverse diameter (mm)	36.2±1.3	38.3±1.9	36.1±2.4	0.05	0.06	1.0
LA anterio-posterior diameter (mm)	27.7±1.1	30.1±1.4	26.8±2.2	0.01	<0.001	0.51
LVEF (%)	69.8±5.0	70.4±5.9	69.8±5.3	NS*	NS*	NS*
LV posterior wall thickness (mm)	7[7-7]	9[8-10]	8[7-8]	0.001	.02	0.24
LA mean (mmHg)	3.7±1.4	8.1±2.8	5.8±2.7	<0.001	0.01	0.09
PA mean(mmHg)	9.8±2.6	15±0.7	11.5±1.7	<0.001	0.01	0.29
Systemic BP mean (mmHg)	70.7±11.8	86.3±13.4	88.4±23.6	0.19	1.0	0.32
LA volume- CARTO (ml)	73.5±12.8	86±15.0	66.4±8.8	<0.001#	<0.001#	0.23#
RA volume-CARTO (ml)	75.1±14.5	89.3±15.9	64.5±8.6			
Conduction Velocity (mean, m/s) –LA	1.58±0.22	1.18±0.28	1.49±0.33	<0.001#	0.001#	<0.001#
Conduction Velocity (mean, m/s) –RA	1.43±0.16	1.03±0.24	1.31±0.29			
CV heterogeneity (%)	9.1±4.9	22.0±6.1	19.7±5.1	<0.001	0.49	<0.001
FD/DP LA (%)	10.8±4.4	53.4±13.6	41.4±11.6	<0.001#	<0.001#	0.30#

FD/DP RA (%)	8.2±2.9	36.0±12.2	31.2±10.6			
Voltage RA (mean, mV)	3.6±0.9	4.1±1.6	3.9±1.2	NS*	NS*	NS*
Voltage LA (mean, mV)	4.4±1.4	4.5±1.7	4.9±1.6	NS*	NS*	NS*
Voltage Heterogeneity (%)	24.6±7.5	32.1±8.8	29.1±4.5	0.01	0.49	0.21
ERP mean (ms) CL 300ms	182±26	180±24	187±27	NS*	NS*	NS*
ERP heterogeneity at CL 300 (%)	10.0±4.2	10.5±3.3	12.4±4.0	0.99	0.67	0.50
ERP mean (ms) CL 450ms	189±29	190±31	194±38	NS*	NS*	NS*
ERP heterogeneity at CL 450 (%)	10.3±3.3	16.3±5.4	13.6±5.1	0.01	0.29	0.32
AF episodes- total	1(0-2)	4.5(2-7)	4(2.5-6)	0.01	0.65	0.07
AF episode duration)(seconds)	2.7[2-5]	7.9[5-17.7]	43[9-226]	0.03	0.08	0.01

* Post hoc test not performed as group main effect was not significant (p >0.05)
# P-value represents overall group effect for both LA and RA in a model that included group, atrium and their interaction.

Figure 1: **Study outline**

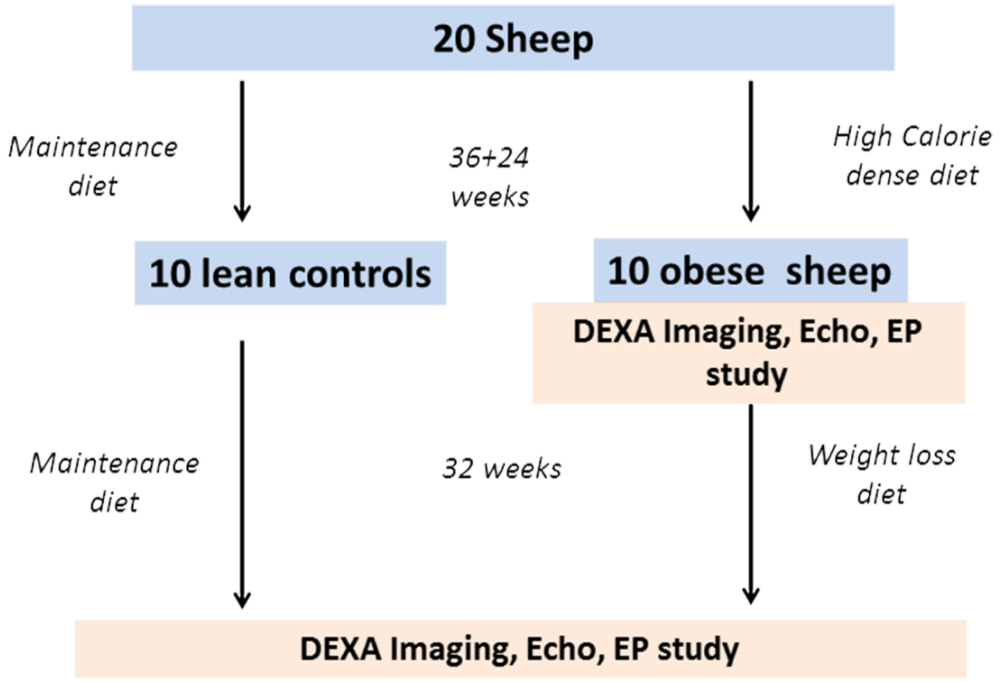

Figure 2: Endocardial conduction velocity and heterogeneity with weight reduction

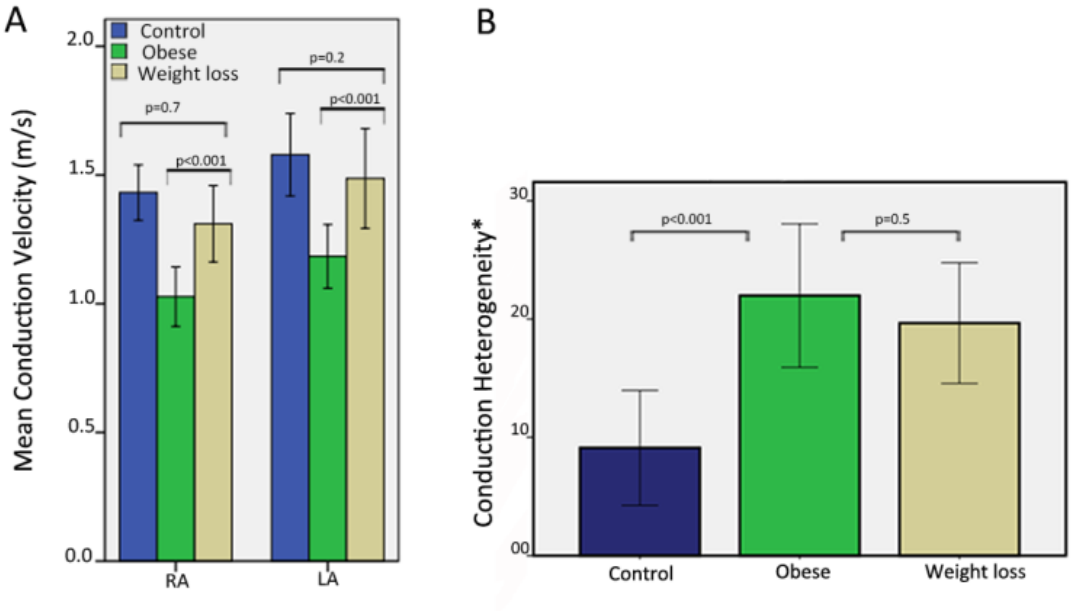

A) Mean conduction velocity (CV) and **B)** CV heterogeneity in control, obese-pre and post weight loss groups in sinus rhythm demonstrating improvement in CV with weight reduction. * Conduction heterogeneity= Variation of CV variation (SD/meanX100%)

Figure 3: Representative bipolar voltage map of the left atrium in sinus rhythm in control and obese group- pre and post weight loss demonstrating reduction in volume and fractionation with weight loss.

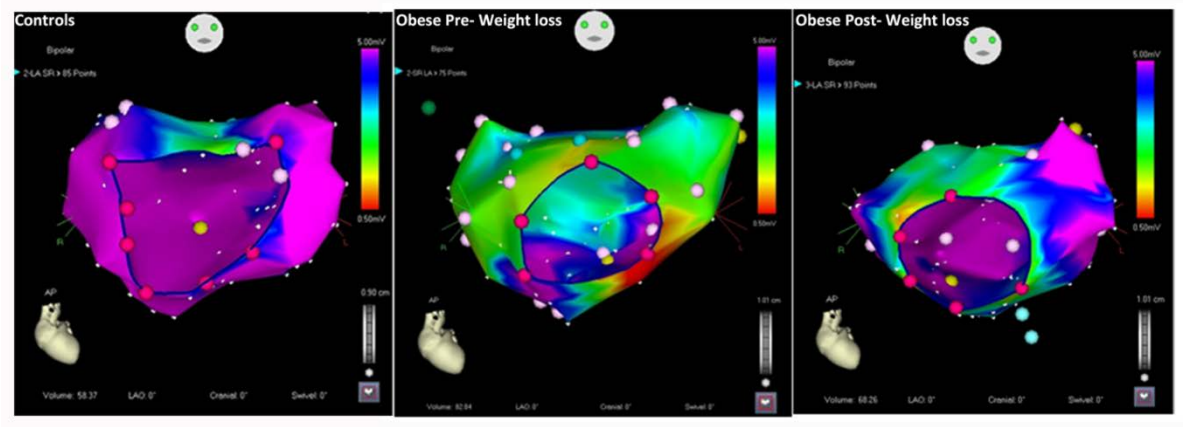

There were no low voltage areas/ electrical scar in the obese animals

Figure 4: ERP distribution in Obese-pre and post weight loss and Control groups.

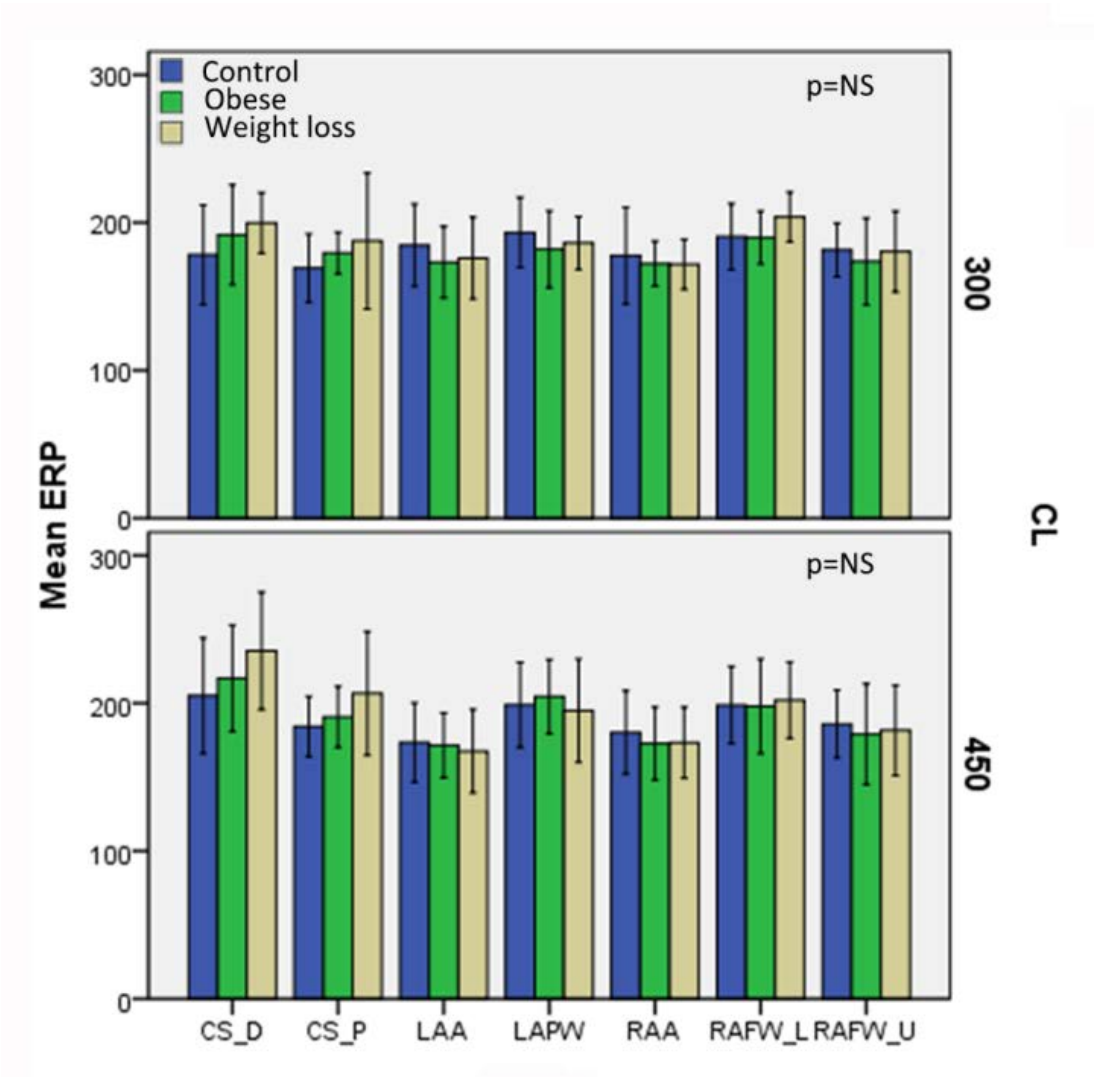

The endocardial ERPs did not change with obesity or weight reduction.

Chapter 5

Cardiovascular Magnetic Resonance imaging of total and atrial pericardial adipose tissue: A validation study and development of a three dimensional pericardial adipose tissue model

5.1 Introduction

The increasing prevalence of atrial fibrillation (AF) has been in-part attributed to the aging population and its associated co-morbidities such as hypertension, coronary artery disease and heart failure. However, there is increasing evidence that obesity contributes to the burden of atrial fibrillation in our population. Analyses from the Framingham and Women Health Studies (WHS) suggest that obesity is associated with an increased risk of AF independent of other traditional risk factors(10,32). These population-based studies have utilized body mass index as a measure of obesity. Recently, pericardial adipose tissue (PAT), both total and atrial, has been demonstrated to predict AF risk independently of weight and other measures of obesity (274,301,309). This has two important implications. Firstly, PAT could have a causal relationship with the risk of AF and it has been hypothesized that this effect could be mediated locally (303,310,311). Secondly, a change in atrial PAT mass with weight change could be a better predictor of the risk of AF as compared to other measures of weight change. Although, ventricular

paracardiac adipose tissue CMR measurement has been validated before, the validation of the patchy and smaller volume of atrial PAT with the gold standard of mass at autopsy has not been previously performed(312). In this study we sought to validate the quantification of atrial and total PAT utilizing a three dimensional atrial PAT model.

5.2 Methods

Ten merino cross sheep with weight ranging from 67 to 103 kilograms were included in the study. All procedures were conducted in accordance with the guidelines outlined in the "Position of the American Heart Association on Research Animal Use" adopted on November 11, 1984 by the American Heart Association. The study protocol was reviewed and approved by the Animal Research Ethics Committees of University of Adelaide and Institute of Medical and Veterinary Services, Adelaide, Australia.

5.2.1 Definitions

The fat deposits around the heart have been defined in this study as:

Epicardial adipose tissue was defined as the adipose tissue between the myocardium and visceral pericardium(313,314).

Paracardiac adipose tissue was defined as the adipose tissue adherent and external to the parietal pericardium(315).

Pericardial adipose tissue was defined the sum of the epicardial and paracardiac adipose tissue(316).

5.2.2 Cardiovascular Magnetic Resonance Protocol and Analysis

All animals underwent CMR immediately prior to euthanasia for the evaluation of pericardial adipose tissue. The CMR was performed using a 1.5 Tesla system (Siemens, Sonata, Erlangen, Germany).The animals were anaesthetized and placed supine within the CMR bore. The animals were mechanically ventilated to allow breath holding sequences to be performed. Sequential steady state free precession (SSFP) short-axis cine sequences were acquired with 6mm slice-thickness and no interslice gaps through both the atrial and the ventricles. Slices were aligned to at 90 degrees to the long axis of the left ventricle, and planned from the most cranial aspect of the left atrium and proceeded caudally to the left ventricular apex. All images were acquired at end expiration with the following parameters (slice thickness 6mm/0mm, TR/TE 52.05 ms/1.74 ms, flip angle 70 degree, matrix 256x150, FOV 380 mm). In order to replicate standard clinical protocols, this study intentionally did not incorporate adipose-specific sequences.

The image analysis was conducted offline using custom made software. The areas of pericardial adipose tissue were traced on consecutive end diastolic images (Figure 1). The ventricular pericardial adipose tissue was defined as adipose tissue from the mitral valve hinge (point of insertion at the annulus) down to the ventricular apex, inclusive of the most inferior margin of the adipose tissue. The atrial pericardial adipose tissue was defined as the pericardial adipose tissue lying above the mitral valve hinge and below the right pulmonary artery. Not all CMR images were of sufficient quality to adequately define the visceral pericardium, particularly in atrial slices, and as a result no attempt was made to differentiate epicardial and paracardiac components of adipose tissue.

In order to quantify total volume of adipose tissue, a three dimensional (3D) model was constructed using semi-automated software developed by the authors. Regions of PAT were marked in each slice followed by linear interpolation of pixel intensities in spaces between consecutive image slices. The total fat volume was quantified on the three dimensional model was converted to mass by multiplying it with a density constant of 0.9.

Assessment of atria, ventricular and total cardiac fat volume measured by CMR scans was performed twice by the primary investigator to determine intra-observer measurement error. An additional independent and experienced investigator also measured the fat volume components to establish an inter-observer agreement. All measures of CMR fat were performed blinded to the autopsy values.

5.2.3 Pericardial fat quantification at Autopsy

The sheep were euthanized following acquisition of CMR images. While the sheep were under general anesthesia, the heart was surgically removed from the sheep thorax, with particular attention paid to retrieving all the pericardial adipose tissue. To ensure that all pericardial fat was collected, the heart was excised with the pulmonary veins, right pulmonary artery and the trachea intact. An incision was made circumferentially along the atrio-ventricular groove and the pericardium peeled back towards the apex (Figure 2; Step 2) and collected as the paracardiac ventricular fat. The remaining pericardium was peeled upwards toward the pulmonary artery with all fat up to the pulmonary artery branches being assigned to paracardiac atrial fat. After the trachea was removed from the heart, the fat was then meticulously dissected from the ventricle and atria to collect the epicardial fat (Figure 2; Step 4).The total pericardial adipose tissue for

the atria and ventricles was calculated as the sum of paracardiac and epicardial components (Figure 2; Step 5).

5.3 Statistical Analysis

Normally distributed continuous data are reported as mean ± standard deviation. The agreement between autopsy total, atrial and ventricular pericardial adipose tissue masses and those derived from CMR were assessed via intra-class correlation coefficients (ICC) and Bland and Altman plots with 95% limits of agreement. Consistency, rather than absolute ICCs were calculated via a two way random effects model because of the expected systematic bias toward lower masses on autopsy due to technical limitations in removing all fat from the ex-vivo heart. The inter- and intra-observer reliability of CMR fat assessment was assessed using the same methodology, except that consistency ICCs were calculated. All tests were performed using PASW (Version 18 IBM, Armonk, NY) with $p<0.05$ deemed significant.

5.4 Results

Ten sheep with a mean weight of 80±8 kg were assessed for both CMR and autopsy pericardial adipose tissue assessment, however one sheep was excluded from further analyses due to CMR artifacts precluding accurate assessment. Mean CMR imaging time was 30 minutes per animal. The additional mean time duration to assess pericardial adipose tissue with the semi-automated software was 5±1.4 minutes per animal. On CMR assessment atrial, ventricular and total adipose tissue were assessed as 37±10, 250±71, 287±77g, respectively. On autopsy, the corresponding values were 29±8, 231±70, 260±74g.

5.4.1 Autopsy pericardial adipose tissue regional distribution

The atrial epicardial adipose tissue was distributed predominately adjacent to posterior wall of left atrium and adjacent to the atrio-ventricular groove. The atrial paracardiac adipose tissue deposits were mainly between the appendages and the great arteries (Figure 2). The ventricular epicardial adipose tissue was distributed predominately along the atrio-ventricular groove and the coronary arteries. In contrast, the paracardiac ventricular fat was evenly distributed over the surface of the pericardium.

5.4.2 Agreement of CMR assessment with Autopsy measures of pericardial adipose tissue

Atrial, ventricular and total CMR pericardial adipose tissue correlated strongly with autopsy measurements (ICC>0.80; p<0.003) (Figure 3). CMR systematically over-estimated *total* autopsy fat by a mean of 26g, within 95% confidence limits of ± 23.0 g. The corresponding ventricular and atrial components were overestimated by a mean of 19.0 g (95% CI ± 19.5gms) and 7.7 g (95% CI ±11.6gms), respectively.

5.4.3 Intra- and inter-observer reliability of CMR assessment of pericardial adipose tissue

Intra- observer reliability for CMR measured atrial, ventricular and total fat mass assessment measures was high (ICC>0.0.993), with 95 % levels of agreement ±5.5% for total fat mass, ±8.3% for atrial fat mass and ±6.6%for ventricular mass (Table 2). Similarly, all components of fat measurement (total, ventricular and atrial) ICCs exceeded 0.991 for inter- observer reliability. The 95% limits of agreement were within ±10.7%, ±7.4% and ±7.2% for atrial, ventricular and total pericardial adipose tissue, respectively (Table 3).

5.5 Discussion

To the best of our knowledge, this is the first study to validate a CMR technique to specifically assess atrial pericardial adipose tissue. Our findings demonstrate that: (1) CMR assessment of atrial, ventricular and total fat has high intra- and inter-observer reproducibility, and (2) CMR quantified atrial and ventricular adipose tissue strongly agrees with ex vivo adipose mass, validating its use as a robust measure of pericardial adiposity. Moreover, the findings were reproducible and the image sequences utilized were those which would normally be acquired during a standard clinical CMR scan. Importantly, this study validates a three dimensional model of atrial pericardial adipose tissue which can be utilized to study regional fat deposits with respect to underlying atrial electrophysiological properties.

Echocardiography and computed tomography have previously been utilized for pericardial fat assessment. However, echocardiography is limited by its inability to obtain pericardial volumes and often sub-optimal imaging windows (317). Moreover, echocardiography has been limited to assessment of ventricular pericardial adipose tissue. Although, volumetric assessment of pericardial adipose tissue can be performed by CT, the exposure to ionizing radiation limits its use, especially if serial measurements are planned (318).

Obesity has been demonstrated, in several population based studies, to be a novel risk factor for atrial fibrillation (31,33,247,289). Its association with hypertension, obstructive sleep apnea, diabetes mellitus, coronary artery disease and congestive heart failure, clouds interpretation of the potential mechanisms by which obesity is linked to atrial fibrillation. Population level studies have suggested that the effect may be mediated through left atrial enlargement (31,33), albeit evidence is

mounting that pericardial adipose tissue, surrounding the heart, may also play a significant role in the development of atrial fibrillation. *Batal et al* suggested that computed-tomography (CT) measured pericardial fat thickness is associated with prevalent AF (301). In participants of the Framingham Heart Study, a community-based cohort, *Thanassoulis et al* observed that higher pericardial fat volumes were associated with a nearly 40% higher odds of prevalent AF(309). *Wong et al* have recently demonstrated that pericardial fat volume is a better predictor than body mass index in predicting severity of atrial fibrillation and even outcomes after ablation (274). As adipose tissue is highly vascular, it is hypothesized that mediators of lipid metabolism and inflammation produced in the pericardial adipose tissue may affect the underlying atrial myocardium in a paracrine manner (303). In addition, epicardial fat has been demonstrated to infiltrate underlying atrial musculature in an obese ovine model(319). This fatty infiltration can mechanically separate muscle fibers and create an area of electrical silence promoting reentry and atrial fibrillation. A recent study has reported the association of elevated dominant frequency with epicardial fat location(320). This study demonstrates that CMR assessment of pericardial fat is an accurate and reproducible measure that could be utilized in future larger clinical cohorts. Furthermore, three dimensional PAT model constructed from CMR slices, allows regional interpretation of local cardiac fat stores, that in future could be utilized in conjunction with electro-anatomic maps to investigate the atrial substrate for atrial fibrillation. This could potentially have implications for planning ablation strategies for atrial fibrillation ablation in obese individuals.

Ventricular paracardiac adipose tissue has previously been validated using CMR(312). This study, to the best of our knowledge, is the first to validate CMR

measure of atrial pericardial fat. Furthermore, in the study by Nelson et al(312), the paracardiac adipose tissue was validated against the histological gold standard. In contrast, in the current study, the total pericardial fat volume was validated, as the epicardial adipose tissue was meticulously removed along with the paracardiac adipose tissue. The provided a more accurate comparison between autopsy and CMR pericardial adipose tissue measures. However, complete removal of epicardial adipose tissue was not possible due to its adherence to underlying myocardium in some cases, and this could be a reason for a small systematic over-estimation by CMR (figure 3).

5.6 Limitations

Fat suppression sequences were intentionally not performed in the study as our intention was to validate measurement of atrial pericardial adipose tissue using a standard clinical CMR protocol. However, fat suppression sequences could improve adjudication of adipose tissue and further improve inter- and intraobserver variability. Furthermore, although stringent attempts were made to completely remove all epicardial adipose tissue at autopsy, this was not always possible.

5.7 Clinical Implications

With the increasing incidence and burden of atrial fibrillation, the identification and characterization of new risk factors is of public health importance(7). Atrial PAT has been demonstrated to predict AF risk independent of other measures of obesity. Given the dual epidemics of obesity and atrial fibrillation, non-invasive CMR measurement of atrial PAT could provide incremental information on the risk

of developing AF. Moreover, atrial pericardial adipose tissue could provide insights in evaluating the variability of AF risk in obese individuals with change in weight(32). The three dimensional model of pericardial fat validated in this study could be utilized to investigate the regional effect of pericardial fat on underlying atrial myocardium. In addition, the information on regional interaction of pericardial fat with adjacent atrial tissue may provide new insights for planning ablation strategies for atrial fibrillation in obese individuals.

5.8 Conclusion

CMR measurement of atrial, ventricular and total pericardial adipose tissue via 3D modeling of fat stores is a reproducible and accurate measure of pericardial fat on autopsy. The measurement of local cardiac fat stores via this methodology could provide a more sensitive tool to examine the potential causal relationship between obesity and atrial fibrillation and examine the regional effect of fat deposition on atrial substrate.

Table 1: Pericardial adipose tissue (PAT) mass as assessed on Autopsy and CMR

Sheep	Total PAT-Autopsy (gms)	Ventricular PAT-Autopsy (gms)	Atrial PAT-Autopsy (gms)	Total PAT-CMR (gms)	Ventricular PAT- CMR (gms)	Atrial PAT-CMR (gms)
1	235	195	40	279	232	47
2	285	265	20	302	273	29
3	414	372	42	446	401	45
4	298	268	30	320	277	42
5	194	172	22	210	184	26
6	253	225	28	267	239	28
7	216	182	34	257	207	50
8	286	260	26	320	279	41
9	160	140	20	177	155	23

Table 2: Intra-observer reproducibility of CMR measures of pericardial adipose tissue (PAT)

PAT	Intra-observer 95% CI (gms)	Intra-observer 95% CI (%)	p value
Total	15.9	5.5	0.001
Ventricular	16.4	6.6	0.001
Atrial	3.1	8.3	0.003

Table 3: Inter-observer reproducibility of CMR measures of pericardial adipose tissue (PAT)

PAT	Inter-observer 95% CI (gms)	Inter-observer 95% CI (%)	p value
Total	20.9	7.2	0.001
Ventricular	18.6	7.4	0.001
Atrial	3.9	10.7	0.001

Figure 1: Three dimensional model of pericardial adipose tissue using semi-automated in-house software.

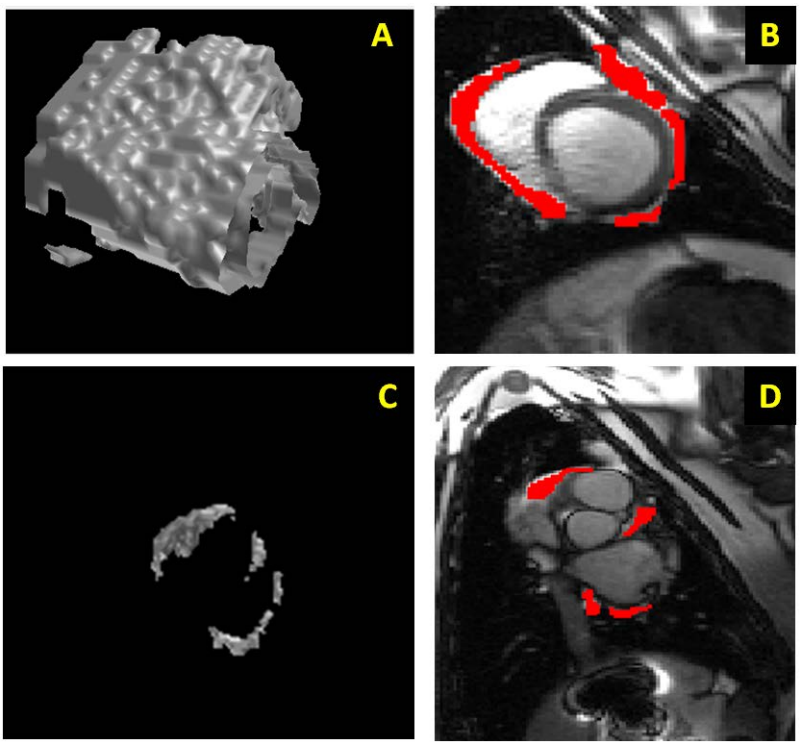

Adipose tissue was marked on each slice followed by interpolation of pixel intensities between consecutive slices. A) A three dimensional rendered model of the ventricular pericardial adipose tissue. B) Short axis view of the left and right ventricles with the pericardial adipose tissue marked in red. C) A three dimensional model of the atrial pericardial adipose tissue. D) A short axis view of the left and right atrium with the pericardial adipose tissue marked in red.

Figure 2: The process of atrial and ventricular pericardial adipose tissue measurement via autopsy.

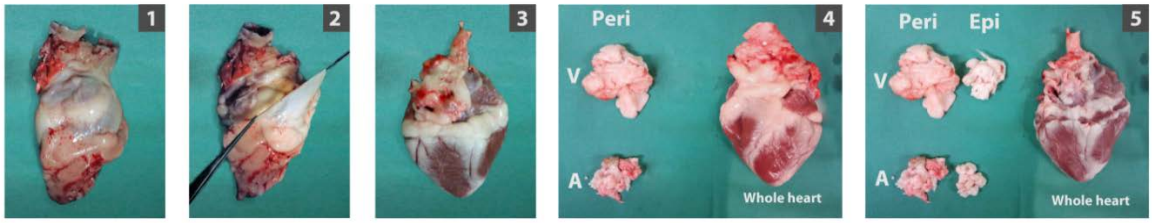

Steps 1) Removal of heart with pulmonary veins, pulmonary artery and part of trachea, 2) Pericardium incised along the atrio-ventricular (AV) groove and was peeled off inferiorly to the ventricular apex to harvest paracardiac ventricular adipose tissue and superiorly to harvest atrial paracardiac adipose tissue., 3) Posterior view of the heart after removal of paracardiac adipose tissue, with epicardial atrial adipose tissue visible posterior (adjacent to posterior LA wall) and laterally along the AV groove, 4) Anterior view of the heart with atrial and ventricular paracardiac adipose tissue to the left. Atrial paracardiac adipose tissue was located between the appendages and the great vessels, with little fat deposition on the appendages, 5) Posterior view of the heart after dissecting the majority of epicardial adipose tissue.

Figure 3: Agreement of CMR assessment with autopsy measures of pericardial adipose tissue

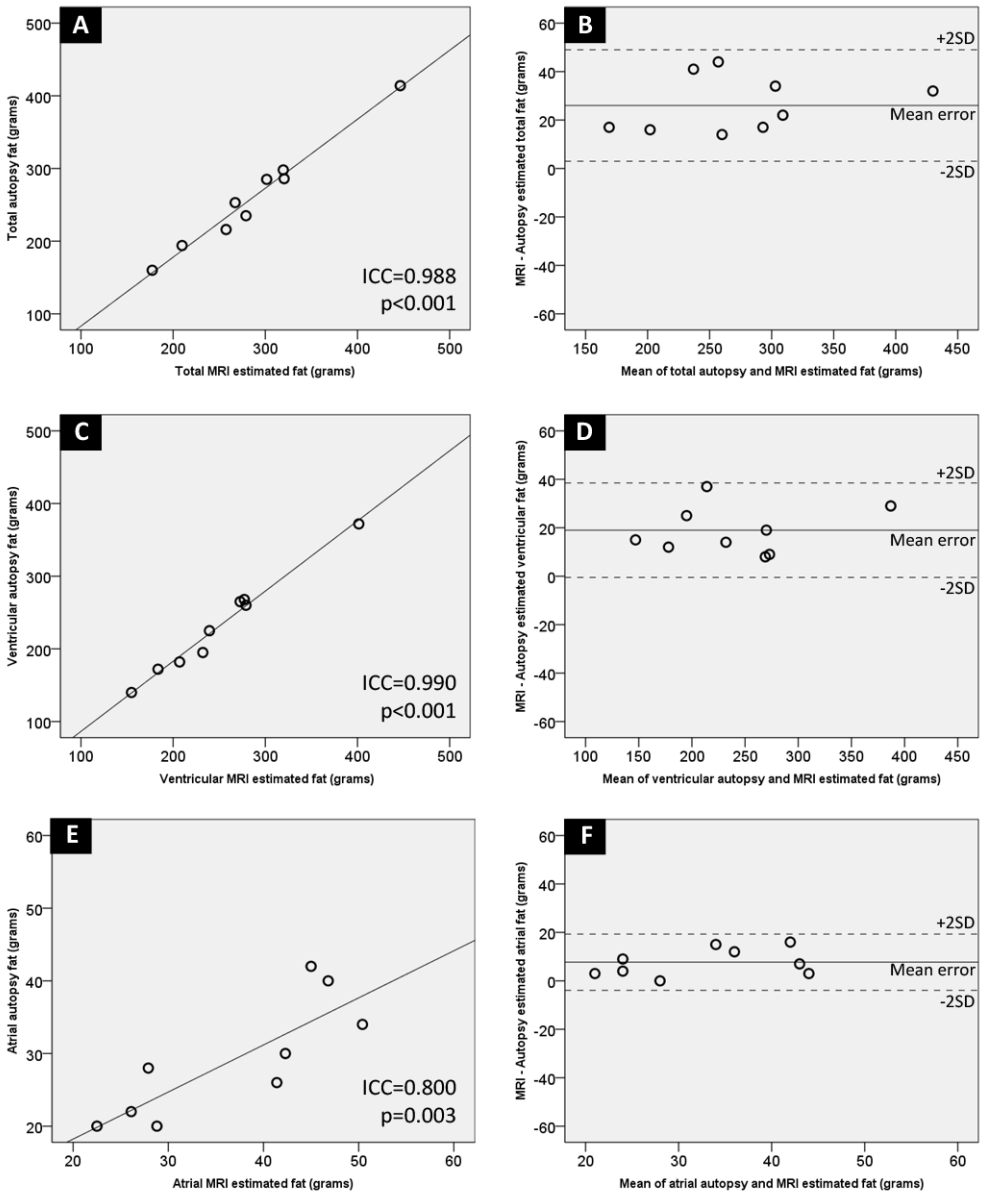

Panel A shows the limits of agreement (ICC) between total pericardial adipose tissue measures on Autopsy and CMR. Panel B represents the degree of agreement, via Bland and Altman plots. Similarly, the panels C, D and E, F represent limits of agreement and Bland and Altman plots for ventricular and atrial pericardial adipose tissue, respectively.

Chapter 6

Epicardial fat depots and atrial remodeling in obese patients with atrial fibrillation: evidence for a direct impact

6.1 Introduction

Atrial fibrillation (AF) is the most common sustained arrhythmia known to affect humans (11). Atrial fibrillation is associated with increased risk of stroke, heart failure and death. It is also recognized as an important cardiovascular cause of hospitalization and contributes significantly to health care costs (7). These observations may in part be due to the growing prevalence of AF, which has been attributed to the aging population and a host of co-morbid conditions (5). Recent observations in epidemiological cohorts have highlighted the role of obesity as an independent risk factor for AF. These studies have suggested a 4-8% increased risk of AF with each additional unit of body mass index (BMI). Whilst in clinical studies obesity frequently co-exists with other established risk factors for AF such as hypertension, diabetes and sleep apnoea, recent experimental studies from our laboratory, on weight gain and sustained obesity have demonstrated diastolic dysfunction, atrial fibrosis and conduction abnormalities in the absence of comorbid conditions(121,321,322). Extension of these findings in a sustained obesity model observed greater epicardial fat depots and fat infiltration of contiguous atrial myocardium, potentially a novel substrate specific to obesity(305). While many studies have evaluated the relationship between systemic measures of adiposity and AF, cardiac ectopic fat depots have only

recently been shown to be associated with propensity and severity of AF(274,276,277). Experimental studies have demonstrated that epicardial fat contributes to atrial substrate development by secreting pro-fibrotic cytokines(216) and directly infiltrating contiguous atrial tissue(305). This study evaluates the electro-anatomic remodeling with obesity and investigates the regional effect of contiguous epicardial fat depots on the contiguous atrial myocardium.

6.2 Methods

Consecutive patients with paroxysmal/persistent AF undergoing first time atrial fibrillation ablation with no contraindication for CMR were enrolled. The patients were divided into obese (BMI≥27) and control (BMI<27) groups. The exclusion criteria included long standing persistent AF, episode of AF (>30 seconds) in 7 days prior to electrophysiology study, contraindication for CMR, restrictive or hypertrophic cardiomyopathy, valvular heart disease, left ventricular dysfunction with LVEF<45%, blood pressure >150/90mmHg, diabetes mellitus with nephropathy, amiodarone use in last 3 months, age<30years, pregnancy, inability to provide informed consent.

Type of AF was defined in accordance to the Heart Rhythm Society Consensus(323). Paroxysmal AF was defined as recurrent AF that terminates spontaneously within seven days. Persistent AF was defined as AF which is sustained beyond seven days, or lasting less than seven days but necessitating pharmacologic or electrical cardioversion. Long standing persistent AF was defined as AF of >1 year duration in which cardioversion has either failed or not

been attempted. Coronary artery disease was defined as greater than 50% stenosis in coronary arteries or a positive stress test (in absence of angiogram).

6.2.1 MRI Protocol and Analysis

Patients underwent cardiac MRI (1.5 Tesla, Siemens Avanto, Siemens Medical Solutions, Erlangen, Germany) in the month prior to ablation. Sequential steady state free precession short-axis cine sequences were acquired with 6mm slice-thickness and no inter-slice gaps through the atria, and 6mm slice-thickness with 4mm gap through the ventricles. Slices were taken from the most cranial aspect of LA and sequentially to the cardiac apex at end expiration. The atria were additionally imaged in the horizontal long-axis plane with 6mm slice-thickness and no inter-slice gaps. Typical imaging parameters were: echo time 1.2ms, repetition time 63.7ms, flip angle 80°, matrix size 192×156, field of view 360-440mm. Epicardial fat volumes were measured offline by two blinded observers using proprietary software (Argus, Siemens Medical Solutions, Erlangen, Germany). CMR measures of cardiac ectopic fat depots have been previously validated by our group in an ex-vivo ovine model and have been demonstrated to be accurate and reproducible(324). Epicardial fat was defined as regions of high signal-intensity between the myoepicardium and parietal pericardium (ie. fat inside the pericardial sac). The ventricular epicardial fat was defined as epicardial adipose tissue from the mitral valve hinge down to the ventricular apex, inclusive of the most inferior margin of the adipose tissue.(324) The atrial epicardial fat was defined as the epicardial adipose tissue subtending to the atria and lying above the mitral valve hinge and below the right pulmonary artery. Areas of fat were traced on consecutive end-diastolic short-axis images and multiplied by the slice-thickness to derive volume. Intra- and inter-observer reproducibility with this technique was excellent (coefficient-of-variation 3.5% and 4.9% respectively). LA volumes were determined by manually tracing endocardial borders in the horizontal long-

axis views in ventricular end-systole and calculated using a modified Simpson's rule.(325)

6.2.2 Electrophysiology Study

Electroanatomic mapping was performed in fasting state prior to ablation. The following catheters were positioned: (i) 10 pole catheter (2-5-2 mm spacing; Daig Electrophysiology) positioned in the coronary sinus as a reference electrode; (ii) Reference patches (Biosense-Webster) positioned along the chest of the patient; and (iii) 3.5 mm tip Navi-Star ablation catheter (Biosense-Webster). The electroanatomic mapping system has been previously described in detail; the accuracy of the sensor position has been previously validated and is 0.8 mm and 5°. In brief, the system records the surface ECG and bipolar electrograms filtered at 30 to 400 Hz from the mapping and reference catheters. Endocardial contact during point acquisition was facilitated by electrogram stability, fluoroscopy, and the catheter icon on the CARTO system. Points were acquired in the auto-freeze mode if the stability criteria in space (6mm) and local activation time (5ms) were met.

Maps were created utilizing a fill threshold of 15 mm in sinus rhythm. Editing of points will be performed offline. Local activation time was manually annotated to the peak of the largest amplitude deflection on bipolar electrograms; in the presence of double potentials, this was annotated at the larger potential. If the bipolar electrogram displayed equivalent maximum positive and negative deflections, the maximum negative deflection on the simultaneously acquired unipolar electrogram was used to annotate the local activation time. Points not conforming to the surface ECG P-wave morphology or <75% of the maximum voltage of the preceding electrogram were excluded. Points within the pulmonary

veins were excluded. The map was edited to ensure an equal density of points throughout the map.

Each point was binned according to location (region), fractionation (presence or absence), low voltage (presence or absence) and bipolar voltage amplitude to allow analysis in a mixed effects model. For the purposes of evaluating regional voltage and conduction velocity differences, the left atrium was segmented offline. The LA was segmented as posterior LA, anterior LA, septal LA, inferior LA, lateral LA, and LA roof. Regional atrial bipolar voltage, fractionation and conduction velocity was analyzed as described below.(92) The following parameters were determined utilizing the electroanatomic maps:

a). *Total atrial activation time* in sinus rhythm;

b). *Regional bipolar voltage and voltage heterogeneity:* previously standardized definitions of scar and regions of low voltage were utilised.(92) Scar was defined as the absence of electrical activity above the noise level of the system (<0.05mV). Areas of low voltage were defined as areas with a bipolar voltage ≤0.5 mV. The heterogeneity of bipolar voltage was determined.

c). *Regional conduction velocity and conduction heterogeneity*. Isochronal activation map (5-ms intervals) of the left atria was created and regional conduction velocity determined in the direction of the wave-front propagation (least isochronal crowding). An approximation of conduction velocity was determined by expressing the distance between 2 points as a function of the difference in local activation time. Mean conduction velocity for each region was determined by averaging the conduction velocity between 3-5 pairs of points, as previously described.(92)

d). *Complex electrograms*. The proportion of points demonstrating complex electrograms was determined using the following definitions: 1) fractionated signals: complex activity of ≥50 ms duration with ≥3 deflections crossing baseline(99); and 2) double potentials: potentials separated by an isoelectric interval where the total electrogram duration was 50 ms. Fractionated and double potentials were combined for analysis.

6.3 Statistical Analysis

Normally distributed continuous data are expressed as mean ± standard deviation. A linear mixed effects model was used for all analyses on continuous data that contained multiple regional measures within each patient (e.g. CV, Voltage). Generalized estimating equations were utilised for nested categorical variables (e.g. % fractionation, % low voltage). To investigate left atrial regional patterns in both approaches, region (posterior LA, anterior LA, septal LA, inferior LA, lateral LA, and LA roof) and group (obese and control) were modeled as fixed effects with an interaction term (region*group). If a significant interaction was present, mixed effects post-hoc test p-values were reported.

For data without multiple measures or levels of data within an individual (eg. fat mass, LA size, LVEF) a conventional unpaired t test were used. Linear regressions between predictor variables of 1) total pericardial fat, 2) atrial pericardial fat 3) left atrial pericardial fat and 4) BMI were correlated with mean posterior LA conduction velocity, mean posterior LA voltage and percent fractionation of posterior LA.

All analyses were performed using SPSS/PASW version21 (SPSS Inc. Chicago, IL). Statistical significance was set as $p<0.05$ and a trend at $p<0.10$.

6.4 Results

A total 30 patients were enrolled in the study. 4 patients were excluded after informed consent due to AF episode in the week prior to electrophysiology study/ablation. The remaining 26 patients were divided into obese (n=16) and control (n=10) based on BMI≥27. The CMR scans were not interpretable in 3 patients and were not analysed.

6.4.1 Group characteristics

The patient characteristics are shown in *table 1*. The body weight of the obese and control groups were 94±13kg and 74±9kg respectively ($p<0.001$). The BMI was 30.2±2.6 and 25.2±1.3 in the obese and controls respectively ($p<0.001$). The two groups did not differ in mean age and prevalence of hypertension, diabetes, heart failure, coronary artery disease and sleep apnoea. There was a similar distribution of the AF type between the two groups ($p=0.42$).

6.4.2 Epicardial fat measures of adiposity

Distribution: Figure 1 demonstrates the representative CMR image showing the left atrial, atrial and ventricular epicardial fat distribution. The left epicardial fat depots were distributed between the right and left pulmonary veins and adjacent to posterior and inferior left atrium. In addition the epicardial pat was deposited along the atrio-ventricular groove. Typically, there was absence of epicardial fat deposits adjacent to the left atrial appendage. The distribution was similar in both obese and control groups.

Epicardial fat and obesity: All epicardial fat measures (ie total, ventricular, atrial and left atrial fat depots) were consistently greater in the obese group as

compared to the controls *(see Table 1)*. The BMI correlated significantly, albeit mildly, with left atrial epicardial fat (R^2=0.38, p=0.002), atrial epicardial fat (R^2=0.40, p=0.001) and total epicardial fat (R^2=0.44, p=0.002).

6.4.3 Electrophysiological remodeling with obesity

The left atrial electroanatomic maps consisted of 74±15 and 70±11 points in obese and control groups respectively (p=0.6). The left atrial activation time trended to be longer (p=0.09) in the obese group (87±16sec) as compared to the control group (74±20sec).

6.4.3.1 Conduction Velocity

The left atrial conduction velocity was reduced in the obese (0.86±0.31m/s) as compared to controls (1.26±0.29m/s) (p<0.001). Although the conduction velocities were more depressed in the posterior and inferior regions (table 2), the regional heterogeneity did not achieve statistical significance (interactive p (group*region) =0.67).

6.4.3.2 Fractionation

There were more complex fractionated signals in the obese group as compared to the controls (p<0.001). There was no interaction between group and region (p=0.32) and the increase in fractionation was similar across different regions in the obese patients (table 2).

6.4.3.3 Left atrial voltage

Figure 2 shows representative voltage LA maps of the control and obese groups.

6.4.3.1.1 Regional differences: Although the mean global voltage was similar in the obese and control groups (obese: 2.24±1.5 vs controls: 2.23±1.9 mV; p=0.8).

However, there were significant differences between group and region (interactive p value<0.001). The posterior and the inferior LA wall had lower regional mean voltages in the obese group as compared to controls (table 2) reaching significance for the posterior LA region (p=0.05). The left atrial region which represents the appendage had increased regional mean voltage in obese group as compared to controls (p=0.01).

Low voltage areas: 13.9% of all points were low voltage in the obese patients as compared to 3.4% in the controls (p=0.005). In addition, there was an interaction between group and region (interactive p=0.005). There were significantly greater low voltage points in the posterior and inferior left atrial regions (posterior LA: p=0.04, inferior LA p=0.05).

6.4.4 Correlation of pericardial fat measures with electrophysiological parameters

There was strong correlation of left atrial epicardial fat volume with atrial epicardial fat volume (R^2=0.86, p<0.001), good correlation with total epicardial fat volume (R^2=0.48, p<0.001) and mild correlation with BMI (R^2=0.38, p=0.002). Left atrial, atrial epicardial fat and BMI correlated significantly with mean left atrial conduction (left atrial fat, R^2=0.30, p=0.008; atrial fat, R^2=0.27, p=0.013; BMI, R^2=0.26, p=0.008). However, left atrial epicardial fat depots predicted a greater percentage of the change in posterior left atrial conduction velocity (left atrial epicardial fat, R^2=0.30, p=0.007; atrial epicardial fat, R^2=0.20, p=0.032; total epicardial fat, R^2=0.16, p=0.063; BMI, R^2=0.22, p=0.014). This is important considering most of the left atrial epicardial fat is clustered posteriorly and spatially related to posterior LA. Similarly, epicardial fat measures correlated

stronger with fractionation as compared to BMI (left atrial epicardial fat, R^2=0.55, p<0.001; atrial epicardial fat, R^2=0.62, p<0.001; total epicardial fat, R^2=0.52, p<0.001, BMI, R^2=0.37, p=0.001).

6.5 Discussion

6.5.1 Major findings

Electro-anatomic remodeling with obesity has been previously demonstrated in preclinical studies(321,322) from our lab and in humans with AF(123). Cardiac ectopic fat depots have been shown to be associated with AF independent of traditional measures of obesity(274,276,277). This study provides further advances the understanding by demonstrating extensive regional electroanatomic changes noted in LA segments contiguous with epicardial fat depots. The major findings are

- Left atrial epicardial fat depots are located contiguous to posterior and inferior LA segments with lateral segment/ appendage being devoid of epicardial fat. In addition epicardial fat was distributed contiguous to AV groove.
- With obesity, there was regional reduction in mean voltage with increased low voltage areas in posterior and inferior LA segments ie segments contiguous to epicardial fat depots.
- Global reduction in conduction velocity in all LA segments with obesity.
- Increased fractionation in all LA segments with obesity.
- Left atrial fat depot (volume) best predicted change in posterior LA conduction. The correlation was weak with other measures of pericardial fat and BMI.
- Epicardial fat measures, as compared to BMI, had a more robust correlation with complex fractioned signals in sinus rhythm.

6.5.2 Association of obesity, pericardial fat and AF

Obesity is increasingly recognized as a novel risk factor that contributes significantly to the rising prevalence of AF(29,31,265,266,326). Epidemiological studies have established the independent role of obesity as a risk factor for AF(31,32,265,266). The study by Gami et al underscored the association of sleep apnoea with obesity and reported an additive effect of the two on the increasing prevalence of AF(29). While these epidemiological studies reported the association utilizing BMI, recent studies have demonstrated that pericardial fat measures are more precise in predicting AF than the traditional measures of obesity(274,275). The largest of the studies to report the association originated from the Framingham Heart Study Offspring and Third Generation Cohorts. In this study involving over two thousand participants, Thanassaulis et al measured pericardial fat with computed tomography (CT) and observed that pericardial fat volume predicted AF risk independent of other measures of adiposity with an OR of 1.28 (95% CI 1.05-1.60, p=0.03) for every standard deviation (SD) increase in pericardial fat volume(276). Total pericardial fat, but not intra-thoracic or visceral fat was associated with AF. Batal et al, studied 169 consecutive patients with CT angiograms for either coronary artery disease or AF and demonstrated that posterior LA fat thickness predicted AF burden, independent of LA area and body mass index(277). In this study, a 10mm increase in posterior LA fat thickness was associated with an OR of 6.06 (95% CI 1.9-19.25, p=0.002). The association between cardiac ectopic fat depots and AF was further confirmed by Al Chekakie et al, who demonstrate that pericardial fat volume (CT) was associated with AF with an OR of 1.13 (for every 10ml increase in pericardial fat volume) after adjusting for BMI, other traditional risk factors and LA enlargement(278). Finally, Wong et al

studied pericardial fat with cardiac magnetic resonance (CMR) in 130 patients and reported the association between pericardial fat volumes with prevalence and severity of AF(274). In this study, both periatrial fat (odds ratio 5.33, 95% CI: 1.25-22.66; p=0.02) and periventricular fat (odds ratio 11.97, 95% CI: 1.69 to 84.88; p=0.01) were predictive of AF after adjusting for other risk factors and BMI. Recently, Shin et al also reported that CT measured epicardial fat volume and peri-atrial fat thickness were associated with prevalence and chronicity of AF(279). However, the term 'pericardial and epicardial fat' has been used interchangeably in AF literature, with some studies defining pericardial fat as fat inside the pericardial sac(276,278) while others defining pericardial fat as a sum of epicardial (fat inside pericardial sac) and paracardial adipose tissue (outside pericardial sac)(274) and others reporting epicardial fat (fat inside pericardial sac)(279). In the present study, epicardial fat measures have been reported and have been defined as fat inside the pericardial sac. Nonetheless, these studies have shown that cardiac ectopic fat depots predict the presence and severity of AF independent of the traditional measures of obesity. This has laid the foundation for the postulate that local cardiac fat deposits create a substrate for AF.

6.5.3 Electroanatomic remodeling with obesity

Structural remodeling and its electrophysiological consequences have emerged as the major factors contributing to the substrate development in patients with risk factors for AF. The importance of diffuse atrial fibrosis and conduction abnormalities for AF substrate was initially defined in experimental heart failure (86). These findings were subsequently confirmed to be the unifying feature of *'remodeling of a different sort'*(86) in other conditions both in pre-clinical studies of heart failure (87), hypertension (88-90) and coronary artery disease (91,116)

and clinical studies of heart failure (92), sinus node disease (93), aging (94), hypertension (96), valvular heart disease (97,98), congenital heart disease (99), and sleep apnea (95). Furthermore, evaluation of patients with "lone AF (117)" has also demonstrated similar findings, suggesting the presence of under recognized (118) or novel risk factors.

Structural remodeling has been observed by our group in an ovine model with sustained obesity. The ovine model, being devoid of sleep apnea and diabetes, allows interpretation without the confabulating effect of associated risk factors usually present with human obesity. In this experimental study, conduction abnormalities, increased atrial voltage heterogeneity and fractionation were demonstrated with sustained obesity after adjusting for hemodynamic stress(321). Up regulation of pro-fibrotic markers, increased atrial fibrosis, fatty infiltration and alteration in connexion expression have been demonstrated to play a role in substrate development for AF in sustained obesity(300).

The careful selection of patients in the present study resulted in similar mean age and prevalence of other risk factors of AF. In keeping with the data in the experimental study, the mean global voltage was similar between the obese and control groups in this study. This is also consistent with the findings of Munger et al in patients undergoing ablation for AF(123).However, the present study further analysed regional voltage differences and demonstrated reduction in voltage in the posterior/ inferior LA and increased voltage in the lateral segment (LAA). Furthermore, low voltage areas were seen in posterior/inferior LA in the obese group, regions spatially related to contiguous epicardial fat. The reduction in voltage in these regions could potentially be the result of fat infiltration of LA myocardium by contiguous fat depots(305). The increase in lateral LA segment

(LAA) may represent hypertrophy due to chronic elevation in LA pressure described in obesity (123,321). The reduction in LA conduction with obesity further extends our preclinical work in the obese ovine model(321). It is also in agreement with findings of Munger et al who have shown slower conduction from the LA entering into the pulmonary veins in obese patients undergoing AF ablation(123). Left atrial epicardial fat volume was more robust predictor of posterior left atrial conduction velocity as compared to other epicardial fat measures and BMI suggesting that pericardial fat may act via paracrine processes to create AF substrate in obesity. Nagashima et al have shown spatial relationship with epicardial fat with high dominant frequency sites but poor correlation with complex fractionated signals(280). The present study demonstrated global increase in fractionation with obesity without any regional differences. In addition, atrial and left atrial epicardial fat volumes in particular correlated strongly with fractionation in sinus rhythm.

6.5.4 Potential mechanistic role of pericardial fat

The epicardial fat is contiguous with atrial myocytes without a separating fascia and shares the same blood supply with the adjacent atrial muscle(304). A preclinical study has demonstrated infiltration of the posterior LA myocardium by the contiguous epicardial fat(305). It is postulated that, in a manner similar to hypothesis proposed for fibrosis, fat cell infiltration could separate muscle fibres and create electrically inert regions promoting conduction abnormality. We propose that reduced voltage in regions contiguous with pericardial fat seen in our study could be the result of fat cell infiltration. Furthermore Venteclef et al have provided insights in the mechanistic link between epicardial fat and AF substrate. They performed elegant experiments in an rat organo-culture model and

demonstrate fibrosis in rat atrial tissue incubated with a secretrome isolated from human epicardial fat(216)The investigators then performed an intervention demonstrating the mediation of fibrosis by activin A, a member of the TGFβ superfamily. It is proposed that profibrotic cytokines may be released from the epicardial fat into the pericardiac sac and may play a role in diffuse atrial fibrosis and conduction abnormalities.

6.6 Limitations

Although the electroanatomic LA maps were segmented into 6 regions for analysis, similar segmentation was not performed for epicardial fat due to the lack of sufficient reproducibility of epicardial fat measures smaller than left atrial epicardial fat volume. However, the epicardial fat was predominantly distributed contiguous to posterior/inferior LA and along AV groove allowing us to draw conclusions.

The effective refractory periods (ERP) for different atrial regions were not evaluated due to the propensity to easily induce AF during ERP testing and lack of consent for multiple cardioversions for research purposes.

6.7 Clinical implications and future directions

The study provides information to fill the gap in literature between the pro-fibrotic cytokine secretion by the epicardial fat (216) and its association with AF(276,277). Considering that the substrate for AF may be reversible (32,297,300), therapies targeted at modulating the secretory function of the epicardial fat may be clinically relevant.

6.8 Conclusion

Patients with obesity and AF demonstrated diffuse LA conduction abnormalities and increased fractionation. In addition, obesity was associated with low voltage areas in posterior and inferior LA, regions that were spatially related to contiguous epicardial fat depots. Left atrial epicardial fat volume was more robust predictor of posterior left atrial conduction velocity than other epicardial fat measures and BMI. This suggests that epicardial fat influences the AF substrate development via local processes.

Table 1: Patient characteristics of the obese and control groups

		Control (n=10)	Obese (n=16)	P value
Demographics	**Age (years)**	59±7	54±9	0.16
	Males (%)	70	100	0.05
Body mass measures	**Weight (Kg)**	74±9	94±13	<0.001
	BMI	25.2±1.3	30.2±2.6	<0.001
	BSA	1.85±0.16	2.10±0.20	0.002
Risk factors for AF (Other than obesity)	**OSA (%)**	0	31	0.12
	Hypertension (%)	40	50	0.70
	DM (%)	0	12.5	0.51
	CAD (%)	0	12.5	0.51
	Heart failure (%)	0	0	1.0
AF type	**Paroxysmal/ persistent (%)**	80/20	62.5/37.5	0.42
Left heart size and function (CMR)	**LA EDV (ml)**	65±15	77±17	0.12
	LA ESV (ml)	43±15	50±14	0.22
	LA EF (%)	35±11	35±10	0.85
	LV EDV (ml)	121±25	137±34	0.21
	LVEF (%)	63±10	65±7	0.57
Epicardial fat measures (CMR)	**Total (ml)**	125±41	177±34	0.01
	Ventricular (ml)	93±26	126±31	0.01
	Atrial (ml)	32±19	52±20	0.02
	Left atrial (ml)	22±11	31±11	0.05

Table 2: Regional electroanatomic remodeling with obesity

		Global	Anterior	Roof	Posterior	Inferior	Septal	Lateral
Voltage (mV)	**Obese**	2.24±1.5	1.94±1.24	2.16±1.41	1.77±1.58	1.95±1.64	1.78±1.25	4.41±2.67
	Control	2.23±1.9	1.90±1.11	2.13±1.28	2.26±1.58	2.36±1.48	1.85±1.13	3.41±1.77
	P value	P (group)=0.77; P (Interactive*) <0.001	0.88	0.78	0.05	0.12	0.74	0.01
Low Voltage (%)	**Obese**	13.9	14.1	8.6	22.5	18.1	11.2	2.4
	Control	3.4	6.1	2.4	6.2	2.3	2.0	1.2
	P value	P (group)=0.005; P (Interactive*)= 0.005	0.23	0.14	0.04	0.05	0.11	0.53
Conduction velocity (m/s)	**Obese**	0.86±0.31	0.81±0.28	0.81±0.20	0.86±0.23	0.74±0.34	0.94±0.40	1.04±0.35
	Control	1.26±0.29	1.16±0.43	1.19±0.24	1.37±0.32	1.21±0.25	1.35±0.26	1.28±0.15
	P value	P (group)<0.001; P (Interactive*)= 0.67	**	**	**	**	**	**
FD/DP (%)	**Obese**	54±17	55	61	51	50	70	34
	Control	25±10	36	28	24	25	37	20
	P value	P (group)<0.001; P (Interactive*)= 0.32	**	**	**	**	**	**

*: Interactive p value group*region
**: post hoc test not performed as interactive p=NS

Figure 1: Pericardial fat representations of left atrial, total atrial and ventricular epicardial fat depots

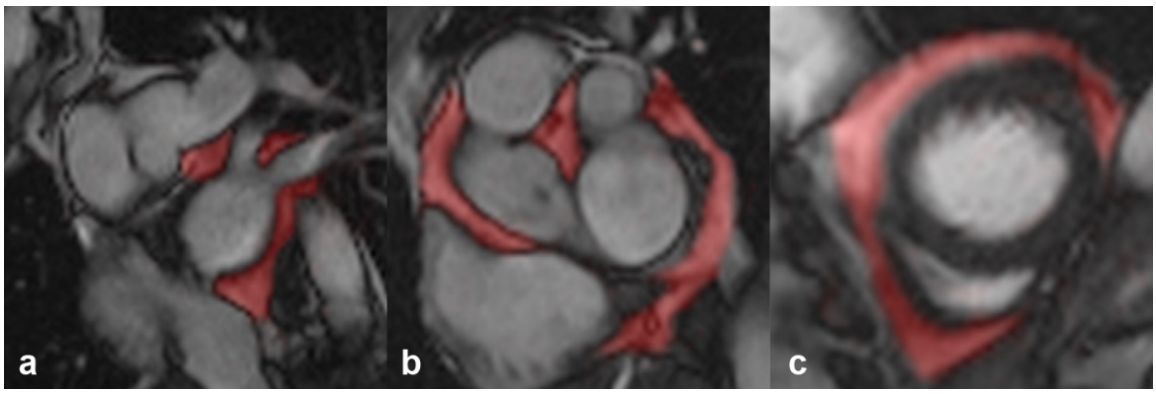

Short axis acquisitions moving apically demonstrating (a) left atrial PAT, b) total atrial PAT and c) ventricular PAT. The fat subtending o the left atrium was located posterior and inferior predominantly.

Figure 2: Representative left atrial voltage maps of the control and obese group

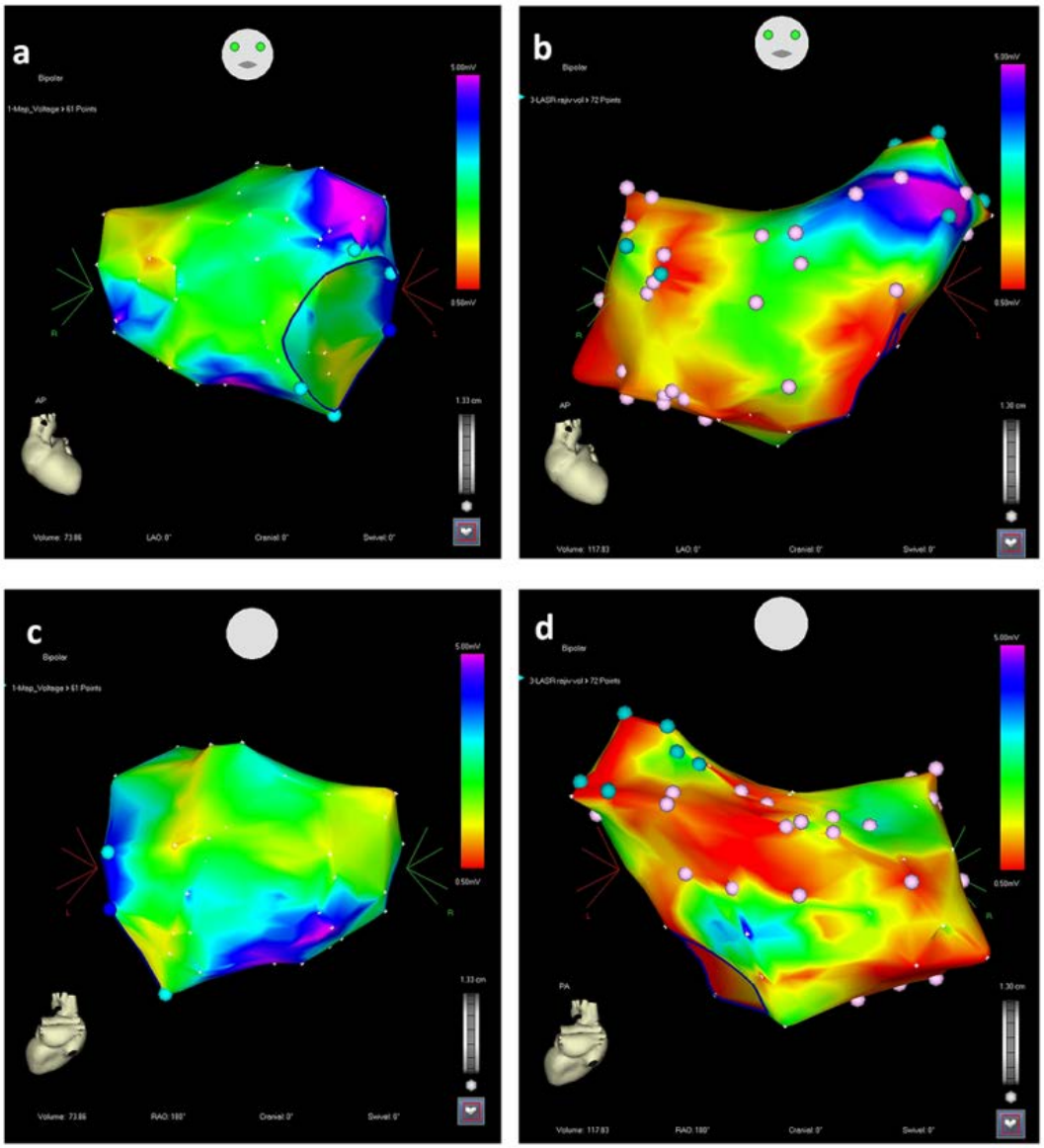

Representative left atrial voltage maps of the control and obese group demonstrating distribution of low voltage areas and increased fractionation in the obese patients. The top panel shows the AP view and the bottom panel shows PA view. Please note the extensive low voltage and fractionation areas in the obese animal. The low voltage regions were predominantly posterior and inferior in distribution

Chapter 7

Conclusion and future directions

This thesis characterizes the atrial remodeling and AF substrate with sustained obesity in an ovine model. It brings forth the role of pericardial fat in creating an AF substrate. It then addresses the reverse remodeling and reversal of AF substrate on intervention with weight reduction in an sustained obese ovine model and highlights that atrial fibrosis is reversible with changes in expression of pro-fibrotic cytokines. The CMR measurement of left atrial, total atrial and ventricular pericardial fat is also validated against the autopsy gold standards. Finally the atrial remodeling in human obesity is characterized with particular attention to the potential direct role of epicardial fat in creating an AF substrate.

In extension of our group's previous work on localized epicardial mapping with short term weight gain, the global endocardial electrophysiological substrate is characterized. Sustained obesity resulted in left atrial dilatation, diastolic dysfunction, elevation of pro-fibrotic cytokines and atrial fibrosis and global conduction abnormalities. In addition to diastolic function and atrial stretch seen with other AF precursors, this thesis provides evidence that pericardial fat may play a direct role in AF substrate. The pericardial fat volume was demonstrated to be increased with obesity both in ovine and human studies. Previous studies have demonstrated that the fat depots around the heart, like other visceral fat depots are endocrine organs and secrete several apokinines. In fact a recent study has demonstrated that activin A, a member of TGF superfamily, is secreted by the

epicardial fat depots and induces atrial fibrosis in an organo-culture model(216). This has led to the hypothesis of a paracrine role of epicardial fat in creating atrial fibrosis. The ovine studies in this thesis demonstrate the elevated expression of TGFβ1 in the atrial tissue with obesity. The increased atrial expression of TGF β1 with sustained obesity and regression on intervention with weight reduction and good correlation with pericardial fat volumes suggested that the fat depots around the heart may be the source of this cytokine. In addition to the paracrine role, this thesis presents the novel finding that epicardial fat can infiltrate contiguous atrial myocardium. We hypothesize that infiltrating fat cells, like fibrosis, may separate cardiomyocytes and cause circuitous conduction promoting re-entry and AF.

The thesis also characterizes the cytokine pathways involved in atrial fibrosis in obesity. TGFβ superfamily and Endothelin pathway have been shown to overactive in human obesity(270,295). This thesis demonstrates that TGFβ1 expression was increased with sustained obesity and decreased with weight reduction and correlated with atrial fibrosis in the obese ovine model. In addition, it was shown that the Endothelin receptor B was upregulated with sustained obesity and downregulated with graded weight reduction in the ovine model. Endothelin receptor B has been previously implicated directly in causing fibrosis in an earlier preclinical intervention study(231). This establishes the important role of these cytokines pathways in obesity.

The electrophysiological substrate was further characterized in sustained obesity. The conduction abnormalities were consistent with both localized epicardial mapping and global endocardial mapping. However, an important feature emerged with atrial refractoriness. There were no significant changes in endocardial ERP

with either sustained obesity or weight reduction. However, the epicardial ERPs decreased with sustained obesity and then increased progressively to control levels with staged weight reduction. The persistence of association even after intervention with weight reduction increases the strength of this relationship. Thus there is an epicardial-endocardial dissociation of atrial refractoriness with sustained obesity. However, this observation is weaken as epicardial and endocardial ERPs were performed in different sheep. We hypothesize that cytokines secreted into the pericardial space by the pericardial fat depots may alter the expression of ion channels resulting in alteration of epicardial atrial refractoriness.

The important question of reversibility of AF substrate was evaluated in a sustained obesity ovine model by intervention with weight reduction. There was not only reversal of epicardial conduction abnormalities, but also down regulation of pro-fibrotic milieu and importantly reversal of atrial fibrosis and diastolic dysfunction. Evaluation of global endocardial electrophysiological substrate suggested similar but less pronounced reversal. This study provides insight into the mechanism of reversal of AF substrate resulting in decreased propensity for AF as has been recently demonstrated in humans by our group(297). This thesis provides evidence that the AF substrate with obesity is reversed though not entirely.

The last section of the thesis characterizes the atrial substrate with human obesity. The obese patients had increase in epicardial fat volumes and non-significant increase in left atrial size. Human obesity was associated with endocardial conduction abnormalities similar to pre-clinical ovine studies. However, the low

voltage areas were seen in human obesity in contrast to the ovine studies. This may be a factor of prolonged exposure to stresses of chronic obesity in humans. Interestingly, the low voltage regions correlated to the location of epicardial fat depots, potentially suggesting a direct of the epicardial fat in creating a substrate for obesity.

This thesis characterizes the AF substrate in sustained obesity in preclinical and clinical studies and sheds light on the underlying mechanisms. It further demonstrates that the obesity related AF substrate is reversible with weight reduction. It also generates hypothesis for further studies. From the mechanistic point of view, future studies directed at evaluating the mRNA expression of pro-fibrotic factors in epicardial fat could further provide information of the direct role of the epicardial fat in creating AF substrate in obesity. Furthermore intervention studies aimed at the pro-fibrotic cytokines could prevent or reverse atrial fibrosis and reduce the risk for AF.

In addition these studies provide a foundation for incorporation of weight reduction program in the holistic management of obese patients with AF.

Chapter 8

References

1. Savelieva I, Camm AJ. Clinical trends in atrial fibrillation at the turn of the millenium. J Intern Med 2001;250:369-72.
2. Steinberg JS. Atrial fibrillation: an emerging epidemic? Heart (British Cardiac Society) 2004;90:239-40.
3. Go AS, Hylek EM, Phillips KA et al. Prevalence of diagnosed atrial fibrillation in adults: national implications for rhythm management and stroke prevention: the AnTicoagulation and Risk Factors in Atrial Fibrillation (ATRIA) Study. JAMA 2001;285:2370-5.
4. Lloyd-Jones DM, Wang TJ, Leip EP et al. Lifetime risk for development of atrial fibrillation: the Framingham Heart Study. Circulation 2004;110:1042-6.
5. Kannel WB, Wolf PA, Benjamin EJ, Levy D. Prevalence, incidence, prognosis, and predisposing conditions for atrial fibrillation: population-based estimates. The American journal of cardiology 1998;82:2N-9N.
6. Miyasaka Y, Barnes ME, Gersh BJ et al. Secular trends in incidence of atrial fibrillation in Olmsted County, Minnesota, 1980 to 2000, and implications on the projections for future prevalence. Circulation 2006;114:119-25.
7. Wong CX, Brooks AG, Leong DP, Roberts-Thomson KC, Sanders P. The increasing burden of atrial fibrillation compared with heart failure and myocardial infarction: a 15-year study of all hospitalizations in australia. Arch Intern Med 2012;172:739-41.
8. Stewart S, Murphy NF, Walker A, McGuire A, McMurray JJ. Cost of an emerging epidemic: an economic analysis of atrial fibrillation in the UK. Heart (British Cardiac Society) 2004;90:286-92.
9. Miyasaka Y, Barnes ME, Gersh BJ et al. Incidence and mortality risk of congestive heart failure in atrial fibrillation patients: a community-based study over two decades. Eur Heart J 2006;27:936-41.
10. Wolf PA, Abbott RD, Kannel WB. Atrial fibrillation as an independent risk factor for stroke: the Framingham Study. Stroke 1991;22:983-8.
11. Benjamin EJ, Wolf PA, D'Agostino RB, Silbershatz H, Kannel WB, Levy D. Impact of atrial fibrillation on the risk of death: the Framingham Heart Study. Circulation 1998;98:946-52.
12. Piccini JP, Hammill BG, Sinner MF et al. Incidence and prevalence of atrial fibrillation and associated mortality among Medicare beneficiaries, 1993-2007. Circulation Cardiovascular quality and outcomes 2012;5:85-93.
13. Miyasaka Y, Barnes ME, Bailey KR et al. Mortality trends in patients diagnosed with first atrial fibrillation: a 21-year community-based study. Journal of the American College of Cardiology 2007;49:986-92.
14. Dulli DA, Stanko H, Levine RL. Atrial fibrillation is associated with severe acute ischemic stroke. Neuroepidemiology 2003;22:118-23.

15. Ott A, Breteler MM, de Bruyne MC, van Harskamp F, Grobbee DE, Hofman A. Atrial fibrillation and dementia in a population-based study. The Rotterdam Study. Stroke 1997;28:316-21.
16. Miyasaka Y, Barnes ME, Petersen RC et al. Risk of dementia in stroke-free patients diagnosed with atrial fibrillation: data from a community-based cohort. Eur Heart J 2007;28:1962-7.
17. Kilander L, Andren B, Nyman H, Lind L, Boberg M, Lithell H. Atrial fibrillation is an independent determinant of low cognitive function: a cross-sectional study in elderly men. Stroke 1998;29:1816-20.
18. Lake FR, Cullen KJ, de Klerk NH, McCall MG, Rosman DL. Atrial fibrillation and mortality in an elderly population. Australian and New Zealand journal of medicine 1989;19:321-6.
19. Benjamin EJ, Levy D, Vaziri SM, D'Agostino RB, Belanger AJ, Wolf PA. Independent risk factors for atrial fibrillation in a population-based cohort. The Framingham Heart Study. JAMA 1994;271:840-4.
20. Davidson E, Weinberger I, Rotenberg Z, Fuchs J, Agmon J. Atrial fibrillation. Cause and time of onset. Arch Intern Med 1989;149:457-9.
21. Robinson K, Frenneaux MP, Stockins B, Karatasakis G, Poloniecki JD, McKenna WJ. Atrial fibrillation in hypertrophic cardiomyopathy: a longitudinal study. Journal of the American College of Cardiology 1990;15:1279-85.
22. Sgarbossa EB, Pinski SL, Maloney JD et al. Chronic atrial fibrillation and stroke in paced patients with sick sinus syndrome. Relevance of clinical characteristics and pacing modalities. Circulation 1993;88:1045-53.
23. Brugada R, Tapscott T, Czernuszewicz GZ et al. Identification of a genetic locus for familial atrial fibrillation. N Engl J Med 1997;336:905-11.
24. Gersh BJ, Solomon A. Lone atrial fibrillation: epidemiology and natural history. American heart journal 1999;137:592-5.
25. Kopecky SL, Gersh BJ, McGoon MD et al. The natural history of lone atrial fibrillation. A population-based study over three decades. N Engl J Med 1987;317:669-74.
26. Frustaci A, Chimenti C, Bellocci F, Morgante E, Russo MA, Maseri A. Histological substrate of atrial biopsies in patients with lone atrial fibrillation. Circulation 1997;96:1180-4.
27. Jais P, Peng JT, Shah DC et al. Left ventricular diastolic dysfunction in patients with so-called lone atrial fibrillation. J Cardiovasc Electrophysiol 2000;11:623-5.
28. Stiles MK, Brooks AG, Roberts-Thomson KC et al. High-density mapping of the sinus node in humans: role of preferential pathways and the effect of remodeling. J Cardiovasc Electrophysiol 2010;21:532-9.
29. Gami AS, Hodge DO, Herges RM et al. Obstructive sleep apnea, obesity, and the risk of incident atrial fibrillation. Journal of the American College of Cardiology 2007;49:565-71.
30. Gami AS, Pressman G, Caples SM et al. Association of atrial fibrillation and obstructive sleep apnea. Circulation 2004;110:364-7.
31. Wang TJ, Parise H, Levy D et al. Obesity and the risk of new-onset atrial fibrillation. JAMA 2004;292:2471-7.
32. Tedrow UB, Conen D, Ridker PM et al. The long- and short-term impact of elevated body mass index on the risk of new atrial fibrillation the WHS

(women's health study). Journal of the American College of Cardiology 2010;55:2319-27.
33. Wanahita N, Messerli FH, Bangalore S, Gami AS, Somers VK, Steinberg JS. Atrial fibrillation and obesity--results of a meta-analysis. American heart journal 2008;155:310-5.
34. Ellinor PT, Yoerger DM, Ruskin JN, MacRae CA. Familial aggregation in lone atrial fibrillation. Human genetics 2005;118:179-84.
35. Oyen N, Ranthe MF, Carstensen L et al. Familial aggregation of lone atrial fibrillation in young persons. Journal of the American College of Cardiology 2012;60:917-21.
36. Mayer A. Rhythmical Pulsation in Scyphomedusae. Washington, DC: Carnegie Institute of Washington, 1906:1-62.
37. Mines GR. On dynamic equilibrium in the heart. The Journal of physiology 1913;46:349-83.
38. Mines GR. On circulating excitations in heart muscles and their possible relation to tachycardia and fibrillation. Trans R Soc Can 1914;4:43-52.
39. Garrey W. The nature of fibrillary contraction of the heart: its relation to tissue mass and form. Am J Physiol 914;33:397-414.
40. Lewis T. Oliver-Sharpey Lectures ON THE NATURE OF FLUTTER AND FIBRILLATION OF THE AURICLE. British medical journal 1921;1:551-5.
41. Lewis T. Oliver-Sharpey Lectures ON THE NATURE OF FLUTTER AND FIBRILLATION OF THE AURICLE. British medical journal 1921;1:590-3.
42. Moe GK, Abildskov JA. Atrial fibrillation as a self-sustaining arrhythmia independent of focal discharge. American heart journal 1959;58:59-70.
43. Moe GK, Rheinboldt WC, Abildskov JA. A Computer Model of Atrial Fibrillation. American heart journal 1964;67:200-20.
44. Allessie MA, Bonke FI, Schopman FJ. Circus movement in rabbit atrial muscle as a mechanism of tachycardia. III. The "leading circle" concept: a new model of circus movement in cardiac tissue without the involvement of an anatomical obstacle. Circ Res 1977;41:9-18.
45. Allessie MA, Bonke FI, Schopman FJ. Circus movement in rabbit atrial muscle as a mechanism of trachycardia. Circ Res 1973;33:54-62.
46. Dillon SM, Allessie MA, Ursell PC, Wit AL. Influences of anisotropic tissue structure on reentrant circuits in the epicardial border zone of subacute canine infarcts. Circ Res 1988;63:182-206.
47. Davidenko JM, Pertsov AV, Salomonsz R, Baxter W, Jalife J. Stationary and drifting spiral waves of excitation in isolated cardiac muscle. Nature 1992;355:349-51.
48. Davidenko JM KP, Chialvo DR, Michaels DC, Jalife J. Sustained vortex-like waves in normal isolated ventricular muscle. Proc Natl Acad Sci USA 1990;87:8785-8789.
49. Krinsky VI. Mathematical models of cardiac arrhythmias (spiral waves). Pharmacology & therapeutics Part B: General & systematic pharmacology 1978;3:539-55.
50. Winfree AT. Varieties of spiral wave behavior: An experimentalist's approach to the theory of excitable media. Chaos 1991;1:303-334.

51. Winfree AT. Erratum: Varieties of spiral wave behavior: An experimentalist's approach to the theory of excitable media [CHAOS 1, 303-334 (1991)]. Chaos 1992;2:273.
52. Narayan SM, Shivkumar K, Krummen DE, Miller JM, Rappel WJ. Panoramic electrophysiological mapping but not electrogram morphology identifies stable sources for human atrial fibrillation: stable atrial fibrillation rotors and focal sources relate poorly to fractionated electrograms. Circ Arrhythm Electrophysiol 2013;6:58-67.
53. Narayan SM, Krummen DE, Shivkumar K, Clopton P, Rappel WJ, Miller JM. Treatment of atrial fibrillation by the ablation of localized sources: CONFIRM (Conventional Ablation for Atrial Fibrillation With or Without Focal Impulse and Rotor Modulation) trial. Journal of the American College of Cardiology 2012;60:628-36.
54. Narayan SM, Patel J, Mulpuru S, Krummen DE. Focal impulse and rotor modulation ablation of sustaining rotors abruptly terminates persistent atrial fibrillation to sinus rhythm with elimination on follow-up: a video case study. Heart Rhythm 2012;9:1436-9.
55. Schuessler RB, Grayson TM, Bromberg BI, Cox JL, Boineau JP. Cholinergically mediated tachyarrhythmias induced by a single extrastimulus in the isolated canine right atrium. Circ Res 1992;71:1254-67.
56. Skanes AC, Mandapati R, Berenfeld O, Davidenko JM, Jalife J. Spatiotemporal periodicity during atrial fibrillation in the isolated sheep heart. Circulation 1998;98:1236-48.
57. Mandapati R, Skanes A, Chen J, Berenfeld O, Jalife J. Stable microreentrant sources as a mechanism of atrial fibrillation in the isolated sheep heart. Circulation 2000;101:194-9.
58. Wu TJ, Doshi RN, Huang HL et al. Simultaneous biatrial computerized mapping during permanent atrial fibrillation in patients with organic heart disease. J Cardiovasc Electrophysiol 2002;13:571-7.
59. Mansour M, Mandapati R, Berenfeld O, Chen J, Samie FH, Jalife J. Left-to-right gradient of atrial frequencies during acute atrial fibrillation in the isolated sheep heart. Circulation 2001;103:2631-6.
60. Morillo CA, Klein GJ, Jones DL, Guiraudon CM. Chronic rapid atrial pacing. Structural, functional, and electrophysiological characteristics of a new model of sustained atrial fibrillation. Circulation 1995;91:1588-95.
61. Li D, Zhang L, Kneller J, Nattel S. Potential ionic mechanism for repolarization differences between canine right and left atrium. Circ Res 2001;88:1168-75.
62. Jalife J, Berenfeld O, Mansour M. Mother rotors and fibrillatory conduction: a mechanism of atrial fibrillation. Cardiovasc Res 2002;54:204-16.
63. Nitta T, Lee R, Watanabe H et al. Radial approach: a new concept in surgical treatment for atrial fibrillation. II. Electrophysiologic effects and atrial contribution to ventricular filling. Ann Thorac Surg 1999;67:36-50.
64. Graffigna A, Pagani F, Minzioni G, Salerno J, Vigano M. Left atrial isolation associated with mitral valve operations. Ann Thorac Surg 1992;54:1093-7; discussion 1098.

65. Haissaguerre M, Jais P, Shah DC et al. Spontaneous initiation of atrial fibrillation by ectopic beats originating in the pulmonary veins. N Engl J Med 1998;339:659-66.
66. Jais P, Haissaguerre M, Shah DC et al. A focal source of atrial fibrillation treated by discrete radiofrequency ablation. Circulation 1997;95:572-6.
67. Chen SA, Hsieh MH, Tai CT et al. Initiation of atrial fibrillation by ectopic beats originating from the pulmonary veins: electrophysiological characteristics, pharmacological responses, and effects of radiofrequency ablation. Circulation 1999;100:1879-86.
68. Haissaguerre M, Jais P, Shah DC et al. Electrophysiological end point for catheter ablation of atrial fibrillation initiated from multiple pulmonary venous foci. Circulation 2000;101:1409-17.
69. Sanders P, Morton JB, Deen VR et al. Immediate and long-term results of radiofrequency ablation of pulmonary vein ectopy for cure of paroxysmal atrial fibrillation using a focal approach. Internal medicine journal 2002;32:202-7.
70. Nathan H, Eliakim M. The junction between the left atrium and the pulmonary veins. An anatomic study of human hearts. Circulation 1966;34:412-22.
71. Nathan H, Gloobe H. Myocardial atrio-venous junctions and extensions (sleeves) over the pulmonary and caval veins. Anatomical observations in various mammals. Thorax 1970;25:317-24.
72. Saito T, Waki K, Becker AE. Left atrial myocardial extension onto pulmonary veins in humans: anatomic observations relevant for atrial arrhythmias. J Cardiovasc Electrophysiol 2000;11:888-94.
73. Hocini M, Ho SY, Kawara T et al. Electrical conduction in canine pulmonary veins: electrophysiological and anatomic correlation. Circulation 2002;105:2442-8.
74. Shah DC, Haissaguerre M, Jais P. Toward a mechanism-based understanding of atrial fibrillation. J Cardiovasc Electrophysiol 2001;12:600-1.
75. Jais P, Hocini M, Macle L et al. Distinctive electrophysiological properties of pulmonary veins in patients with atrial fibrillation. Circulation 2002;106:2479-85.
76. Blom NA, Gittenberger-de Groot AC, DeRuiter MC, Poelmann RE, Mentink MM, Ottenkamp J. Development of the cardiac conduction tissue in human embryos using HNK-1 antigen expression: possible relevance for understanding of abnormal atrial automaticity. Circulation 1999;99:800-6.
77. Chen YJ, Chen SA, Chen YC et al. Effects of rapid atrial pacing on the arrhythmogenic activity of single cardiomyocytes from pulmonary veins: implication in initiation of atrial fibrillation. Circulation 2001;104:2849-54.
78. Chen YJ, Chen YC, Yeh HI, Lin CI, Chen SA. Electrophysiology and arrhythmogenic activity of single cardiomyocytes from canine superior vena cava. Circulation 2002;105:2679-85.
79. Lau CP, Tse HF, Ayers GM. Defibrillation-guided radiofrequency ablation of atrial fibrillation secondary to an atrial focus. Journal of the American College of Cardiology 1999;33:1217-26.
80. Todd DM, Fynn SP, Hobbs WJ, Fitzpatrick AP, Garratt CJ. Prevalence and significance of focal sources of atrial arrhythmia in patients undergoing

cardioversion of persistent atrial fibrillation. J Cardiovasc Electrophysiol 2000;11:616-22.
81. Haissaguerre M, Jais P, Shah DC et al. Catheter ablation of chronic atrial fibrillation targeting the reinitiating triggers. J Cardiovasc Electrophysiol 2000;11:2-10.
82. Zhou S, Chang CM, Wu TJ et al. Nonreentrant focal activations in pulmonary veins in canine model of sustained atrial fibrillation. Am J Physiol Heart Circ Physiol 2002;283:H1244-52.
83. Weerasooriya R, Khairy P, Litalien J et al. Catheter ablation for atrial fibrillation: are results maintained at 5 years of follow-up? Journal of the American College of Cardiology 2011;57:160-6.
84. Allessie MA, Boyden PA, Camm AJ et al. Pathophysiology and prevention of atrial fibrillation. Circulation 2001;103:769-77.
85. Wijffels MC, Kirchhof CJ, Dorland R, Allessie MA. Atrial fibrillation begets atrial fibrillation. A study in awake chronically instrumented goats. Circulation 1995;92:1954-68.
86. Li D, Fareh S, Leung TK, Nattel S. Promotion of atrial fibrillation by heart failure in dogs: atrial remodeling of a different sort. Circulation 1999;100:87-95.
87. Lau DH, Psaltis PJ, Mackenzie L et al. Atrial remodeling in an ovine model of anthracycline-induced nonischemic cardiomyopathy: remodeling of the same sort. J Cardiovasc Electrophysiol 2011;22:175-82.
88. Lau DH, Mackenzie L, Kelly DJ et al. Short-term hypertension is associated with the development of atrial fibrillation substrate: a study in an ovine hypertensive model. Heart Rhythm 2010;7:396-404.
89. Lau DH, Mackenzie L, Kelly DJ et al. Hypertension and atrial fibrillation: evidence of progressive atrial remodeling with electrostructural correlate in a conscious chronically instrumented ovine model. Heart Rhythm 2010;7:1282-90.
90. Kistler PM, Sanders P, Dodic M et al. Atrial electrical and structural abnormalities in an ovine model of chronic blood pressure elevation after prenatal corticosteroid exposure: implications for development of atrial fibrillation. Eur Heart J 2006;27:3045-56.
91. Alasady M, Shipp NJ, Brooks AG et al. Myocardial infarction and atrial fibrillation: importance of atrial ischemia. Circ Arrhythm Electrophysiol 2013;6:738-45.
92. Sanders P, Morton JB, Davidson NC et al. Electrical remodeling of the atria in congestive heart failure: electrophysiological and electroanatomic mapping in humans. Circulation 2003;108:1461-8.
93. Sanders P, Morton JB, Kistler PM et al. Electrophysiological and electroanatomic characterization of the atria in sinus node disease: evidence of diffuse atrial remodeling. Circulation 2004;109:1514-22.
94. Kistler PM, Sanders P, Fynn SP et al. Electrophysiologic and electroanatomic changes in the human atrium associated with age. Journal of the American College of Cardiology 2004;44:109-16.
95. Dimitri H, Ng M, Brooks AG et al. Atrial remodeling in obstructive sleep apnea: implications for atrial fibrillation. Heart Rhythm 2012;9:321-7.

96. Medi C, Kalman JM, Spence SJ et al. Atrial electrical and structural changes associated with longstanding hypertension in humans: implications for the substrate for atrial fibrillation. J Cardiovasc Electrophysiol 2011;22:1317-24.
97. John B, Stiles MK, Kuklik P et al. Reverse remodeling of the atria after treatment of chronic stretch in humans: implications for the atrial fibrillation substrate. Journal of the American College of Cardiology 2010;55:1217-26.
98. John B, Stiles MK, Kuklik P et al. Electrical remodelling of the left and right atria due to rheumatic mitral stenosis. Eur Heart J 2008;29:2234-43.
99. Roberts-Thomson KC, John B, Worthley SG et al. Left atrial remodeling in patients with atrial septal defects. Heart Rhythm 2009;6:1000-6.
100. Gaspo R, Bosch RF, Talajic M, Nattel S. Functional mechanisms underlying tachycardia-induced sustained atrial fibrillation in a chronic dog model. Circulation 1997;96:4027-35.
101. Anne W, Willems R, Holemans P et al. Self-terminating AF depends on electrical remodeling while persistent AF depends on additional structural changes in a rapid atrially paced sheep model. J Mol Cell Cardiol 2007;43:148-58.
102. Goette A, Honeycutt C, Langberg JJ. Electrical remodeling in atrial fibrillation. Time course and mechanisms. Circulation 1996;94:2968-74.
103. Qi XY, Yeh YH, Xiao L et al. Cellular signaling underlying atrial tachycardia remodeling of L-type calcium current. Circ Res 2008;103:845-54.
104. Yue L, Feng J, Gaspo R, Li GR, Wang Z, Nattel S. Ionic remodeling underlying action potential changes in a canine model of atrial fibrillation. Circ Res 1997;81:512-25.
105. Yue L, Melnyk P, Gaspo R, Wang Z, Nattel S. Molecular mechanisms underlying ionic remodeling in a dog model of atrial fibrillation. Circ Res 1999;84:776-84.
106. Voigt N, Maguy A, Yeh YH et al. Changes in I K, ACh single-channel activity with atrial tachycardia remodelling in canine atrial cardiomyocytes. Cardiovasc Res 2008;77:35-43.
107. Voigt N, Friedrich A, Bock M et al. Differential phosphorylation-dependent regulation of constitutively active and muscarinic receptor-activated IK,ACh channels in patients with chronic atrial fibrillation. Cardiovasc Res 2007;74:426-37.
108. Gaspo R, Bosch RF, Bou-Abboud E, Nattel S. Tachycardia-induced changes in Na+ current in a chronic dog model of atrial fibrillation. Circ Res 1997;81:1045-52.
109. Cha TJ, Ehrlich JR, Zhang L, Nattel S. Atrial ionic remodeling induced by atrial tachycardia in the presence of congestive heart failure. Circulation 2004;110:1520-6.
110. van der Velden HM, Ausma J, Rook MB et al. Gap junctional remodeling in relation to stabilization of atrial fibrillation in the goat. Cardiovasc Res 2000;46:476-86.
111. Ausma J, Litjens N, Lenders MH et al. Time course of atrial fibrillation-induced cellular structural remodeling in atria of the goat. J Mol Cell Cardiol 2001;33:2083-94.
112. Ausma J, Wijffels M, Thone F, Wouters L, Allessie M, Borgers M. Structural changes of atrial myocardium due to sustained atrial fibrillation in the goat. Circulation 1997;96:3157-63.

113. Ausma J, van der Velden HM, Lenders MH et al. Reverse structural and gap-junctional remodeling after prolonged atrial fibrillation in the goat. Circulation 2003;107:2051-8.
114. Avitall B, Bi J, Mykytsey A, Chicos A. Atrial and ventricular fibrosis induced by atrial fibrillation: evidence to support early rhythm control. Heart Rhythm 2008;5:839-45.
115. Burstein B, Qi XY, Yeh YH, Calderone A, Nattel S. Atrial cardiomyocyte tachycardia alters cardiac fibroblast function: a novel consideration in atrial remodeling. Cardiovasc Res 2007;76:442-52.
116. Nishida K, Qi XY, Wakili R et al. Mechanisms of atrial tachyarrhythmias associated with coronary artery occlusion in a chronic canine model. Circulation 2011;123:137-46.
117. Stiles MK, John B, Wong CX et al. Paroxysmal lone atrial fibrillation is associated with an abnormal atrial substrate: characterizing the "second factor". Journal of the American College of Cardiology 2009;53:1182-91.
118. Lau DH, Middeldorp ME, Brooks AG et al. Aortic stiffness in lone atrial fibrillation: a novel risk factor for arrhythmia recurrence. PLoS One 2013;8:e76776.
119. Korantzopoulos P, Kokkoris S, Liu T, Protopsaltis I, Li G, Goudevenos JA. Atrial fibrillation in end-stage renal disease. Pacing and clinical electrophysiology : PACE 2007;30:1391-7.
120. Kato T, Yamashita T, Sekiguchi A et al. What are arrhythmogenic substrates in diabetic rat atria? J Cardiovasc Electrophysiol 2006;17:890-4.
121. Abed HS, Samuel CS, Lau DH et al. Obesity results in progressive atrial structural and electrical remodeling: Implications for atrial fibrillation. Heart Rhythm 2013;10:90-100.
122. Iwasaki YK, Shi Y, Benito B et al. Determinants of atrial fibrillation in an animal model of obesity and acute obstructive sleep apnea. Heart Rhythm 2012;9:1409-1416 e1.
123. Munger TM, Dong YX, Masaki M et al. Electrophysiological and hemodynamic characteristics associated with obesity in patients with atrial fibrillation. Journal of the American College of Cardiology 2012;60:851-60.
124. Feinberg WM, Blackshear JL, Laupacis A, Kronmal R, Hart RG. Prevalence, age distribution, and gender of patients with atrial fibrillation. Analysis and implications. Arch Intern Med 1995;155:469-73.
125. Friberg J, Scharling H, Gadsboll N, Jensen GB. Sex-specific increase in the prevalence of atrial fibrillation (The Copenhagen City Heart Study). The American journal of cardiology 2003;92:1419-23.
126. Goette A, Juenemann G, Peters B et al. Determinants and consequences of atrial fibrosis in patients undergoing open heart surgery. Cardiovasc Res 2002;54:390-6.
127. Anyukhovsky EP, Sosunov EA, Chandra P et al. Age-associated changes in electrophysiologic remodeling: a potential contributor to initiation of atrial fibrillation. Cardiovasc Res 2005;66:353-63.
128. Michelucci A, Padeletti L, Fradella GA et al. Aging and atrial electrophysiologic properties in man. Int J Cardiol 1984;5:75-81.

129. DuBrow IW, Fisher EA, Denes P, Hastreiter AR. The influence of age on cardiac refractory periods in man. Pediatric research 1976;10:135-9.
130. Sakabe K, Fukuda N, Nada T et al. Age-related changes in the electrophysiologic properties of the atrium in patients with no history of atrial fibrillation. Japanese heart journal 2003;44:385-93.
131. Sakabe K, Fukuda N, Soeki T et al. Relation of age and sex to atrial electrophysiological properties in patients with no history of atrial fibrillation. Pacing and clinical electrophysiology : PACE 2003;26:1238-44.
132. Kojodjojo P, Kanagaratnam P, Markides V, Davies DW, Peters N. Age-related changes in human left and right atrial conduction. J Cardiovasc Electrophysiol 2006;17:120-7.
133. Roberts-Thomson KC, Kistler PM, Sanders P et al. Fractionated atrial electrograms during sinus rhythm: relationship to age, voltage, and conduction velocity. Heart Rhythm 2009;6:587-91.
134. Conen D, Tedrow UB, Koplan BA, Glynn RJ, Buring JE, Albert CM. Influence of systolic and diastolic blood pressure on the risk of incident atrial fibrillation in women. Circulation 2009;119:2146-52.
135. investigators. TS. Effect of enalapril on mortality and the development of heart failure in asymptomatic patients with reduced left ventricular ejection fractions. The SOLVD Investigattors. N Engl J Med 1992;327:685-91.
136. Deedwania PC, Singh BN, Ellenbogen K, Fisher S, Fletcher R, Singh SN. Spontaneous conversion and maintenance of sinus rhythm by amiodarone in patients with heart failure and atrial fibrillation: observations from the veterans affairs congestive heart failure survival trial of antiarrhythmic therapy (CHF-STAT). The Department of Veterans Affairs CHF-STAT Investigators. Circulation 1998;98:2574-9.
137. Carson PE, Johnson GR, Dunkman WB, Fletcher RD, Farrell L, Cohn JN. The influence of atrial fibrillation on prognosis in mild to moderate heart failure. The V-HeFT Studies. The V-HeFT VA Cooperative Studies Group. Circulation 1993;87:VI102-10.
138. Group TCTS. Effects of enalapril on mortality in severe congestive heart failure. Results of the Cooperative North Scandinavian Enalapril Survival Study (CONSENSUS). The CONSENSUS Trial Study Group. N Engl J Med 1987;316:1429-35.
139. Shinagawa K, Shi YF, Tardif JC, Leung TK, Nattel S. Dynamic nature of atrial fibrillation substrate during development and reversal of heart failure in dogs. Circulation 2002;105:2672-8.
140. Li D, Shinagawa K, Pang L et al. Effects of angiotensin-converting enzyme inhibition on the development of the atrial fibrillation substrate in dogs with ventricular tachypacing-induced congestive heart failure. Circulation 2001;104:2608-14.
141. Boyden PA, Tilley LP, Albala A, Liu SK, Fenoglio JJ, Jr., Wit AL. Mechanisms for atrial arrhythmias associated with cardiomyopathy: a study of feline hearts with primary myocardial disease. Circulation 1984;69:1036-47.
142. Boixel C, Fontaine V, Rucker-Martin C et al. Fibrosis of the left atria during progression of heart failure is associated with increased matrix

metalloproteinases in the rat. Journal of the American College of Cardiology 2003;42:336-44.
143. Yeh YH, Wakili R, Qi XY et al. Calcium-handling abnormalities underlying atrial arrhythmogenesis and contractile dysfunction in dogs with congestive heart failure. Circ Arrhythm Electrophysiol 2008;1:93-102.
144. Li D, Melnyk P, Feng J et al. Effects of experimental heart failure on atrial cellular and ionic electrophysiology. Circulation 2000;101:2631-8.
145. Selzer A, Cohn KE. Natural history of mitral stenosis: a review. Circulation 1972;45:878-90.
146. Grigioni F, Avierinos JF, Ling LH et al. Atrial fibrillation complicating the course of degenerative mitral regurgitation: determinants and long-term outcome. Journal of the American College of Cardiology 2002;40:84-92.
147. Schwartz R, Myerson RM, Lawrence T, Nichols HT. Mitral stenosis, massive pulmonary hemorrhage, and emergency valve replacement. N Engl J Med 1966;275:755-8.
148. Diker E, Aydogdu S, Ozdemir M et al. Prevalence and predictors of atrial fibrillation in rheumatic valvular heart disease. The American journal of cardiology 1996;77:96-8.
149. Verheule S, Wilson E, Everett Tt, Shanbhag S, Golden C, Olgin J. Alterations in atrial electrophysiology and tissue structure in a canine model of chronic atrial dilatation due to mitral regurgitation. Circulation 2003;107:2615-22.
150. Fan K, Lee KL, Chow WH, Chau E, Lau CP. Internal cardioversion of chronic atrial fibrillation during percutaneous mitral commissurotomy: insight into reversal of chronic stretch-induced atrial remodeling. Circulation 2002;105:2746-52.
151. Konstantinides S, Geibel A, Olschewski M et al. A comparison of surgical and medical therapy for atrial septal defect in adults. N Engl J Med 1995;333:469-73.
152. Gatzoulis MA, Freeman MA, Siu SC, Webb GD, Harris L. Atrial arrhythmia after surgical closure of atrial septal defects in adults. N Engl J Med 1999;340:839-46.
153. Arat N, Sokmen Y, Altay H, Ozcan F, Ilkay E. Left and right atrial myocardial deformation properties in patients with an atrial septal defect. Echocardiography 2008;25:401-7.
154. Morton JB, Sanders P, Vohra JK et al. Effect of chronic right atrial stretch on atrial electrical remodeling in patients with an atrial septal defect. Circulation 2003;107:1775-82.
155. Fang F, Yu CM, Sanderson JE et al. Prevalence and determinants of incomplete right atrial reverse remodeling after device closure of atrial septal defects. The American journal of cardiology 2011;108:114-9.
156. Krahn AD, Manfreda J, Tate RB, Mathewson FA, Cuddy TE. The natural history of atrial fibrillation: incidence, risk factors, and prognosis in the Manitoba Follow-Up Study. Am J Med 1995;98:476-84.
157. Eldar M, Canetti M, Rotstein Z et al. Significance of paroxysmal atrial fibrillation complicating acute myocardial infarction in the thrombolytic era. SPRINT and Thrombolytic Survey Groups. Circulation 1998;97:965-70.
158. Hunt D, Sloman G, Penington C. Effects of atrial fibrillation on prognosis of acute myocardial infarction. British heart journal 1978;40:303-7.

159. Asanin M, Perunicic J, Mrdovic I et al. Significance of recurrences of new atrial fibrillation in acute myocardial infarction. Int J Cardiol 2006;109:235-40.
160. Siu CW, Jim MH, Ho HH et al. Transient atrial fibrillation complicating acute inferior myocardial infarction: implications for future risk of ischemic stroke. Chest 2007;132:44-9.
161. James TN. Myocardial infarction and atrial arrhythmias. Circulation 1961;24:761-76.
162. Nielsen FE, Andersen HH, Gram-Hansen P, Sorensen HT, Klausen IC. The relationship between ECG signs of atrial infarction and the development of supraventricular arrhythmias in patients with acute myocardial infarction. American heart journal 1992;123:69-72.
163. Rechavia E, Strasberg B, Mager A et al. The incidence of atrial arrhythmias during inferior wall myocardial infarction with and without right ventricular involvement. American heart journal 1992;124:387-91.
164. Shimizu A, Nozaki A, Rudy Y, Waldo AL. Onset of induced atrial flutter in the canine pericarditis model. Journal of the American College of Cardiology 1991;17:1223-34.
165. Sugiura T, Iwasaka T, Takahashi N et al. Atrial fibrillation in inferior wall Q-wave acute myocardial infarction. The American journal of cardiology 1991;67:1135-6.
166. Sugiura T, Iwasaka T, Takahashi N et al. Factors associated with atrial fibrillation in Q wave anterior myocardial infarction. American heart journal 1991;121:1409-12.
167. Shaw RM, Rudy Y. Electrophysiologic effects of acute myocardial ischemia: a theoretical study of altered cell excitability and action potential duration. Cardiovasc Res 1997;35:256-72.
168. Shaw RM, Rudy Y. Electrophysiologic effects of acute myocardial ischemia. A mechanistic investigation of action potential conduction and conduction failure. Circ Res 1997;80:124-38.
169. Olgin JE, Sih HJ, Hanish S et al. Heterogeneous atrial denervation creates substrate for sustained atrial fibrillation. Circulation 1998;98:2608-14.
170. Alasady M, Abhayaratna WP, Leong DP et al. Coronary artery disease affecting the atrial branches is an independent determinant of atrial fibrillation after myocardial infarction. Heart Rhythm 2011;8:955-60.
171. Sinno H, Derakhchan K, Libersan D, Merhi Y, Leung TK, Nattel S. Atrial ischemia promotes atrial fibrillation in dogs. Circulation 2003;107:1930-6.
172. Young T, Skatrud J, Peppard PE. Risk factors for obstructive sleep apnea in adults. JAMA 2004;291:2013-6.
173. Peppard PE, Young T, Palta M, Dempsey J, Skatrud J. Longitudinal study of moderate weight change and sleep-disordered breathing. JAMA 2000;284:3015-21.
174. Kanagala R, Murali NS, Friedman PA et al. Obstructive sleep apnea and the recurrence of atrial fibrillation. Circulation 2003;107:2589-94.
175. Jongnarangsin K, Chugh A, Good E et al. Body mass index, obstructive sleep apnea, and outcomes of catheter ablation of atrial fibrillation. J Cardiovasc Electrophysiol 2008;19:668-72.

176. Levy P, Pepin JL, Arnaud C et al. Intermittent hypoxia and sleep-disordered breathing: current concepts and perspectives. Eur Respir J 2008;32:1082-95.
177. Somers VK, Dyken ME, Clary MP, Abboud FM. Sympathetic neural mechanisms in obstructive sleep apnea. The Journal of clinical investigation 1995;96:1897-904.
178. Romero-Corral A, Somers VK, Pellikka PA et al. Decreased right and left ventricular myocardial performance in obstructive sleep apnea. Chest 2007;132:1863-70.
179. Hoffmann MS, Singh P, Wolk R, Romero-Corral A, Raghavakaimal S, Somers VK. Microarray studies of genomic oxidative stress and cell cycle responses in obstructive sleep apnea. Antioxidants & redox signaling 2007;9:661-9.
180. Tang RB, Dong JZ, Liu XP et al. Obstructive sleep apnoea risk profile and the risk of recurrence of atrial fibrillation after catheter ablation. Europace 2009;11:100-5.
181. Patel D, Mohanty P, Di Biase L et al. Safety and efficacy of pulmonary vein antral isolation in patients with obstructive sleep apnea: the impact of continuous positive airway pressure. Circ Arrhythm Electrophysiol;3:445-51.
182. Matiello M, Nadal M, Tamborero D et al. Low efficacy of atrial fibrillation ablation in severe obstructive sleep apnoea patients. Europace;12:1084-9.
183. Fein AS, Shvilkin A, Shah D et al. Treatment of obstructive sleep apnea reduces the risk of atrial fibrillation recurrence after catheter ablation. Journal of the American College of Cardiology 2013;62:300-5.
184. Caples SM, Somers VK. CPAP treatment for obstructive sleep apnoea in heart failure: expectations unmet. Eur Heart J 2007;28:1184-6.
185. Spach MS. Mounting evidence that fibrosis generates a major mechanism for atrial fibrillation. Circ Res 2007;101:743-5.
186. Spach MS, Boineau JP. Microfibrosis produces electrical load variations due to loss of side-to-side cell connections: a major mechanism of structural heart disease arrhythmias. Pacing and clinical electrophysiology : PACE 1997;20:397-413.
187. Anne W, Willems R, Roskams T et al. Matrix metalloproteinases and atrial remodeling in patients with mitral valve disease and atrial fibrillation. Cardiovasc Res 2005;67:655-66.
188. Luo MH, Li YS, Yang KP. Fibrosis of collagen I and remodeling of connexin 43 in atrial myocardium of patients with atrial fibrillation. Cardiology 2007;107:248-53.
189. Ohtani K, Yutani C, Nagata S, Koretsune Y, Hori M, Kamada T. High prevalence of atrial fibrosis in patients with dilated cardiomyopathy. Journal of the American College of Cardiology 1995;25:1162-9.
190. Verheule S, Tuyls E, Gharaviri A et al. Loss of continuity in the thin epicardial layer because of endomysial fibrosis increases the complexity of atrial fibrillatory conduction. Circ Arrhythm Electrophysiol 2013;6:202-11.
191. Verheule S, Sato T, Everett Tt et al. Increased vulnerability to atrial fibrillation in transgenic mice with selective atrial fibrosis caused by overexpression of TGF-beta1. Circ Res 2004;94:1458-65.
192. Kumagai K, Nakashima H, Urata H, Gondo N, Arakawa K, Saku K. Effects of angiotensin II type 1 receptor antagonist on electrical and structural

remodeling in atrial fibrillation. Journal of the American College of Cardiology 2003;41:2197-204.
193. Lee KW, Everett THt, Rahmutula D et al. Pirfenidone prevents the development of a vulnerable substrate for atrial fibrillation in a canine model of heart failure. Circulation 2006;114:1703-12.
194. Neuberger HR, Schotten U, Verheule S et al. Development of a substrate of atrial fibrillation during chronic atrioventricular block in the goat. Circulation 2005;111:30-7.
195. Revel JP, Karnovsky MJ. Hexagonal array of subunits in intercellular junctions of the mouse heart and liver. The Journal of cell biology 1967;33:C7-C12.
196. Manjunath CK, Goings GE, Page E. Proteolysis of cardiac gap junctions during their isolation from rat hearts. The Journal of membrane biology 1985;85:159-68.
197. Beyer EC, Paul DL, Goodenough DA. Connexin43: a protein from rat heart homologous to a gap junction protein from liver. The Journal of cell biology 1987;105:2621-9.
198. Barker RJ, Price RL, Gourdie RG. Increased association of ZO-1 with connexin43 during remodeling of cardiac gap junctions. Circ Res 2002;90:317-24.
199. Gutstein DE, Morley GE, Tamaddon H et al. Conduction slowing and sudden arrhythmic death in mice with cardiac-restricted inactivation of connexin43. Circ Res 2001;88:333-9.
200. Peters NS, Coromilas J, Severs NJ, Wit AL. Disturbed connexin43 gap junction distribution correlates with the location of reentrant circuits in the epicardial border zone of healing canine infarcts that cause ventricular tachycardia. Circulation 1997;95:988-96.
201. Duffy HS, Wit AL. Is there a role for remodeled connexins in AF? No simple answers. J Mol Cell Cardiol 2008;44:4-13.
202. Verheule S, van Batenburg CA, Coenjaerts FE, Kirchhoff S, Willecke K, Jongsma HJ. Cardiac conduction abnormalities in mice lacking the gap junction protein connexin40. J Cardiovasc Electrophysiol 1999;10:1380-9.
203. Bikou O, Thomas D, Trappe K et al. Connexin 43 gene therapy prevents persistent atrial fibrillation in a porcine model. Cardiovasc Res 2011;92:218-25.
204. Reisner Y, Meiry G, Zeevi-Levin N et al. Impulse conduction and gap junctional remodelling by endothelin-1 in cultured neonatal rat ventricular myocytes. J Cell Mol Med 2009;13:562-73.
205. Gabbiani G. The myofibroblast in wound healing and fibrocontractive diseases. The Journal of pathology 2003;200:500-3.
206. Nattel S. New ideas about atrial fibrillation 50 years on. Nature 2002;415:219-26.
207. Rosenkranz S. TGF-beta1 and angiotensin networking in cardiac remodeling. Cardiovasc Res 2004;63:423-32.
208. Attisano L, Wrana JL. Signal transduction by the TGF-beta superfamily. Science 2002;296:1646-7.
209. Santander C, Brandan E. Betaglycan induces TGF-beta signaling in a ligand-independent manner, through activation of the p38 pathway. Cellular signalling 2006;18:1482-91.

210. Liu S, Xu SW, Kennedy L et al. FAK is required for TGFbeta-induced JNK phosphorylation in fibroblasts: implications for acquisition of a matrix-remodeling phenotype. Molecular biology of the cell 2007;18:2169-78.
211. Leask A, Abraham DJ. TGF-beta signaling and the fibrotic response. FASEB journal : official publication of the Federation of American Societies for Experimental Biology 2004;18:816-27.
212. Hinz B, Phan SH, Thannickal VJ, Galli A, Bochaton-Piallat ML, Gabbiani G. The myofibroblast: one function, multiple origins. The American journal of pathology 2007;170:1807-16.
213. Leask A, Abraham DJ. All in the CCN family: essential matricellular signaling modulators emerge from the bunker. Journal of cell science 2006;119:4803-10.
214. Leask A. Targeting the TGFbeta, endothelin-1 and CCN2 axis to combat fibrosis in scleroderma. Cellular signalling 2008;20:1409-14.
215. Verrecchia F, Chu ML, Mauviel A. Identification of novel TGF-beta /Smad gene targets in dermal fibroblasts using a combined cDNA microarray/promoter transactivation approach. The Journal of biological chemistry 2001;276:17058-62.
216. Venteclef N, Guglielmi V, Balse E et al. Human epicardial adipose tissue induces fibrosis of the atrial myocardium through the secretion of adipo-fibrokines. Eur Heart J 2013.
217. Kuwahara F, Kai H, Tokuda K et al. Transforming growth factor-beta function blocking prevents myocardial fibrosis and diastolic dysfunction in pressure-overloaded rats. Circulation 2002;106:130-5.
218. Sugden PH, Clerk A. Regulation of the ERK subgroup of MAP kinase cascades through G protein-coupled receptors. Cellular signalling 1997;9:337-51.
219. Marrero MB, Schieffer B, Paxton WG et al. Direct stimulation of Jak/STAT pathway by the angiotensin II AT1 receptor. Nature 1995;375:247-50.
220. Tsai CT, Lai LP, Kuo KT et al. Angiotensin II activates signal transducer and activators of transcription 3 via Rac1 in atrial myocytes and fibroblasts: implication for the therapeutic effect of statin in atrial structural remodeling. Circulation 2008;117:344-55.
221. Campbell SE, Katwa LC. Angiotensin II stimulated expression of transforming growth factor-beta1 in cardiac fibroblasts and myofibroblasts. J Mol Cell Cardiol 1997;29:1947-58.
222. Yang F, Chung AC, Huang XR, Lan HY. Angiotensin II induces connective tissue growth factor and collagen I expression via transforming growth factor-beta-dependent and -independent Smad pathways: the role of Smad3. Hypertension 2009;54:877-84.
223. Gao X, He X, Luo B, Peng L, Lin J, Zuo Z. Angiotensin II increases collagen I expression via transforming growth factor-beta1 and extracellular signal-regulated kinase in cardiac fibroblasts. Eur J Pharmacol 2009;606:115-20.
224. De Mello WC, Specht P. Chronic blockade of angiotensin II AT1-receptors increased cell-to-cell communication, reduced fibrosis and improved impulse propagation in the failing heart. Journal of the renin-angiotensin-aldosterone system : JRAAS 2006;7:201-5.
225. Shibasaki Y, Nishiue T, Masaki H et al. Impact of the angiotensin II receptor antagonist, losartan, on myocardial fibrosis in patients with end-stage renal

disease: assessment by ultrasonic integrated backscatter and biochemical markers. Hypertension research : official journal of the Japanese Society of Hypertension 2005;28:787-95.
226. Chatziantoniou C, Boffa JJ, Ardaillou R, Dussaule JC. Nitric oxide inhibition induces early activation of type I collagen gene in renal resistance vessels and glomeruli in transgenic mice. Role of endothelin. The Journal of clinical investigation 1998;101:2780-9.
227. Belloni AS, Rossi GP, Andreis PG et al. Endothelin adrenocortical secretagogue effect is mediated by the B receptor in rats. Hypertension 1996;27:1153-9.
228. Shi-wen X, Kennedy L, Renzoni EA et al. Endothelin is a downstream mediator of profibrotic responses to transforming growth factor beta in human lung fibroblasts. Arthritis and rheumatism 2007;56:4189-94.
229. Shi-Wen X, Rodriguez-Pascual F, Lamas S et al. Constitutive ALK5-independent c-Jun N-terminal kinase activation contributes to endothelin-1 overexpression in pulmonary fibrosis: evidence of an autocrine endothelin loop operating through the endothelin A and B receptors. Molecular and cellular biology 2006;26:5518-27.
230. Shephard P, Hinz B, Smola-Hess S, Meister JJ, Krieg T, Smola H. Dissecting the roles of endothelin, TGF-beta and GM-CSF on myofibroblast differentiation by keratinocytes. Thrombosis and haemostasis 2004;92:262-74.
231. Seccia TM, Belloni AS, Kreutz R et al. Cardiac fibrosis occurs early and involves endothelin and AT-1 receptors in hypertension due to endogenous angiotensin II. Journal of the American College of Cardiology 2003;41:666-73.
232. Mulder P, Richard V, Derumeaux G et al. Role of endogenous endothelin in chronic heart failure: effect of long-term treatment with an endothelin antagonist on survival, hemodynamics, and cardiac remodeling. Circulation 1997;96:1976-82.
233. Xie S, Sukkar MB, Issa R, Oltmanns U, Nicholson AG, Chung KF. Regulation of TGF-beta 1-induced connective tissue growth factor expression in airway smooth muscle cells. American journal of physiology Lung cellular and molecular physiology 2005;288:L68-76.
234. Mori T, Kawara S, Shinozaki M et al. Role and interaction of connective tissue growth factor with transforming growth factor-beta in persistent fibrosis: A mouse fibrosis model. Journal of cellular physiology 1999;181:153-9.
235. Shi-wen X, Stanton LA, Kennedy L et al. CCN2 is necessary for adhesive responses to transforming growth factor-beta1 in embryonic fibroblasts. The Journal of biological chemistry 2006;281:10715-26.
236. Hayata N, Fujio Y, Yamamoto Y et al. Connective tissue growth factor induces cardiac hypertrophy through Akt signaling. Biochemical and biophysical research communications 2008;370:274-8.
237. Kennedy L, Liu S, Shi-Wen X et al. CCN2 is necessary for the function of mouse embryonic fibroblasts. Experimental cell research 2007;313:952-64.
238. Bonner JC. Regulation of PDGF and its receptors in fibrotic diseases. Cytokine & growth factor reviews 2004;15:255-73.
239. Rajkumar VS, Shiwen X, Bostrom M et al. Platelet-derived growth factor-beta receptor activation is essential for fibroblast and pericyte recruitment during

cutaneous wound healing. The American journal of pathology 2006;169:2254-65.
240. Burstein B, Libby E, Calderone A, Nattel S. Differential behaviors of atrial versus ventricular fibroblasts: a potential role for platelet-derived growth factor in atrial-ventricular remodeling differences. Circulation 2008;117:1630-41.
241. Tuuminen R, Nykanen AI, Krebs R et al. PDGF-A, -C, and -D but not PDGF-B increase TGF-beta1 and chronic rejection in rat cardiac allografts. Arteriosclerosis, thrombosis, and vascular biology 2009;29:691-8.
242. Carnes CA, Chung MK, Nakayama T et al. Ascorbate attenuates atrial pacing-induced peroxynitrite formation and electrical remodeling and decreases the incidence of postoperative atrial fibrillation. Circ Res 2001;89:E32-8.
243. Mihm MJ, Yu F, Carnes CA et al. Impaired myofibrillar energetics and oxidative injury during human atrial fibrillation. Circulation 2001;104:174-80.
244. Korantzopoulos P, Kolettis TM, Galaris D, Goudevenos JA. The role of oxidative stress in the pathogenesis and perpetuation of atrial fibrillation. Int J Cardiol 2007;115:135-43.
245. Liu T, Li G, Li L, Korantzopoulos P. Association between C-reactive protein and recurrence of atrial fibrillation after successful electrical cardioversion: a meta-analysis. Journal of the American College of Cardiology 2007;49:1642-8.
246. Aviles RJ, Martin DO, Apperson-Hansen C et al. Inflammation as a risk factor for atrial fibrillation. Circulation 2003;108:3006-10.
247. Aime-Sempe C, Folliguet T, Rucker-Martin C et al. Myocardial cell death in fibrillating and dilated human right atria. Journal of the American College of Cardiology 1999;34:1577-86.
248. Mevorach D. Opsonization of apoptotic cells. Implications for uptake and autoimmunity. Annals of the New York Academy of Sciences 2000;926:226-35.
249. Allessie M, Ausma J, Schotten U. Electrical, contractile and structural remodeling during atrial fibrillation. Cardiovasc Res 2002;54:230-46.
250. Chen CL, Huang SK, Lin JL et al. Upregulation of matrix metalloproteinase-9 and tissue inhibitors of metalloproteinases in rapid atrial pacing-induced atrial fibrillation. J Mol Cell Cardiol 2008;45:742-53.
251. Friedrichs K, Klinke A, Baldus S. Inflammatory pathways underlying atrial fibrillation. Trends in molecular medicine 2011;17:556-63.
252. Rudolph V, Andrie RP, Rudolph TK et al. Myeloperoxidase acts as a profibrotic mediator of atrial fibrillation. Nature medicine 2010;16:470-4.
253. Chen MC, Chang JP, Liu WH et al. Increased inflammatory cell infiltration in the atrial myocardium of patients with atrial fibrillation. The American journal of cardiology 2008;102:861-5.
254. Li YY, McTiernan CF, Feldman AM. Interplay of matrix metalloproteinases, tissue inhibitors of metalloproteinases and their regulators in cardiac matrix remodeling. Cardiovasc Res 2000;46:214-24.
255. Thomas CV, Coker ML, Zellner JL, Handy JR, Crumbley AJ, 3rd, Spinale FG. Increased matrix metalloproteinase activity and selective upregulation in LV myocardium from patients with end-stage dilated cardiomyopathy. Circulation 1998;97:1708-15.

256. Gomez DE, Alonso DF, Yoshiji H, Thorgeirsson UP. Tissue inhibitors of metalloproteinases: structure, regulation and biological functions. European journal of cell biology 1997;74:111-22.
257. Spinale FG, Coker ML, Bond BR, Zellner JL. Myocardial matrix degradation and metalloproteinase activation in the failing heart: a potential therapeutic target. Cardiovasc Res 2000;46:225-38.
258. Spinale FG, Coker ML, Heung LJ et al. A matrix metalloproteinase induction/activation system exists in the human left ventricular myocardium and is upregulated in heart failure. Circulation 2000;102:1944-9.
259. Cleutjens JP, Kandala JC, Guarda E, Guntaka RV, Weber KT. Regulation of collagen degradation in the rat myocardium after infarction. J Mol Cell Cardiol 1995;27:1281-92.
260. Zhang W, Zhong M, Yang GR et al. Matrix metalloproteinase-9/tissue inhibitors of metalloproteinase-1 expression and atrial structural remodeling in a dog model of atrial fibrillation: inhibition with angiotensin-converting enzyme. Cardiovascular pathology : the official journal of the Society for Cardiovascular Pathology 2008;17:399-409.
261. Hoit BD, Takeishi Y, Cox MJ et al. Remodeling of the left atrium in pacing-induced atrial cardiomyopathy. Molecular and cellular biochemistry 2002;238:145-50.
262. Xu J, Cui G, Esmailian F et al. Atrial extracellular matrix remodeling and the maintenance of atrial fibrillation. Circulation 2004;109:363-8.
263. Flegal KM, Carroll MD, Ogden CL, Johnson CL. Prevalence and trends in obesity among US adults, 1999-2000. JAMA 2002;288:1723-7.
264. Kurth T, Gaziano JM, Berger K et al. Body mass index and the risk of stroke in men. Arch Intern Med 2002;162:2557-62.
265. Dublin S, French B, Glazer NL et al. Risk of new-onset atrial fibrillation in relation to body mass index. Arch Intern Med 2006;166:2322-8.
266. Frost L, Hune LJ, Vestergaard P. Overweight and obesity as risk factors for atrial fibrillation or flutter: the Danish Diet, Cancer, and Health Study. Am J Med 2005;118:489-95.
267. Vaziri SM, Larson MG, Benjamin EJ, Levy D. Echocardiographic predictors of nonrheumatic atrial fibrillation. The Framingham Heart Study. Circulation 1994;89:724-30.
268. Kenchaiah S, Evans JC, Levy D et al. Obesity and the risk of heart failure. N Engl J Med 2002;347:305-13.
269. Weil BR, Westby CM, Van Guilder GP, Greiner JJ, Stauffer BL, DeSouza CA. Enhanced endothelin-1 system activity with overweight and obesity. Am J Physiol Heart Circ Physiol 2011;301:H689-95.
270. Fain JN, Tichansky DS, Madan AK. Transforming growth factor beta1 release by human adipose tissue is enhanced in obesity. Metabolism: clinical and experimental 2005;54:1546-51.
271. Fruhbeck G. The adipose tissue as a source of vasoactive factors. Current medicinal chemistry Cardiovascular and hematological agents 2004;2:197-208.
272. Paradise NF, Pilati CF, Payne WR, Finkelstein JA. Left ventricular function of the isolated, genetically obese rat's heart. Am J Physiol 1985;248:H438-44.

273. Zhou YT, Grayburn P, Karim A et al. Lipotoxic heart disease in obese rats: implications for human obesity. Proc Natl Acad Sci U S A 2000;97:1784-9.
274. Wong CX, Abed HS, Molaee P et al. Pericardial fat is associated with atrial fibrillation severity and ablation outcome. Journal of the American College of Cardiology 2011;57:1745-51.
275. Britton KA, Fox CS. Ectopic fat depots and cardiovascular disease. Circulation 2011;124:e837-41.
276. Thanassoulis G, Massaro JM, O'Donnell CJ et al. Pericardial fat is associated with prevalent atrial fibrillation: the Framingham Heart Study. Circ Arrhythm Electrophysiol 2010;3:345-50.
277. Batal O, Schoenhagen P, Shao M et al. Left atrial epicardial adiposity and atrial fibrillation. Circ Arrhythm Electrophysiol 2010;3:230-6.
278. Al Chekakie MO, Welles CC, Metoyer R et al. Pericardial fat is independently associated with human atrial fibrillation. Journal of the American College of Cardiology 2010;56:784-8.
279. Shin SY, Yong HS, Lim HE et al. Total and interatrial epicardial adipose tissues are independently associated with left atrial remodeling in patients with atrial fibrillation. J Cardiovasc Electrophysiol 2011;22:647-55.
280. Nagashima K, Okumura Y, Watanabe I et al. Does location of epicardial adipose tissue correspond to endocardial high dominant frequency or complex fractionated atrial electrogram sites during atrial fibrillation? Circ Arrhythm Electrophysiol 2012;5:676-83.
281. Wolf PA, Dawber TR, Thomas HE, Jr., Kannel WB. Epidemiologic assessment of chronic atrial fibrillation and risk of stroke: the Framingham study. Neurology 1978;28:973-7.
282. Brand FN, Abbott RD, Kannel WB, Wolf PA. Characteristics and prognosis of lone atrial fibrillation. 30-year follow-up in the Framingham Study. JAMA 1985;254:3449-53.
283. Murphy NF, MacIntyre K, Stewart S, Hart CL, Hole D, McMurray JJ. Long-term cardiovascular consequences of obesity: 20-year follow-up of more than 15 000 middle-aged men and women (the Renfrew-Paisley study). Eur Heart J 2006;27:96-106.
284. Wang TJ, Parise H, Levy D et al. Obesity and the risk of new-onset atrial fibrillation. JAMA : the journal of the American Medical Association 2004;292:2471-7.
285. McCann JP, Bergman EN, Beermann DH. Dynamic and static phases of severe dietary obesity in sheep: food intakes, endocrinology and carcass and organ chemical composition. The Journal of nutrition 1992;122:496-505.
286. Gepstein L, Hayam G, Ben-Haim SA. A novel method for nonfluoroscopic catheter-based electroanatomical mapping of the heart. In vitro and in vivo accuracy results. Circulation 1997;95:1611-22.
287. Bradford MM. A rapid and sensitive method for the quantitation of microgram quantities of protein utilizing the principle of protein-dye binding. Anal Biochem 1976;72:248-54.
288. Wood JP, Chidlow G, Graham M, Osborne NN. Energy substrate requirements for survival of rat retinal cells in culture: the importance of glucose and monocarboxylates. J Neurochem 2005;93:686-97.

289. Wilhelmsen L, Rosengren A, Lappas G. Hospitalizations for atrial fibrillation in the general male population: morbidity and risk factors. J Intern Med 2001;250:382-9.
290. Iwasaki YK, Shi Y, Benito B et al. Determinants of atrial fibrillation in an animal model of obesity and acute obstructive sleep apnea. Heart rhythm : the official journal of the Heart Rhythm Society 2012;9:1409-1416 e1.
291. Leask A. Potential therapeutic targets for cardiac fibrosis: TGFbeta, angiotensin, endothelin, CCN2, and PDGF, partners in fibroblast activation. Circ Res 2010;106:1675-80.
292. Savelieva I, Kakouros N, Kourliouros A, Camm AJ. Upstream therapies for management of atrial fibrillation: review of clinical evidence and implications for European Society of Cardiology guidelines. Part II: secondary prevention. Europace : European pacing, arrhythmias, and cardiac electrophysiology : journal of the working groups on cardiac pacing, arrhythmias, and cardiac cellular electrophysiology of the European Society of Cardiology 2011;13:610-25.
293. Lammers WJ, Schalij MJ, Kirchhof CJ, Allessie MA. Quantification of spatial inhomogeneity in conduction and initiation of reentrant atrial arrhythmias. The American journal of physiology 1990;259:H1254-63.
294. Zamani N, Brown CW. Emerging roles for the transforming growth factor-{beta} superfamily in regulating adiposity and energy expenditure. Endocr Rev 2011;32:387-403.
295. Weil BR, Westby CM, Van Guilder GP, Greiner JJ, Stauffer BL, DeSouza CA. Enhanced endothelin-1 system activity with overweight and obesity. Am J Physiol Heart Circ Physiol 2011;301:H689-95.
296. Lijnen PJ, Petrov VV, Fagard RH. Induction of cardiac fibrosis by transforming growth factor-beta(1). Mol Genet Metab 2000;71:418-35.
297. Abed HS, Wittert GA, Leong DP et al. Effect of weight reduction and cardiometabolic risk factor management on symptom burden and severity in patients with atrial fibrillation: a randomized clinical trial. JAMA 2013;310:2050-60.
298. Gepstein L, Hayam G, Shpun S, Ben-Haim SA. Hemodynamic evaluation of the heart with a nonfluoroscopic electromechanical mapping technique. Circulation 1997;96:3672-80.
299. Sanders P, Kistler PM, Morton JB, Spence SJ, Kalman JM. Remodeling of sinus node function in patients with congestive heart failure: reduction in sinus node reserve. Circulation 2004;110:897-903.
300. Mahajan R, Brooks AG, Shipp N et al. AF and obesity: Impact of weight reduction on the atrial substrate. Heart Rhythm 2013:S484.
301. Batal O, Schoenhagen P, Shao M et al. Left atrial epicardial adiposity and atrial fibrillation. Circulation 2010;3:230-6.
302. Al Chekakie MO, Welles CC, Metoyer R et al. Pericardial fat is independently associated with human atrial fibrillation. Journal of the American College of Cardiology 2010;56:784-8.
303. Lin YK, Chen YJ, Chen SA. Potential atrial arrhythmogenicity of adipocytes: implications for the genesis of atrial fibrillation. Med Hypotheses 2010;74:1026-9.

304. Marchington JM, Mattacks CA, Pond CM. Adipose tissue in the mammalian heart and pericardium: structure, foetal development and biochemical properties. Comp Biochem Physiol B 1989;94:225-32.
305. Mahajan R, Brooks, A.G, Shipp, N., Finnie, J.W., Manavis, J., Grover, S, Selvanayagam, J.B., Thanigaimani, S., Abed, H.S., Alasady, M., Roberts-Thomson, K.C.,Sanders, P. Epicardial fat infiltration of atrial musculature creates the substrate for atrial fibrillation in obesity. Heart Rhythm 2012;9:S124.
306. Hao J, Ju H, Zhao S, Junaid A, Scammell-La Fleur T, Dixon IM. Elevation of expression of Smads 2, 3, and 4, decorin and TGF-beta in the chronic phase of myocardial infarct scar healing. J Mol Cell Cardiol 1999;31:667-78.
307. John B, Stiles MK, Kuklik P et al. Reverse remodeling of the atria after treatment of chronic stretch in humans: implications for the atrial fibrillation substrate. Journal of the American College of Cardiology 2010;55:1217-26.
308. Lau DH, Psaltis PJ, Carbone A et al. Atrial protective effects of n-3 polyunsaturated fatty acids: a long-term study in ovine chronic heart failure. Heart Rhythm 2011;8:575-82.
309. Thanassoulis G, Massaro JM, O'Donnell CJ et al. Pericardial fat is associated with prevalent atrial fibrillation: the Framingham Heart Study. Circ Arrhythm Electrophysiol 2010;3:345-50.
310. Shen MJ, Choi EK, Tan AY et al. Neural mechanisms of atrial arrhythmias. Nature reviews 2011;9:30-9.
311. Scherlag BJ, Nakagawa H, Jackman WM et al. Electrical stimulation to identify neural elements on the heart: their role in atrial fibrillation. Journal of interventional cardiac electrophysiology : an international journal of arrhythmias and pacing 2005;13 Suppl 1:37-42.
312. Nelson AJ, Worthley MI, Psaltis PJ et al. Validation of cardiovascular magnetic resonance assessment of pericardial adipose tissue volume. J Cardiovasc Magn Reson 2009;11:15.
313. Iacobellis G, Corradi D, Sharma AM. Epicardial adipose tissue: anatomic, biomolecular and clinical relationships with the heart. Nat Clin Pract Cardiovasc Med 2005;2:536-43.
314. Sacks HS, Fain JN. Human epicardial adipose tissue: a review. American heart journal 2007;153:907-17.
315. Sironi AM, Gastaldelli A, Mari A et al. Visceral fat in hypertension: influence on insulin resistance and beta-cell function. Hypertension 2004;44:127-33.
316. Wheeler GL, Shi R, Beck SR et al. Pericardial and visceral adipose tissues measured volumetrically with computed tomography are highly associated in type 2 diabetic families. Invest Radiol 2005;40:97-101.
317. Iacobellis G, Ribaudo MC, Assael F et al. Echocardiographic epicardial adipose tissue is related to anthropometric and clinical parameters of metabolic syndrome: a new indicator of cardiovascular risk. The Journal of clinical endocrinology and metabolism 2003;88:5163-8.
318. Gorter PM, van Lindert AS, de Vos AM et al. Quantification of epicardial and peri-coronary fat using cardiac computed tomography; reproducibility and relation with obesity and metabolic syndrome in patients suspected of coronary artery disease. Atherosclerosis 2008;197:896-903.

319. Mahajan R BA, Finnie JW, Manavis J, Grover S, Selvanayagam JB, Thanigaimani S, Abed H, Alasady M, Roberts-Thomson KC, Sanders P. Epicardial fatty infiltration of atrial musculature creates the substrate for atrial fibrillation in obesity. Heart Rhythm 2012;9:S124.
320. Nagashima K, Okumura Y, Watanabe I et al. Does location of epicardial adipose tissue correspond to endocardial high dominant frequency or complex fractionated atrial electrogram sites during atrial fibrillation? Circ Arrhythm Electrophysiol 2012;5:676-83.
321. Mahajan R, Brooks AG, Shipp N et al. Obesity and atrial fibrillation: Endocardial electroanatomic and structural remodelling with obesity in an ovine model. Heart, Lung and Circulation 2011;20S.
322. Mahajan R, Brooks, A.G., Shipp,N., Manavis,J., Wood,J.P., Finnie,J., Samuel, C., Royce, S., Abed,H.S., Kuklik, P., Alasady, A., Lau, D.L., Roberts-Thomson, K.C., Sanders, P. Obesity and Weight Reduction: Impact on the Substrate for Atrial Fibrillation. Circulation 2012;126:A12204.
323. Calkins H, Kuck KH, Cappato R et al. 2012 HRS/EHRA/ECAS expert consensus statement on catheter and surgical ablation of atrial fibrillation: recommendations for patient selection, procedural techniques, patient management and follow-up, definitions, endpoints, and research trial design: a report of the Heart Rhythm Society (HRS) Task Force on Catheter and Surgical Ablation of Atrial Fibrillation. Developed in partnership with the European Heart Rhythm Association (EHRA), a registered branch of the European Society of Cardiology (ESC) and the European Cardiac Arrhythmia Society (ECAS); and in collaboration with the American College of Cardiology (ACC), American Heart Association (AHA), the Asia Pacific Heart Rhythm Society (APHRS), and the Society of Thoracic Surgeons (STS). Endorsed by the governing bodies of the American College of Cardiology Foundation, the American Heart Association, the European Cardiac Arrhythmia Society, the European Heart Rhythm Association, the Society of Thoracic Surgeons, the Asia Pacific Heart Rhythm Society, and the Heart Rhythm Society. Heart Rhythm 2012;9:632-696 e21.
324. Mahajan R, Kuklik, P., Grover, S., Brooks, A.G., Wong, C.X., Sanders, P., Selvanayagam, J.B. Cardiovascular magnetic resonance of total and atrial pericardial adipose tissue: A validation study and development of a 3 dimensional pericardial adipose tissue model. Journal of Cardiovascular Magnetic Resonance 2013;15:73-79.
325. Teo KS, Dundon BK, Molaee P et al. Percutaneous closure of atrial septal defects leads to normalisation of atrial and ventricular volumes. J Cardiovasc Magn Reson 2008;10:55.
326. Tsang TS, Barnes ME, Miyasaka Y et al. Obesity as a risk factor for the progression of paroxysmal to permanent atrial fibrillation: a longitudinal cohort study of 21 years. Eur Heart J 2008;29:2227-33.